

# A conditional gradient homotopy method with applications to Semidefinite Programming

Pavel Dvurechensky<sup>1</sup>, Gabriele Iomazzo<sup>4</sup>, Shimrit Shtern<sup>2</sup>, and Mathias Staudigl<sup>\*3</sup>

<sup>1</sup>Weierstrass Institute for Applied Analysis and Stochastics, Mohrenstr. 39, 10117 Berlin, Germany, (Pavel.Dvurechensky@wias-berlin.de)

<sup>2</sup>Faculty of Data and Decision Sciences, Technion - Israel Institute of Technology, Haifa, Israel, (shimrit@technion.ac.il)

<sup>3</sup>Department of Mathematics, 68159 Mannheim, B6, Germany, (mathias.staudigl@uni-mannheim.de)

<sup>4</sup>Zuse Institute Berlin, Berlin, Germany, (iomazzo@zib.de)

January 31, 2025

## Abstract

We propose a new homotopy-based conditional gradient method for solving convex optimization problems with a large number of simple conic constraints. Instances of this template naturally appear in semidefinite programming problems arising as convex relaxations of combinatorial optimization problems. Our method is a double-loop algorithm in which the conic constraint is treated via a self-concordant barrier, and the inner loop employs a conditional gradient algorithm to approximate the analytic central path, while the outer loop updates the accuracy imposed on the temporal solution and the homotopy parameter. Our theoretical iteration complexity is competitive when confronted to state-of-the-art SDP solvers, with the decisive advantage of cheap projection-free subroutines. Preliminary numerical experiments are provided for illustrating the practical performance of the method.

## 1 Introduction

In this paper we investigate a new algorithm for solving a large class of convex optimization problems with conic constraints of the following form:

$$\min_x g(x) \quad \text{s.t. } x \in X, \mathcal{P}(x) \in K \subseteq H. \quad (\text{P})$$

The objective function  $g : E \rightarrow (-\infty, \infty]$  is assumed to be closed, convex, and proper,  $X \subseteq E$  is a compact convex set,  $\mathcal{P} : E \rightarrow H$  is an affine mapping between two finite-dimensional Euclidean vector spaces  $E$  and  $H$ , and  $K$  is a closed convex pointed cone. Problem (P) is sufficiently generic to cover many optimization settings considered in the literature.

*Example 1.1* (Packing SDP). The model template (P) covers the large class of packing semidefinite programs (SDPs) [14, 24]. In this problem class we have  $E = \mathbb{S}^n$  – the space of symmetric  $n \times n$  matrices, a collection of positive semidefinite input matrices  $\mathbf{A}_1, \dots, \mathbf{A}_m \in \mathbb{S}_+^n$ , with constraints given by  $\mathcal{P}(\mathbf{X}) = [1 - \text{tr}(\mathbf{A}_1\mathbf{X}); \dots; 1 - \text{tr}(\mathbf{A}_m\mathbf{X})]^\top$  and  $K = \mathbb{R}_+^m$ , coupled with the objective function  $g(\mathbf{X}) = \text{tr}(C\mathbf{X})$  and the set  $X = \{\mathbf{X} \in \mathbb{S}_+^n \mid \text{tr}(\mathbf{X}) \leq \rho\}$ . Special instances of packing SDPs include the MaxCut SDP relaxation of [19], the Lovasz- $\theta$  function SDP, among many others; see [23].

\*Corresponding Author

*Example 1.2* (Covering SDP). A dual formulation of the packing SDP is the covering problem [14]. In its normalized version, the problem reads as

$$\min_x \sum_{i=1}^m x_i \quad \text{s.t.} \sum_{i=1}^m x_i \mathbf{A}_i - \mathbf{I} \geq 0, x \in \mathbb{R}_+^m,$$

where  $\mathbf{A}_1, \dots, \mathbf{A}_m \in \mathbb{S}_+^n$  are given input matrices. This can be seen as a special case of problem (P) with  $g(x) = \sum_{i=1}^m x_i$ ,  $\mathcal{P}(x) = \sum_{i=1}^m x_i \mathbf{A}_i - \mathbf{I}$ ,  $\mathbf{K} = \mathbb{S}_+^n$ ,  $\mathbf{H} = \mathbb{S}^n$ ,  $\mathbf{E} = \mathbb{R}^m$ , and the constraint set  $\mathbf{X} = \{x \in \mathbb{R}_+^m \mid \sum_{i=1}^m x_i \leq \rho\}$  for some large  $\rho$  added to the problem for the compactification purposes.

*Example 1.3* (Relative entropy programs). Relative entropy programs are conic optimization problems in which a linear functional of a decision variable is minimized subject to linear constraints and conic constraints specified by a *relative entropy cone*. The relative entropy cone is defined for triples  $(u, v, w) \in \mathbb{R}^n \times \mathbb{R}^n \times \mathbb{R}^n$  via Cartesian products of the following elementary cone

$$\mathbf{K}_{\text{RE}}^{(1)} = \{(v, \lambda, \delta) \in \mathbb{R}_+ \times \mathbb{R}_+ \times \mathbb{R} \mid -v \log\left(\frac{\lambda}{v}\right) \leq \delta\}.$$

As the function  $\mathbb{R}_{++}^2 \ni (v, \lambda) \mapsto -v \log(\lambda/v)$  is the perspective transform of the negative logarithm, we know that it is a convex function [4]. Hence,  $\mathbf{K}_{\text{RE}}^{(1)}$  is a convex cone. The relative entropy cone is accordingly defined as  $\mathbf{K} = \prod_{i=1}^n \mathbf{K}_{\text{RE}}^{(1)}$ . This set appears in many important applications, containing estimation of dynamical systems and the optimization of quantum channels; see [5] for an overview.

*Example 1.4* (Relative Entropy entanglement). The relative entropy of entanglement (REE) is an important measure for entanglement for a given quantum state in quantum information theory [31]. Obtaining accurate bounds on the REE is a major problem in quantum information theory. In [44] the following problem is used to find a lower bound to the REE:

$$\begin{aligned} \min_x g(x) &= \text{tr}[\rho(\log(\rho) - \log(x))] \\ \text{s.t.} \quad x &\in \mathbb{H}_+^n, \text{tr}(x) = 1, \mathcal{P}(x) \in \mathbb{H}_+^n, \end{aligned}$$

where  $\mathbb{H}_+^n$  is the cone of  $n \times n$  Hermitian positive semi-definite matrices, and  $\mathcal{P}(x)$  is the so-called partial transpose operator, which is a linear symmetric operator (see [22]).  $\rho \in \mathbb{H}_+^n$  is a given quantum reference state. We obtain a problem of the form (P), upon the identification  $\mathbf{E} = \mathbb{H}^n$  the space of  $n \times n$  Hermitian matrices, and  $\mathbf{K} = \mathbb{H}_+^n$ , and  $\mathbf{X} = \{x \in \mathbf{E} \mid x \in \mathbb{H}_+^n, \text{tr}(x) = 1\}$ .

The model template (P) can be solved with moderate accuracy using fast proximal gradient methods, like FISTA and related acceleration tricks [12]. In this formalism, the constraints imposed on the optimization problem have to be included in proximal operators which essentially means that one can calculate a projection onto the feasible set. Unfortunately, the computation of proximal operators can impose a significant burden and even lead to intractability of gradient-based methods. This is in particular the case in SDPs with a large number of constraints and decision variables, such as in convex relaxations of NP-hard combinatorial optimization problems [28]. Other prominent examples in machine learning are  $k$ -means clustering [32],  $k$ -nearest neighbor classification [36], sparse PCA [8], kernel learning [27], among many others. In many of these mentioned applications, it is not only the size of the problem that challenges the application of off-the-shelf solvers, but also the desire to obtain sparse solutions. As a result, the Conditional Gradient (CndG) method [17] has seen renewed interest in large-scale convex programming, since it only requires computing a Linear Minimization Oracle (LMO) at each iteration. Compared to proximal methods, CndG features significantly reduced computational costs (e.g. when  $\mathbf{X}$  is a spectrahedron), tractability and interpretability (e.g. it generates solutions as a combination of atoms of  $\mathbf{X}$ ).

**Our approach** In this paper we propose a CndG framework for solving (P) with rigorous iteration complexity guarantees. Our approach retains the simplicity of CndG, but allows to disentangle the different sources of complexity describing the problem. Specifically, we study the performance of a new *homotopy/path-following method*, which iteratively approaches a solution of problem (P). To develop the path-following argument we start by decomposing the feasible set into two components. We assume that  $X$  is a compact convex set which admits efficient applications of CndG. The challenging constraints are embodied by the membership condition  $\mathcal{P}(x) \in K$ . These are conic restrictions on the solution, and in typical applications of our method we have to manage a lot of them. Our approach deals with these constraints via a *logarithmically homogeneous barrier* for the cone  $K$ . [30] introduced this class of functions in connection with polynomial-time interior point methods. It is a well-known fact that any closed convex cone admits a logarithmically homogeneous barrier (the universal barrier) [30, Thm. 2.5.1]. A central assumption of our approach is that we have a practical representation of a logarithmically homogeneous barrier for the cone  $K$ . As many restrictions appearing in applications are linear or PSD inequalities, this assumption is rather mild. Exploiting the announced decomposition, we approximate the target problem (P) by a family of parametric penalty-based composite convex optimization problems formulated in terms of the *potential function*

$$\min_{x \in X} \{V_t(x) := \frac{1}{t}F(x) + g(x)\}. \quad (1.1)$$

This potential function involves a path-following/homotopy parameter  $t > 0$ , and  $F$  is a barrier function defined over the set  $\mathcal{P}^{-1}(K)$ . By minimizing the function  $V_t$  over the set  $X$  for a sequence of increasing values of  $t$ , we can trace the *analytic central path*  $z^*(t)$  of (1.1) as it converges to a solution of (P). The practical implementation of this path-following scheme is achieved via a double-loop algorithm in which the inner loop performs a number of CndG updating steps on the potential function  $V_t$ , and the outer-loop readjusts the parameter  $t$  as well as the desired tolerance imposed on the CndG-solver. Importantly, unlike existing primal-dual methods for (P) (e.g. [41]), our approach generates a sequence of feasible points for the original problem (P).

**Comparison to the literature** Exact homotopy/path-following methods were developed in statistics and signal processing in the context of the  $\ell_1$ -regularized least squares problem (LASSO) [34] to compute the entire regularization path. Relatedly, approximate homotopy methods have been studied in this context as well [21, 37], and superior empirical performance has been reported for seeking sparse solutions. [38] is the first reference which investigates the complexity of a proximal gradient homotopy method for the LASSO problem. To our best knowledge, our paper provides the first complexity analysis of a homotopy CndG algorithm to compute an approximate solution close to the analytic central path for the optimization template (P). Our analysis is heavily influenced by recent papers [43] and [42]. They study a generalized CndG algorithm designed for solving a composite convex optimization problem, in which the smooth part is given by a *logarithmically homogeneous barrier*. Unlike [43], we analyze a more complicated dynamic problem in which the objective changes as we update the penalty parameter, and we propose important practical extensions including line-search and inexact-LMO versions of the CndG algorithm for reducing the potential function (1.1). Furthermore, we analyze the complexity of the whole path-following process in order to approximate a solution to the initial non-penalized problem (P).

**Main Results** One of the challenging questions is how to design a penalty parameter updating schedule, and we develop a practical answer to this question. Specifically, our contributions can be summarized as follows:

- We introduce a simple CndG framework for solving problem (P) and prove that it achieves a  $\tilde{O}(\varepsilon^{-2})$  iteration complexity, where  $\tilde{O}(\cdot)$  hides polylogarithmic factors (Theorem 3.3).
- We provide two extensions for the inner-loop CndG algorithm solving the potential minimization problem (1.1): a line-search and an inexact-LMO version. For both, we show that the complexity of the inner and the outer loop are the same as in the basic variant up to constant factors.
- We present practically relevant applications of our framework, including instances of SDPs arising from convex relaxations of NP-hard combinatorial optimization problems, and provide promising results of the numerical experiments.

Direct application of existing CndG frameworks [40, 41] for solving (P) would require projection onto  $K$ , which may be complicated if, e.g.,  $K$  is a PSD cone. Moreover, these algorithms do not produce feasible iterates but rather approximate solutions with primal optimality and dual feasibility guarantees. For specific instances of SDPs, the theoretical complexity achieved by our method matches or even improves the state-of-the-art iteration complexity results reported in the literature. For packing and covering types of SDPs, the state-of-the-art upper complexity bound reported in [14] is worse than ours since their algorithm has complexity  $\tilde{O}(C_1\varepsilon^{-2.5} + C_2\varepsilon^{-2})$ , where  $C_1, C_2$  are constants depending on the problem data<sup>1</sup>. For SDPs with linear equality constraints and spectrahedron constraints, the primal-dual method CGAL [41] produces *approximately optimal* and *approximately feasible* points in  $O(\varepsilon^{-2})$  iterations. Our method is purely primal, generating feasible points anytime. At the same time, our method shares the same theoretical iteration complexity as CGAL and can deal with additional conic constraints embodied by the membership restriction  $\mathcal{P}(x) \in K$  without use of projection. We expect that this added feature will allow us to apply our method to handle challenging scientific computing questions connected to the quantum information theory, such as bounding the relative entropy of entanglement of quantum states (cf. Example 1.4 and [15, 16, 44]).

**Organization of the paper** This paper is organized as follows: Section 2 introduces the notation and terminology we use throughout this paper. Section 3 presents the basic algorithm under consideration in this paper. In section 4 we describe an inexact version of our basic homotopy method. Section 5 contains a detailed complexity analysis of our scheme when an exact LMO is available. The corresponding statements under our inexact LMO are performed in Appendix A. Section 6 reports the performance of our method in solving relevant examples of SDPs and gives some first comparisons with existing approaches. In particular, numerical results on the mixing time problem of a finite Markov Chain, and synthetic examples aimed at testing the robustness to scaling are reported there. Appendix B contains further results on the numerical experiments.

## 2 Notation and Preliminaries

Let  $E$  be a finite-dimensional Euclidean vector space,  $E^*$  its dual space, which is formed by all linear functions on  $E$ . The value of function  $s \in E^*$  at  $x \in E$  is denoted by  $\langle s, x \rangle$ . Let  $B : E \rightarrow E^*$  be a positive definite self-adjoint operator. Define the primal and dual norms

$$\|h\|_B = \langle Bh, h \rangle^{1/2}, \text{ and } \|s\|_B^* = \langle s, B^{-1}s \rangle^{1/2}$$

---

<sup>1</sup>The notation  $\tilde{O}$  hides polylogarithmic factors

for  $h \in E$  and  $s \in E^*$ , respectively. If  $B$  is the identity operator, we simplify notation to  $\|h\|$  and  $\|s\|_*$ , respectively for the primal and the dual norm. For a linear operator  $A : E \rightarrow E^*$  we define the operator norm

$$\|A\| = \max_{h \in E: \|h\| \leq 1} \|Ah\|_*.$$

For a differentiable function  $f(x)$  with  $\text{dom}(f) \subseteq E$ , we denote by  $f'(x) \in E^*$  its gradient, by  $f''(x) : E \rightarrow E^*$  its Hessian, and by  $f'''(x)$  its third derivative. Accordingly, given directions  $h_1, h_2, h_3 \in E$  the first, second, and third directional derivatives of  $f$  are denoted respectively as  $f'(x)[h_1], f''(x)[h_1, h_2], f'''(x)[h_1, h_2, h_3]$ .

## 2.1 Self-Concordant Functions

Let  $Q$  be an open and convex subset of  $E$ . A function  $f : E \rightarrow (-\infty, \infty]$  is *self-concordant* (SC) on  $Q$  if  $f \in C^3(Q)$  and for all  $x \in Q, h \in E$ , we have  $|f'''(x)[h, h, h]| \leq 2(f''(x)[h, h])^{3/2}$ . In case where  $\text{cl}(Q)$  is a closed, convex, and pointed (i.e., contains no line) cone, we have more structure. We call  $f$  a  *$\nu$ -canonical barrier* for  $Q$ , denoted by  $f \in \mathcal{B}_\nu(Q)$ , if it is SC and

$$\forall (x, t) \in Q \times (0, \infty): \quad f(tx) = f(x) - \nu \log(t).$$

From [30, Prop. 2.3.4], the following properties are satisfied by a  $\nu$ -canonical barrier for each  $x \in Q, h \in E, t > 0$ :

$$f'(tx) = t^{-1} f'(x), \tag{2.1}$$

$$f'(x)[h] = -f''(x)[x, h], \tag{2.2}$$

$$f'(x)[x] = -\nu, \tag{2.3}$$

$$f''(x)[x, x] = \nu. \tag{2.4}$$

We define the local norm  $\|h\|_{f''(x)} := (f''(x)[h, h])^{1/2}$  for all  $x \in \text{dom}(f)$  and  $h \in E$ . SC functions are in general not Lipschitz smooth. Still, we have access to a version of a descent lemma of the following form [29, Thm. 5.1.9]:

$$f(x+h) \leq f(x) + f'(x)[h] + \omega_*(\|h\|_{f''(x)}) \tag{2.5}$$

for all  $x \in \text{dom}(f)$  and  $h \in E$  such that  $\|h\|_{f''(x)} < 1$ , where  $\omega_*(t) = -t - \log(1-t)$ . It also holds true that [29, Thm. 5.1.8]

$$f(x+h) \geq f(x) + f'(x)[h] + \omega(\|h\|_{f''(x)}) \tag{2.6}$$

for all  $x \in \text{dom}(f)$  and  $h \in E$  such that  $x+h \in \text{dom}(f)$ , where  $\omega(t) = t - \log(1+t)$  for  $t \geq 0$ .

A classical and useful bound is [29, Lemma 5.1.5]:

$$\frac{t^2}{2-t} \leq \omega_*(t) \leq \frac{t^2}{2(1-t)} \quad \forall t \in [0, 1). \tag{2.7}$$

## 2.2 The Optimization Problem

The following assumptions are made for the rest of this paper.

**Assumption 1.** The function  $g : E \rightarrow (-\infty, \infty]$  is closed and convex and continuous on  $\text{dom}(g)$ . The quantity  $\Omega_g := \max_{x, y \in \text{dom}(g) \cap X} |g(x) - g(y)|$  is finite.

**Assumption 2.**  $K \subset H$  is a closed convex pointed cone with  $\text{int}(K) \neq \emptyset$ , admitting a  $\nu$ -canonical barrier  $f \in \mathcal{B}_\nu(K)$ .

The next assumption transports the barrier setup from the codomain  $K$  to the domain  $\mathcal{P}^{-1}(K)$ . This is a common operation in the framework of the "barrier calculus" developed in [30, Section 5.1].

**Assumption 3.** The map  $\mathcal{P} : E \rightarrow H$  is linear, and  $F(x) := f(\mathcal{P}(x))$  is a  $\nu$ -canonical barrier on the cone  $\mathcal{P}^{-1}(K)$ , i.e.  $F \in \mathcal{B}_\nu(\mathcal{P}^{-1}(K))$ .

Note that  $\text{dom}(F) = \text{int } \mathcal{P}^{-1}(K)$ .

*Example 2.1.* Considering the normalised covering problem presented in Example 1.2. [14] solve this problem via a logarithmic potential function method [30], involving the logarithmically homogeneous barrier  $f(\mathbf{X}) = \log \det(\mathbf{X})$  for  $\mathbf{X} \in \mathbb{S}_+^n$ . This is a typical choice in Newton-type methods to impose the semi-definiteness constraint. However, in our projection-free environment, we use the power of the linear minimisation oracle to obtain search directions which leaves the cone of positive semidefinite matrices invariant. Instead, we employ barrier functions to incorporate the additional linear constraints in (P). Hence, we set  $F(x) = f(\mathcal{P}(x)) = \log \det(\sum_{i=1}^m x_i \mathbf{A}_i - \mathbf{I})$  to absorb the constraint  $\mathcal{P}(x) \in \mathbb{S}_+^n$ . In particular, this frees us from matrix inversions, and related computationally intensive steps coming with Newton and interior-point methods.

**Assumption 4.**  $X$  is a nonempty compact convex set in  $E$ , and  $C := X \cap \text{dom}(F) \cap \text{dom}(g) \neq \emptyset$ .

Let  $\text{Opt} := \min\{g(x) | x \in X, \mathcal{P}(x) \in K\}$ . Thanks to assumptions 2 and 4,  $\text{Opt}$  is attained. Our goal is to find an  $\varepsilon$ -solution of problem (P), defined as follows.

**Definition 2.1.** Given a tolerance  $\varepsilon > 0$ , we say that  $z_\varepsilon^*$  is an  $\varepsilon$ -solution for (P) if  $z_\varepsilon^*$  is a *feasible* solution of problem (P) with objective at most  $\varepsilon$  higher than  $\text{Opt}$ , that is,

$$z_\varepsilon^* \in \mathcal{P}^{-1}(K) \cap X \text{ and } g(z_\varepsilon^*) - \text{Opt} \leq \varepsilon.$$

Given  $t > 0$ , define

$$\text{Opt}(t) := \min_{x \in X} \{V_t(x) = \frac{1}{t}F(x) + g(x)\}, \text{ and } z^*(t) \in \{x \in X | V_t(x) = \text{Opt}(t)\}. \quad (2.8)$$

The following Lemma shows that the path  $t \mapsto z^*(t)$  traces a trajectory in the interior of the feasible set which can be used to approximate a solution of the original problem (P), provided the penalty parameter  $t$  is chosen large enough.

**Lemma 2.2.** For all  $t > 0$ , it holds that  $z^*(t) \in C$ . In particular,

$$g(z^*(t)) - \text{Opt} \leq \frac{\nu}{t}. \quad (2.9)$$

*Proof.* Since  $F \in \mathcal{B}_\nu(\mathcal{P}^{-1}(K))$ , it follows immediately that  $z^*(t) \in \text{dom}(F) \cap X$ . By Fermat's principle we have

$$0 \in \frac{1}{t}F'(z^*(t)) + \partial g(z^*(t)) + \text{NC}_X(z^*(t)).$$

Convexity and [29, Thm. 5.3.7] implies that for all  $z \in \text{dom}(F) \cap X$ , we have

$$g(z) \geq g(z^*(t)) - \frac{1}{t}F'(z^*(t))[z - z^*(t)] \geq g(z^*(t)) - \frac{\nu}{t}.$$

Let  $z^*$  be a feasible point satisfying  $g(z^*) = \text{Opt}$ . Choosing a sequence  $\{z^j\}_{j \in \mathbb{N}} \subset \text{dom}(F) \cap X$  with  $z^j \rightarrow z^*$ , the continuity on  $\text{dom}(g)$  gives

$$\text{Opt} \geq g(z^*(t)) - \frac{\nu}{t}.$$

■

### 3 Algorithm

In this section we first describe a new CndG method for solving general conic constrained convex optimization problems of the form (2.8), for a fixed  $t > 0$ . This procedure serves as the inner loop of our homotopy method. The path-following strategy in the outer loop is then explained in Section 3.2.

#### 3.1 The Proposed CndG Solver

The computational efficiency of our approach relies on the availability of a suitably defined minimisation oracle:

**Assumption 5.** For any  $c \in \mathbf{E}^*$ , the auxiliary problem

$$\mathcal{L}_g(c) := \operatorname{argmin}_{s \in X} \{\langle c, s \rangle + g(s)\} \quad (3.1)$$

is easily solvable.

We can compute the gradient and Hessian of  $F$  as

$$F'(x) = f'(\mathcal{P}(x))\mathcal{P}'(x), \quad F''(x)[s, t] = f''(\mathcal{P}(x))[\mathcal{P}(s), \mathcal{P}(t)] \quad \forall x \in \operatorname{int} \mathcal{P}^{-1}(\mathbf{K}).$$

This means that we obtain a local norm on  $\mathbf{H}$  given by

$$\|w\|_x := F''(x)[w, w]^{1/2} \quad \forall (x, w) \in \operatorname{int} \mathcal{P}^{-1}(\mathbf{K}) \times \mathbf{H}.$$

Note that in order to evaluate the local norm we do not need to compute the full Hessian  $F''(x)$ . It only requires a directional derivative, which is potentially easy to do numerically.

A Linear Minimization Oracle (LMO) is defined as an oracle producing the vector field

$$s_t(x) \in \mathcal{L}_g(t^{-1}F'(x)). \quad (3.2)$$

Note that our analysis does not rely on a specific tie-breaking rule, so any member of the set  $\mathcal{L}_g(t^{-1}F'(x))$  will be acceptable.

To measure solution accuracy and overall algorithmic progress, we introduce two *merit functions*:

$$\mathbf{Gap}_t(x) := t^{-1}F'(x)[x - s_t(x)] + g(x) - g(s_t(x)), \text{ and} \quad (3.3)$$

$$\Delta_t(x) := V_t(x) - V_t(z^*(t)). \quad (3.4)$$

Note that  $\mathbf{Gap}_t(x) \geq 0$  and  $\Delta_t(x) \geq 0$  for all  $x \in \operatorname{dom}(F)$ . Moreover, convexity together with the definition of the point  $z^*(t)$ , gives

$$\begin{aligned} 0 \leq \Delta_t(x) &= t^{-1}[F(x) - F(z^*(t))] + g(x) - g(z^*(t)) \\ &\leq t^{-1}F'(x)[x - z^*(t)] + g(x) - g(z^*(t)) \\ &\leq t^{-1}F'(x)[x - s_t(x)] + g(x) - g(s_t(x)) = \mathbf{Gap}_t(x). \end{aligned}$$

Hence,

$$\mathbf{Gap}_t(x) \geq \Delta_t(x) \quad \forall x \in \operatorname{dom}(F) \cap \operatorname{dom}(g). \quad (3.5)$$

---

**Algorithm 1**  $\text{CG}(x^0, \varepsilon, t)$ 

---

**Input:**  $(x^0, t) \in \mathbf{C} \times (0, \infty)$  initial state;  $\varepsilon > 0$  accuracy level  
**for**  $k = 0, 1, \dots$  **do**  
  **if**  $\text{Gap}_t(x^k) > \varepsilon$  **then**  
    Obtain  $s^k = s_t(x^k)$  defined in (3.2).  
     $\alpha_k = \alpha_t(x^k)$  defined in (3.8).  
    Set  $x^{k+1} = x^k + \alpha_k(s^k - x^k)$ .  
  **else**  
    STOP. Return iteration index  $k$  and last iterate  $x^k$ .  
  **end if**  
**end for**

---

Define

$$e_t(x) := \|s_t(x) - x\|_x. \quad (3.6)$$

Then, for  $\alpha \in [0, \min\{1, 1/e_t(x)\}]$ , we get from (2.5)

$$F(x + \alpha(s_t(x) - x)) \leq F(x) + \alpha F'(x)[s_t(x) - x] + \omega_*(\alpha e_t(x)).$$

Together with the convexity of  $g$ , this implies

$$V_t(x + \alpha(s_t(x) - x)) \leq V_t(x) - \alpha \text{Gap}_t(x) + t^{-1} \omega_*(\alpha e_t(x)) = V_t(x) - \eta_{t,x}(\alpha), \quad (3.7)$$

where

$$\eta_{t,x}(\alpha) := \alpha \text{Gap}_t(x) - t^{-1} \omega_*(\alpha e_t(x)) = \alpha \text{Gap}_t(x) + t^{-1} (\alpha e_t(x) + \log(1 - \alpha e_t(x))).$$

Optimising this expression w.r.t  $\alpha \in [0, 1]$ , we obtain the analytic step-size policy

$$\alpha_t(x) := \min \left\{ 1, \frac{t \text{Gap}_t(x)}{e_t(x)(e_t(x) + t \text{Gap}_t(x))} \right\} \in [0, 1/e_t(x)]. \quad (3.8)$$

Equipped with this step strategy, procedure  $\text{CG}(x^0, \varepsilon, t)$ , described in Algorithm 1, constructs a sequence  $\{x_t^k\}_{k \geq 0}$  which produces an approximately-optimal solution in terms of the merit function  $\text{Gap}_t(\cdot)$  and the potential function  $\text{gap } \Delta_t$ . Specifically, our main results on the performance of Algorithm 1 are the following iteration complexity estimates, which are proven in Section 5.

**Proposition 3.1.** *Given  $\eta, t > 0$ , Algorithm  $\text{CG}(x_t^0, \eta, t)$  requires at most*

$$R(x_t^0, \eta, t) := \lceil 5.3(v + t\Delta_t(x_t^0) + t\Omega_g) \log(10.6t\Delta_t(x_t^0)) \rceil + \lceil \frac{24}{t\eta} (v + t\Omega_g)^2 \rceil, \quad (3.9)$$

*iterations in order to reach a point  $x_t^k$  satisfying  $\text{Gap}_t(x_t^k) \leq \eta$  for the first time.*

**Proposition 3.2.** *Given  $\eta, t > 0$ , Algorithm  $\text{CG}(x_t^0, \eta, t)$  requires at most*

$$N(x_t^0, \eta, t) := \lceil 5.3(v + t\Delta_t(x_t^0) + t\Omega_g) \log(10.6t\Delta_t(x_t^0)) \rceil + \lceil 12(v + t\Omega_g)^2 \left( \frac{1}{t\eta} - \frac{1}{t\Delta_t(x_t^0)} \right)_+ \rceil \quad (3.10)$$

*iterations, in order to reach a point  $x_t^k$  satisfying  $\Delta_t(x_t^k) \leq \eta$  for the first time.*

---

**Algorithm 2** Method Homotopy( $x^0, \varepsilon, f$ )

---

**Input:**  $x^0 \in \mathbf{C}$ ,  $f \in \mathcal{B}_\nu(\mathbf{K})$ ,  $t_0, \eta_0 > 0$ .

**Parameters:**  $\varepsilon, \sigma \in (0, 1)$ .

**Initialize:**  $x_{t_0}^0 = x^0$ ,  $I = \lceil \frac{\log(2\eta_0/\varepsilon)}{\log(1/\sigma)} \rceil$ .

**for**  $i = 0, 1, \dots, I - 1$  **do**

    Set  $\hat{x}_i$  the output of  $\text{CG}(x_{t_i}^0, \eta_i, t_i)$ .

    Update  $t_{i+1} = t_i/\sigma$ ,  $\eta_{i+1} = \sigma\eta_i$ ,  $x_{t_{i+1}}^0 = \hat{x}_i$ .

**end for**

Set  $\hat{z} = \hat{x}_I$  the output of  $\text{CG}(x_{t_I}^0, \eta_I, t_I)$ .

---

### 3.2 Updating the Homotopy Parameter

Our analysis so far focuses on minimisation of the potential function  $V_t(x)$  for a fixed  $t > 0$ . However, in order to solve the initial problem (P), one must trace the sequence of approximate solutions  $\{z^*(t)\}_{t \geq 0}$  as  $t \uparrow \infty$ . The construction of such an increasing sequence of homotopy parameters is the purpose of this section.

Let  $\{\eta_i\}_{i \geq 0}, \{t_i\}_{i \geq 0}$  be a sequence of approximation errors and homotopy parameters. For each run  $i$ , we activate procedure  $\text{CG}(x_{t_i}^0, \eta_i, t_i)$  with the given configuration  $(\eta_i, t_i)$ . For  $i = 0$ , we assume to have an admissible initial point  $x_{t_0}^0 = x^0$  available. For  $i \geq 1$ , we restart Algorithm 1 using a kind of warm-start strategy by choosing  $x_{t_i}^0 = x_{t_{i-1}}^{R_{i-1}}$ , where  $R_{i-1} \leq R(x_{t_{i-1}}^0, \eta_{i-1}, t_{i-1})$  denotes the first iterate  $k$  of Algorithm  $\text{CG}(x_{t_{i-1}}^0, \eta_{i-1}, t_{i-1})$  satisfying  $\text{Gap}_{t_{i-1}}(x_{t_{i-1}}^k) \leq \eta_{i-1}$ . Note that  $R_{i-1}$  is upper bounded by the constant  $R(x_{t_{i-1}}^0, \eta_{i-1}, t_{i-1})$  defined in Proposition 3.1. After the  $i$ -th restart, let us call the obtained iterate  $\hat{x}_i := x_{t_i}^{R_i}$ . In this way we obtain a sequence  $\{\hat{x}_i\}_{i \geq 0}$ , consisting of candidates for approximately following the central path, as they are  $\eta_i$ -close in terms of the gap  $\text{Gap}_{t_i}$  (and, hence, in terms of the function gap) to the stage  $t_i$ 's optimal point  $z^*(t_i)$ . We update the parameters  $(\eta_i, t_i)$  as follows:

- The sequence of homotopy parameters is determined as  $t_i = t_0\sigma^{-i}$  for  $\sigma \in (0, 1)$  until the last round of  $\text{Homotopy}(x^0, \varepsilon, f)$  is reached.
- The sequence of accuracies requested in the algorithm  $\text{CG}(x_{t_i}^0, \eta_i, t_i)$  is updated by  $\eta_i = \eta_0\sigma^i$ .
- The Algorithm stops after  $I \equiv I(\sigma, \eta_0, \varepsilon) = \lceil \frac{\log(2\eta_0/\varepsilon)}{\log(1/\sigma)} \rceil$  updates of the accuracy and homotopy parameters and yields an  $\varepsilon$ -approximate solution of problem (P).

Our updating strategy for the parameters ensures "detailed balance"  $t_i\eta_i = t_0\eta_0$ . This equilibrating choice between the increasing homotopy parameter and the decreasing accuracy parameter is sensible, because the iteration complexity of the CndG solver is inversely proportional to  $t_i\eta_i$  (cf. Proposition 3.1). Making the judicious choice  $\eta_0 t_0 = 2\nu$ , yields a compact assessment of the total complexity of method  $\text{Homotopy}(x^0, \varepsilon, f)$ .

**Theorem 3.3.** Choose  $t_0 = \frac{\nu}{\Omega_g}$  and  $\eta_0 = 2\Omega_g$ . The total iteration complexity of method  $\text{Homotopy}(x^0, \varepsilon, f)$  to find an  $\varepsilon$ -solution of (P) is

$$\text{Comp1}(x^0, \varepsilon, f) = \tilde{\mathcal{O}} \left( \frac{384\Omega_g^2\nu}{\varepsilon^2(1-\sigma^2)} + \Omega_g \log(21.2\nu(1 + (2/\varepsilon)\Omega_g)) \frac{21.2\nu}{\varepsilon} \frac{2-\sigma}{1-\sigma} \right), \quad (3.11)$$

where  $\tilde{\mathcal{O}}$  hides polylogarithmic factors in  $\varepsilon^{-1}$ .

---

**Algorithm 3** CndG with line search:  $\text{LCG}(x^0, \varepsilon, t)$ 

---

**Input:**  $(x^0, t) \in \mathcal{C} \times (0, \infty)$  initial state;  $\varepsilon > 0$  accuracy level  
**for**  $k = 0, 1, \dots$  **do**  
  **if**  $\text{Gap}_t(x^k) > \varepsilon$  **then**  
    Same as Algorithm 1, but with step size strategy (4.1).  
  **else**  
    STOP. Return iteration index  $k$  and last iterate  $x^k$ .  
  **end if**  
**end for**

---

*Remark 3.1.* The theorem leaves open the choice of the parameter  $\sigma$ . We treat  $\sigma$  as a hyperparameter that should be calibrated by the user. The proof of Theorem 3.3 can be found in Section 5.

## 4 Modifications and Extensions

### 4.1 Line Search

The step size policy employed in Algorithm 1 is inversely proportional to the local norm  $e_t(x)$ . In particular, its derivation is based on the a-priori restriction that we force our iterates to stay within a trust-region defined by the Dikin ellipsoid. This restriction may force the method to take very small steps, and as a result display bad performance in practice. A simple remedy would be to employ a line search. Given  $(x, t) \in \text{dom}(F) \times (0, +\infty)$ , let

$$\gamma_t(x) = \underset{\gamma \in [0,1] \text{ s.t. } x + \gamma(s_t(x) - x) \in \text{dom}(F)}{\text{argmin}} V_t(x + \gamma(s_t(x) - x)). \quad (4.1)$$

Thanks to the barrier structure of the potential function  $V_t$ , some useful consequences can be drawn from the definition of  $\gamma_t(x)$ . First,  $\gamma_t(x) \in \{\gamma \geq 0 \mid x + \gamma(s_t(x) - x) \in \text{dom}(F)\}$ . This implies  $x + \gamma_t(x)(s_t(x) - x) \in \mathcal{X} \cap \text{dom}(F) \cap \text{dom}(g)$ . Second, since  $\alpha_t(x)$  is also contained in the latter set, we have

$$V_t(x + \gamma_t(x)(s_t(x) - x)) \leq V_t(x + \alpha_t(x)(s_t(x) - x)) \quad \forall (x, t) \in \text{dom}(F) \times (0, +\infty).$$

Via a comparison principle, this allows us to deduce the analysis of the sequence produced by  $\text{LCG}(x^0, \varepsilon, t)$  from the analysis of the sequence induced by  $\text{CG}(x^0, \varepsilon, t)$ . Indeed, if  $\{\xi_t^k\}_{k \geq 0}$  is the sequence constructed by the line search procedure  $\text{LCG}(x^0, \eta, t)$ , then we have  $V_t(\xi_t^{k+1}) \leq V_t(\xi_t^k + \alpha_t(\xi_t^k)(s_t(\xi_t^k) - \xi_t^k))$  for all  $k$ . Hence, we can perform the complexity analysis on the majorising function as in the analysis of procedure  $\text{CG}(x^0, \varepsilon, t)$ . Consequently, all the complexity-related estimates for the method  $\text{CG}(x^0, \eta, t)$  apply verbatim to the sequence  $\{\xi_t^k\}_{k \geq 0}$  induced by the method  $\text{LCG}(x^0, \eta, t)$ .

### 4.2 Algorithm with inexact LMO

A key assumption in our approach so far is that we can obtain an exact answer from the LMO (3.2). In this section we consider the case when our search direction subproblem is solved only with some pre-defined accuracy, a setting that is of particular interest in optimization problems defined over matrix variables. As an illustration, let us consider instances of (P) where  $\mathcal{X}$  is the spectrahedron of symmetric matrices, namely  $\mathcal{X} = \{\mathbf{X} \in \mathbb{R}^{n \times n} \mid \mathbf{X} \geq 0, \text{tr}(\mathbf{X}) = 1\}$ . For these instances solving the subproblem (3.1) with  $g = \text{tr}(\mathbf{C}\mathbf{X})$  corresponds to computing the leading

eigenvector of a symmetric matrix, which when  $n$  is very large is typically computed inexactly using iterative methods. We therefore relax our definition of the LMO by allowing for an Inexact Linear Minimization Oracle (ILMO), featuring additive and multiplicative errors. To define our ILMO, let

$$\Gamma_t(x, s) := \frac{1}{t}F'(x)[x - s] + g(x) - g(s) \quad t > 0, (x, s) \in \mathbf{C} \times \mathbf{C}.$$

By definition of the point  $s_t(x)$  in (3.2) and of the gap function  $\text{Gap}_t(x)$ , we have  $\Gamma_t(x, s) \leq \text{Gap}_t(x)$  for all  $s \in \mathbf{C}$ .

**Definition 4.1.** Given  $t > 0, \delta \in (0, 1]$ , and  $\theta > 0$ , we call an oracle producing a point  $\tilde{s}_t(x) \in \mathbf{C}$  a  $(\delta, \theta)$ -ILMO, such that

$$\widetilde{\text{Gap}}_t(x) \geq \delta(\text{Gap}_t(x) - \theta), \text{ where } \widetilde{\text{Gap}}_t(x) \equiv \Gamma_t(x, \tilde{s}_t(x)). \quad (4.2)$$

We write  $\tilde{s}_t(x) \in \mathcal{L}_g^{(\delta, \theta)}(t^{-1}\nabla F(x))$  for any direction  $\tilde{s}_t(x)$  satisfying (4.2).

We note that a  $(0, 0)$ -ILMO returns a search point satisfying inclusion (3.2). We therefore refer to the case where we can design a  $(0, 0)$ -ILMO as the *exact oracle case*. Moreover, a  $(1, \theta)$ -ILMO is an oracle that only features additive errors. This relaxation for inexact computations has been considered in previous work, such as [10, 18, 25]. The combination of multiplicative error  $\delta$  and additive error  $\theta$  displayed in (4.2) is similar to the oracle constructed in [26]. The above definition can also be interpreted as follows. The answer  $s_t(x)$  of the exact LMO solves the maximization problem  $\max_{s \in \mathbf{X}} \{\Gamma_t(x, s) = t^{-1}F'(x)[x - s] + g(x) - g(s)\}$  and the optimal value in this problem is nonnegative. Thus, (4.2) can be interpreted as the requirement that the point  $\tilde{s}_t(x)$  solves the same problem up to the additive error  $\theta$  and the multiplicative error  $\delta$  (i.e. because it is itself the output of a convex optimisation routine). We emphasize that our analysis does not depend on the specific choice of the point  $\tilde{s}_t(x)$ .

Equipped with these concepts, we can derive an analytic step-size policy as in the exact regime. Let  $x \in \mathbf{C}$  be given,  $\tilde{s}_t(x) \in \mathcal{L}_g^{(\delta, \theta)}(t^{-1}\nabla F(x))$ , and  $\alpha \in (0, 1)$  small enough so that  $\alpha\|\tilde{s}_t(x) - x\|_x \equiv \alpha\tilde{e}_t(x) \in (0, 1)$ . Just like in (3.7), we can then obtain the upper bound

$$V_t(x + \alpha(\tilde{s}_t(x) - x)) \leq V_t(x) - \alpha\widetilde{\text{Gap}}_t(x) + \frac{1}{t}\omega_*(\alpha\tilde{e}_t(x)).$$

Optimizing the upper bound with respect to  $\alpha$  gives us the analytic step-size criterion

$$\tilde{\alpha}_t(x) := \min \left\{ 1, \frac{t\widetilde{\text{Gap}}_t(x)}{\tilde{e}_t(x)(\tilde{e}_t(x) + t\widetilde{\text{Gap}}_t(x))} \right\}. \quad (4.3)$$

The  $(\delta, \theta)$ -ILMO, and the step size policy (4.3) are enough to define a CndG-update with inexact computations that are executed by a function  $P(x, t, \delta, \theta)$ , defined in Algorithm 4.

---

**Algorithm 4** Function  $P(x, t, \delta, \theta)$

---

Obtain  $\tilde{s}_t(x) \in \mathcal{L}_g^{(\delta, \theta)}(t^{-1}\nabla F(x))$ ;  
Obtain  $\tilde{\alpha}_t(x)$  defined in (4.3);  
Update  $x \leftarrow x + \tilde{\alpha}_t(x)(\tilde{s}_t(x) - x)$ .

---

To use this method within a bona fide algorithm, we would need to introduce some stopping criterion. Ideally, such a stopping criterion should aim at making the merit functions  $\text{Gap}_t$  or  $\Delta_t$

---

**Algorithm 5**  $\text{ICG}(x, t, \eta, \delta, \theta)$ 

---

**Input:**  $x \in \mathbf{C}, \delta \in (0, 1], \theta > 0, t > 0, \eta > 0$ .  
**for**  $k = 0, 1, \dots$  **do**  
  **if**  $\widetilde{\text{Gap}}_t(x^k) > \eta\delta$  **then**  
     $x^{k+1} = P(x^k, t, \delta, \theta)$   
  **else**  
    STOP. Return iteration index  $k$  and last iterate  $x^k$ .  
  **end if**  
**end for**

---

small. However, our inexact oracle does not allow us to make direct inferences on the values of these merit functions. Hence, we need to come up with a stopping rule that uses only quantities that are observable and that are coupled with these merit functions. The natural optimality measure for the inexact oracle case is thus  $\widetilde{\text{Gap}}_t(x)$ . Indeed, by the very definition of our inexact oracle, if, for accuracy  $\eta > 0$ , we have arrived at an iterate  $x$  for which  $\widetilde{\text{Gap}}_t(x) \leq \delta\eta$ , we know from (4.2) that  $\text{Gap}_t(x) \leq \eta + \theta$ . Therefore, by making  $\theta$  a function of  $\eta$ , we would attain essentially the same accuracy as the exact implementation requires when running Algorithm 1. This is the main idea leading to the development of Algorithm 5.

There are two types of iteration complexity guarantees that we can derive for  $\text{ICG}(x, t, \eta, \delta, \theta)$ . One is concerned with upper bounding the number of iterations after which our stopping criterion will be satisfied. The other is an upper bound on the number of iterations needed to make the potential function gap  $\Delta_t(x^k)$  smaller than  $\eta + \theta$ . The derivation of these estimates is rather technical and follows closely the complexity analysis of the exact regime. We therefore only present the statements here and invite the reader to consult the Appendix A for a detailed proof.

**Proposition 4.2.** *Assume that  $\eta, \theta, t > 0, \delta \in (0, 1]$ , and  $x^0 \in \mathbf{C}$ . Algorithm  $\text{ICG}(x^0, t, \eta, \delta, \theta)$  requires at most*

$$\begin{aligned} \tilde{R}_t(x^0, \eta, \delta, \theta) := & \left\lceil \frac{5.3(t\delta(\Delta_t(x^0) - \theta) + \nu + t\Omega_g)}{\delta} \log \left( \min \left\{ \frac{10.6t\Delta_t(x^0)}{(1 - 10.6t\theta)_+}, \frac{\Delta_t(x^0)}{\eta} \right\} \right) \right\rceil \\ & + \left\lceil \frac{12(\nu + t\Omega_g)^2}{t\delta^2\eta} \left( 2 + \frac{\theta}{\eta} \right) \right\rceil + 1 \end{aligned} \quad (4.4)$$

iterations in order to reach a point  $x^k$  satisfying  $\widetilde{\text{Gap}}_t(x^k) \leq \eta\delta$  for the first time.

**Proposition 4.3.** *Assume that  $\eta, \theta, t > 0, \delta \in (0, 1]$ , and  $x^0 \in \mathbf{C}$ . Algorithm  $\text{ICG}(x^0, t, \eta, \delta, \theta)$  requires at most*

$$\begin{aligned} \tilde{N}(x^0, \eta, \delta, \theta) := & \left\lceil \frac{5.3(t\delta(\Delta_t(x^0) - \theta) + \nu + t\Omega_g)}{\delta} \log \left( \min \left\{ \frac{10.6t\Delta_t(x^0)}{(1 - 10.6t\theta)_+}, \frac{\Delta_t(x^0)}{\eta} \right\} \right) \right\rceil \\ & + \left\lceil \frac{12(\nu + t\Omega_g)^2}{t\delta^2} \left( \frac{1}{\eta} - \frac{1}{\Delta_t(x^0) - \theta} \right)_+ \right\rceil + 1 \end{aligned} \quad (4.5)$$

iterations, in order to reach a point  $x^k$  satisfying  $\Delta_t(x^k) \leq \eta + \theta$  for the first time.

**Updating the Homotopy Parameter in the Inexact Case** We are now in a position to describe the outer loop of our algorithm with ILMO. The construction is very similar to Algorithm 2. As

---

**Algorithm 6** Inexact Homotopy( $x^0, \varepsilon, f, \delta$ )

---

**Input:**  $x^0 \in \mathbf{C}$ ,  $f \in \mathcal{B}_\nu(\mathbf{K})$ ,  $\delta \in (0, 1]$ .

**Parameters:**  $\varepsilon, t_0, \theta_0 = \eta_0 > 0, \sigma \in (0, 1)$ .

**Initialisation:**  $x_{t_0}^0 = x^0, I = \lceil \frac{\log(3\eta_0/\varepsilon)}{\log(1/\sigma)} \rceil$ .

**for**  $i = 0, 1, \dots, I - 1$  **do**

    Set  $\hat{x}_i$  the output of ICG( $x_{t_i}^0, t_i, \eta_i, \delta, \theta_i$ ).

    Update  $t_{i+1} = t_i/\sigma, \eta_{i+1} = \sigma\eta_i, \theta_{i+1} = \sigma\theta_{i+1}, x_{t_{i+1}}^0 = \hat{x}_i$ .

**end for**

$\hat{z} = \hat{x}_I$  the output of ICG( $x_{t_I}^0, t_I, \eta_I, \delta, \theta_I$ ).

---

before, our aim is to reach an  $\varepsilon$ -solution (Definition 2.1). Let  $\{t_i\}_{i \geq 0}, \{\eta_i\}_{i \geq 0}, \{\theta_i\}_{i \geq 0}$  be sequences of homotopy parameters, accuracies in the inner loop, and ILMO inexactnesses. For each run  $i$ , we activate procedure ICG( $x_{t_i}^0, t_i, \eta_i, \delta, \theta_i$ ) with the given configuration  $(t_i, \eta_i, \theta_i)$ . For  $i = 0$ , we assume to have an admissible initial point  $x_{t_0}^0 = x^0$  available. For  $i \geq 1$ , we restart Algorithm 5 using a kind of warm-start strategy by choosing  $x_{t_i}^0 = x_{t_{i-1}}^{R_{i-1}}$ , where  $\tilde{R}_{i-1} \leq \tilde{R}_{t_{i-1}}(x_{t_{i-1}}^0, \eta_{i-1}, \delta, \theta_{i-1})$  is the first iterate  $k$  of Algorithm ICG( $x_{t_{i-1}}^0, t_{i-1}, \eta_{i-1}, \delta, \theta_{i-1}$ ) satisfying  $\widetilde{\text{Gap}}_{t_{i-1}}(x_{t_{i-1}}^k) \leq \eta_{i-1}\delta$ . Note  $\tilde{R}_{i-1}$  is upper bounded by the mentioned number, by means of Proposition 4.2. After the  $i$ -th restart, let us call the obtained iterate  $\hat{x}_i := x_{t_i}^{\tilde{R}_i}$ . In this way we generate a sequence  $\{\hat{x}_i\}_{i \geq 0}$ , consisting of candidates for approximately following the central path, as they are  $(\eta_i + \theta_i)$ -close in terms of  $\text{Gap}_{t_i}$  (and, hence, in terms of the potential function gap  $\Delta_{t_i}$ ). We update the parameters  $(t_i, \eta_i, \theta_i)$  as follows:

- The sequence of homotopy parameters is determined as  $t_i = t_0\sigma^{-i}$  for  $\sigma \in (0, 1)$  until the last round of Inexact Homotopy( $x^0, \varepsilon, f, \delta$ ) is reached.
- The sequences of accuracies in the inner loop and ILMO inexactnesses requested in procedure ICG( $x_{t_i}^0, t_i, \eta_i, \delta, \theta_i$ ) is updated by  $\eta_i = \eta_0\sigma^i, \theta_i = \theta_0\sigma^i$ .
- The Algorithm stops after  $I \equiv I(\sigma, \eta_0, \varepsilon) = \lceil \frac{\log(3\eta_0/\varepsilon)}{\log(1/\sigma)} \rceil$  updates of the accuracy and homotopy parameters, and yields an  $\varepsilon$ -approximate solution of problem (P).

We underline that it is not necessary to stop the algorithm after a prescribed number of iterations and it is essentially an any-time convergent algorithm.

Our updating strategy for the parameters ensures that  $t_i\eta_i = t_i\theta_i = t_0\eta_0 = t_0\theta_0$ . We will make the judicious choice  $\eta_0 t_0 = 2\nu$  to obtain an overall assessment of the iteration complexity of method Inexact Homotopy( $x^0, \varepsilon, f, \delta$ ). The proof is given in Appendix A.

**Theorem 4.4.** Choose  $t_0 = \frac{\nu}{\Omega_g}$  and  $\theta_0 = \eta_0 = 2\Omega_g$ . The total iteration complexity, i.e. the number of CndG steps, of method Inexact Homotopy( $x^0, \varepsilon, f, \delta$ ) to find an  $\varepsilon$ -solution of (P) is  $\text{CompI}(x^0, \varepsilon, f, \delta) = O\left(\frac{\nu\Omega_g^2}{\delta^2\varepsilon^2(1-\sigma^2)}\right)$ .

## 5 Complexity Analysis

In this section, we give a detailed presentation of the analysis of the iteration complexity of Algorithm 2.

## 5.1 Analysis of procedure $\text{CG}(x^0, \varepsilon, t)$

Recall  $\Omega_g := \max_{x, y \in \text{dom}(g) \cap \mathcal{X}} |g(x) - g(y)|$  and  $\mathbf{C} = \text{dom}(F) \cap \mathcal{X} \cap \text{dom}(g)$ . The following estimate can be established as in [43, Prop. 3]. We therefore omit its simple proof.

**Lemma 5.1.** *For all  $(x, t) \in \mathbf{C} \times (0, \infty)$ , we have*

$$t^{-1} \mathbf{e}_t(x) \leq \nu/t + \text{Gap}_t(x) + \Omega_g. \quad (5.1)$$

Observe that

$$\begin{aligned} \mathbf{e}_t(x) &= \|s_t(x) - x\|_x = \sqrt{F''(x)[s_t(x) - x, s_t(x) - x]} \\ &\geq \nu^{-1/2} |F'(x)[s_t(x) - x]| \\ &= \frac{t}{\sqrt{\nu}} |\text{Gap}_t(x) - g(x) + g(s_t(x))| \\ &\geq \frac{t}{\sqrt{\nu}} (\text{Gap}_t(x) - \Omega_g). \end{aligned} \quad (5.2)$$

### 5.1.1 Proof of Proposition 3.2

The proof mainly follows the steps of the proof of Theorem 1 in [43]. The main technical challenge in our analysis is taking care of the penalty parameter  $t$ . A main step in the complexity analysis is the identification of two convergence regimes, depending on the magnitude of the merit function  $\text{Gap}_t$ .

**Lemma 5.2.** *Define  $\mathbf{a}_t := \frac{\nu}{t} + \Omega_g$ , and the partition*

$$\mathbb{K}_I(t) = \{k \in \mathbb{N} \mid \text{Gap}_t(x_t^k) > \mathbf{a}_t\}, \quad \mathbb{K}_{II}(t) = \mathbb{N} \setminus \mathbb{K}_I(t).$$

*If  $k \in \mathbb{K}_I(t)$  we have*

$$\Delta_t(x_t^k) - \Delta_t(x_t^{k+1}) \geq \frac{1}{5.3} \frac{G_t^k}{\nu + tG_t^k + t\Omega_g} \geq \frac{\Delta_t(x_t^k)}{5.3(\nu + t\Omega_g + t\Delta_t(x_t^k))}, \quad (5.3)$$

*and if  $k \in \mathbb{K}_{II}(t)$  we have*

$$\frac{1}{\Delta_t(x_t^{k+1})} \geq \frac{1}{\Delta_t(x_t^k)} + \frac{t}{12(\nu + t\Omega_g)^2} \quad (5.4)$$

*In particular,  $\{\Delta_t(x_t^k)\}_{k \in \mathbb{N}}$  is monotonically decreasing.*

Before proving this Lemma, let us explain how we use it to estimate the total number of iterations needed by method  $\text{CG}(x^0, \varepsilon, t)$  until the stopping criterion is satisfied. Motivated by the two different regimes identified in Lemma 5.2, we can bound the number of iterations produced by  $\text{CG}(x_t^0, \eta, t)$  before the stopping criterion  $\Delta_t(x_t^k) \leq \eta$  applies in two steps: First, we bound the number of iterations which the algorithm spends in the set  $\mathbb{K}_I(t)$ ; Second we bound the number of iterations the algorithm spends in  $\mathbb{K}_{II}(t)$ . Combining these two upper bounds, yields the total iteration bound reported in Proposition 3.2.

*Proof of Lemma 5.2.* Assume that iteration  $k$  is in phase  $\mathbb{K}_I(t)$ . To reduce notational clutter, we set  $\mathbf{e}_t^k \equiv \mathbf{e}_t(x_t^k)$  and  $G_t^k \equiv \text{Gap}_t(x_t^k)$ . Combining the condition  $G_t^k > \frac{\nu}{t} + \Omega_g$  of phase  $\mathbb{K}_I(t)$  with (5.2), we deduce that  $\mathbf{e}_t^k \geq \sqrt{\nu} \geq 1$ . This in turn implies  $\frac{tG_t^k}{\mathbf{e}_t^k(\mathbf{e}_t^k + tG_t^k)} < \frac{tG_t^k}{\mathbf{e}_t^k + tG_t^k} < 1$ . Hence, at this iteration, algorithm  $\text{CG}(x^0, \varepsilon, t)$  chooses the step sizes  $\alpha_k = \frac{tG_t^k}{\mathbf{e}_t^k(\mathbf{e}_t^k + tG_t^k)}$ . The per-iteration reduction of the potential function can be estimated as

$$\begin{aligned} V_t(x_t^{k+1}) &\leq V_t(x_t^k) - \frac{G_t^k}{\mathbf{e}_t^k} \frac{tG_t^k}{\mathbf{e}_t^k + tG_t^k} + \frac{1}{t} \omega_* \left( \frac{tG_t^k}{\mathbf{e}_t^k + tG_t^k} \right) \\ &= V_t(x_t^k) - \frac{G_t^k}{\mathbf{e}_t^k} + \frac{1}{t} \log \left( 1 + \frac{tG_t^k}{\mathbf{e}_t^k} \right) \\ &= V_t(x_t^k) - \frac{1}{t} \omega \left( \frac{tG_t^k}{\mathbf{e}_t^k} \right) \end{aligned} \quad (5.5)$$

where  $\omega(\tau) = \tau - \log(1 + \tau)$  and  $\omega_*(t) = -\tau - \log(1 - \tau)$ . This readily yields  $\Delta_t(x_t^k) - \Delta_t(x_t^{k+1}) \geq \frac{1}{t} \omega \left( \frac{tG_t^k}{\mathbf{e}_t^k} \right)$  and implies that  $\{\Delta_t(x_t^k)\}_{k \in \mathbb{K}_I(t)}$  is monotonically decreasing. For  $k \in \mathbb{K}_I(t)$ , we also see  $\frac{tG_t^k}{\nu + tG_t^k + t\Omega_g} > \frac{1}{2}$ . Together with (5.1), this implies

$$\frac{tG_t^k}{\mathbf{e}_t^k} \geq \frac{G_t^k}{\nu/t + G_t^k + \Omega_g} = \frac{tG_t^k}{\nu + tG_t^k + t\Omega_g} > \frac{1}{2}. \quad (5.6)$$

Using (3.5), the monotonicity of  $\omega(\cdot)$  and that  $\omega(\tau) \geq \frac{\tau}{5.3}$  for  $\tau \geq 1/2$  (see [43, Prop. 1]), the fact that the function  $x \mapsto \frac{x}{a+tx}$  is strictly increasing for  $t, a > 0$ , we arrive at

$$\Delta_t(x_t^k) - \Delta_t(x_t^{k+1}) \geq \frac{1}{5.3} \frac{G_t^k}{\nu + tG_t^k + t\Omega_g} \geq \frac{\Delta_t(x_t^k)}{5.3(\nu + t\Omega_g + t\Delta_t(x_t^k))}. \quad (5.7)$$

Next, consider an integer  $k \in \mathbb{K}_{II}(t)$ . We have to distinguish the iterates using large steps ( $\alpha_k = 1$ ), from those using short steps ( $\alpha_k < 1$ ). Let us first consider the case where  $\alpha_k = 1$ . Then,  $tG_t^k \geq \mathbf{e}_t^k(tG_t^k + \mathbf{e}_t^k)$ , which implies  $\mathbf{e}_t^k \in (0, 1)$ , and  $G_t^k \geq \frac{(\mathbf{e}_t^k)^2}{t(1-\mathbf{e}_t^k)}$ . Moreover, using (2.7), we readily obtain

$$\begin{aligned} V_t(x_t^{k+1}) &\leq V_t(x_t^k) - G_t^k + \frac{1}{t} \omega_*(\mathbf{e}_t^k) \\ &\leq V_t(x_t^k) - G_t^k + \frac{1}{t} \frac{(\mathbf{e}_t^k)^2}{2(1-\mathbf{e}_t^k)} \\ &\leq V_t(x_t^k) - \frac{G_t^k}{2}. \end{aligned}$$

Therefore,

$$\Delta_t(x_t^k) - \Delta_t(x_t^{k+1}) \geq \frac{G_t^k}{2} \geq \frac{1}{2} \frac{(G_t^k)^2}{\nu/t + \Omega_g} = \frac{1}{2} \frac{t(G_t^k)^2}{\nu + t\Omega_g} \geq \frac{1}{12} \frac{t(G_t^k)^2}{(\nu + t\Omega_g)^2}.$$

In the regime where  $\alpha_k < 1$ , we obtain the estimate  $\Delta_t(x_t^k) - \Delta_t(x_t^{k+1}) \geq \frac{1}{12} \frac{t(G_t^k)^2}{(\nu + t\Omega_g)^2}$ , by following the same reasoning as in [43]. Using the relation  $G_t^k \geq \Delta_t(x_t^k) \geq \Delta_t(x_t^{k+1})$ , we conclude

$$\frac{1}{\Delta_t(x_t^{k+1})} - \frac{1}{\Delta_t(x_t^k)} \geq \frac{t}{12(\nu + t\Omega_g)^2}.$$

■

We now exploit this monotonicity of the potential function gap in order to upper bound the number of iterations which Algorithm CG( $x_t^0, \eta, t$ ) spends in the disjoint phases  $\mathbb{K}_I(t)$  and  $\mathbb{K}_{II}(t)$ , respectively.

*Proof of Proposition 3.2.* Given the pair  $(t, \eta) \in (0, \infty)^2$ , denote by  $N \equiv N(x_t^0, \eta, t)$  the upper bound defined in (3.10). We separate  $N$  into two parts, corresponding with stages  $\mathbb{K}_I(t)$  and  $\mathbb{K}_{II}(t)$ , as they are defined in the proof of Lemma 5.2. We will show that  $N = K_t(x_t^0) + M$  where  $K_t(x_t^0)$  is a bound on the number of iterates within  $\mathbb{K}_I(t)$  and  $M$  is bound on the number of iterates within  $\mathbb{K}_{II}(t)$  until  $\Delta_t(x_t^k) \leq \eta$  is reached.

Note that Lemma 5.2 ensures that for all  $k \in \mathbb{N} = \mathbb{K}_I(t) \cup \mathbb{K}_{II}(t)$ , it holds that  $\Delta_t(x_t^{k+1}) \leq \Delta_t(x_t^k)$ , i.e. the sequence  $\Delta_t(x_t^k)$  is monotonically decreasing.

We begin by deriving an expression for  $K_t(x_t^0)$ , the number of iterations which CG( $x_t^0, \eta, t$ ) spends in  $\mathbb{K}_I(t)$ . To that end, let  $\{k_i\}_{i \in \mathbb{N}}$  denote the increasing set of indices enumerating the elements of the set  $\mathbb{K}_I(t)$ . From (5.7) and  $\Delta_t(x_t^{k_{i+1}}) \leq \Delta_t(x_t^{k_i+1}) \leq \Delta_t(x_t^{k_i}) \leq \Delta_t(x_t^0)$ , we conclude

$$\Delta_t(x_t^{k_i}) \left[ 1 - \frac{1}{5.3(\nu + t\Omega_g + t\Delta_t(x_t^0))} \right] \geq \Delta_t(x_t^{k_{i+1}}) \geq \Delta_t(x_t^{k_{i+1}}). \quad (5.8)$$

Setting  $q_t := \frac{1}{5.3(\nu + t\Omega_g + t\Delta_t(x_t^0))} \in (0, 1)$  (since  $\nu \geq 1$ ), we arrive at the recursion

$$\Delta_t(x_t^{k_i}) \leq (1 - q_t)^i \Delta_t(x_t^0) \leq \exp(-q_t i) \Delta_t(x_t^0).$$

Furthermore, by definition, all  $k_i \in \mathbb{K}_I(t)$  satisfy  $G_t^{k_i} \geq a_t = \frac{\nu}{t} + \Omega_g$ , so that (5.6) yields

$$\Delta_t(x_t^{k_i}) \geq \Delta_t(x_t^{k_i}) - \Delta_t(x_t^{k_{i+1}}) \geq \frac{G_t^{k_i}}{5.3(\nu + tG_t^{k_i} + t\Omega_g)} \geq \frac{1}{10.6t}.$$

Hence,  $\frac{1}{10.6t\Delta_t(x_t^0)} \leq \exp(-q_t |\mathbb{K}_I(t)|)$ , and

$$K_t(x_t^0) := \lceil 5.3(\nu + t\Delta_t(x_t^0) + t\Omega_g) \log(10.6t\Delta_t(x_t^0)) \rceil \quad (5.9)$$

yields the upper bound.

We proceed analogously with the analysis on the set  $\mathbb{K}_{II}(t)$ . Let  $\{\ell_j\}_{j \in \mathbb{N}_0}$  the increasing set of indices enumerating the elements of the set  $\mathbb{K}_{II}(t)$ , and  $M = N - K_t(x_t^0)$  the upper bound on iterations in this set. Using inequality (5.4) for  $k := \ell_j$  together with the monotonicity of  $\Delta_t(x_t^k)$  results in

$$\frac{1}{\Delta_t(x_t^{\ell_{j+1}})} \geq \frac{1}{\Delta_t(x_t^{\ell_{j+1}})} \geq \frac{1}{\Delta_t(x_t^{\ell_j})} + \frac{t}{12(\nu + t\Omega_g)^2}. \quad (5.10)$$

Telescoping the inequality (5.10) together with  $\Delta_t(x_t^{\ell_1}) \leq \Delta_t(x_t^0)$  we get

$$\frac{1}{\Delta_t(x_t^{\ell_M})} \geq \frac{1}{\Delta_t(x_t^{\ell_0})} + \frac{Mt}{12(\nu + t\Omega_g)^2} \geq \frac{1}{\Delta_t(x_t^0)} + \frac{Mt}{12(\nu + t\Omega_g)^2}.$$

Thus,  $\Delta_t(x_t^{\ell_M}) \leq \eta$ , is satisfied for  $M = \lceil 12(\nu + t\Omega_g)^2 (\frac{1}{\eta} - \frac{1}{t\Delta_t(x_t^0)})_+ \rceil$ . This demonstrates that at most  $N = K_t(x_t^0) + M$  iterations of CG( $x_t^0, \eta, t$ ) are sufficient for achieving  $\Delta_t(x_t^k) \leq \eta$ . ■

### 5.1.2 Proof of Proposition 3.1

Using the bound  $K_t(x_t^0)$  on the number of iterations in  $\mathbb{K}_I(t)$  from the proof of Proposition 3.2, we are left to bound the number of iteration in  $\mathbb{K}_{II}(t)$ , until the condition  $G_t^k \leq \eta$  is satisfied.

Let  $\{k_j(t)\}_j$  denote the increasing set of indices enumerating the elements of the set  $\mathbb{K}_{II}(t)$ . From (5.4) we know that

$$\Delta_t(x_t^{k_{j+1}(t)}) - \Delta_t(x_t^{k_j(t)}) \leq -\frac{1}{12} \frac{t(G_t^{k_j(t)})^2}{(v + t\Omega_g)^2}, \text{ and } G_t^{k_j(t)} \geq \Delta_t(x_t^{k_j(t)}) \geq \Delta_t(x_t^{k_{j-1}(t)}).$$

Set  $d_j \equiv \Delta_t(x_t^{k_j(t)})$  and  $\frac{1}{M} \equiv \frac{t}{12(v+t\Omega_g)^2}$ ,  $\Gamma_j \equiv G_t^{k_j(t)}$ . We thus obtain the recursion

$$d_{j+1} \leq d_j - \frac{\Gamma_j^2}{M}, \quad \Gamma_j \geq d_j,$$

and we can apply [43, Prop. 2.4] directly to the above recursion to obtain the estimates

$$d_j \leq \frac{M}{j}, \quad \text{and } \min\{\Gamma_0, \dots, \Gamma_j\} \leq \frac{2M}{j}.$$

Since the algorithm terminates when we obtain an iterate with  $\Gamma_j = \mathbf{Gap}_t(x_t^{k_j(t)}) \leq \eta$ , it is sufficient to stop at the label  $j$  is reached satisfying  $\frac{2M}{j} \leq \eta$ . Solving this for  $j$  yields

$$j \leq \left\lceil \frac{24(v + t\Omega_g)^2}{t\eta} \right\rceil. \tag{5.11}$$

Combining the bound (5.11) with  $K_t(x_t^0)$ , we obtain the total complexity estimate postulated in Proposition 3.1.

## 5.2 Analysis of the outer loop and proof of Theorem 3.3

Let  $I \equiv I(\eta_0, \sigma, \varepsilon) = \lceil \frac{\log(2\eta_0/\varepsilon)}{\log(1/\sigma)} \rceil$  denote the a-priori fixed number of updates of the accuracy and homotopy parameter. We set  $\hat{x}_i \equiv x_{t_i}^{R_i}$ , the last iterate of procedure  $\text{CG}(x_{t_i}^0, \eta_i, t_i)$  satisfying  $\Delta_{t_i}(\hat{x}_i) \leq \mathbf{Gap}_{t_i}(\hat{x}_i) \leq \eta_i$ . From this, using the definition of the gap function, we deduce that

$$g(\hat{x}_i) - g(z^*(t_i)) \leq \mathbf{Gap}_{t_i}(\hat{x}_i) + \frac{1}{t_i} F'(\hat{x}_i)[z^*(t_i) - \hat{x}_i] \leq \eta_i + \frac{\nu}{t_i}. \tag{5.12}$$

Hence, using Lemma 2.2, we observe

$$g(\hat{x}_i) - \text{Opt} = g(\hat{x}_i) - g(z^*(t_i)) + g(z^*(t_i)) - \text{Opt} \leq \eta_i + \frac{2\nu}{t_i}. \tag{5.13}$$

Since  $t_i = \frac{2\nu}{\eta_i}$ , we obtain  $g(\hat{x}_i) - \text{Opt} \leq 2\eta_i$ . We next estimate the initial gap  $\Delta_{t_{i+1}}(x_{t_{i+1}}^0) = \Delta_{t_{i+1}}(\hat{x}_i)$  incurred by our warm-start strategy. Observe that

$$\begin{aligned} V_{t_{i+1}}(x_{t_{i+1}}^0) - V_{t_{i+1}}(z^*(t_{i+1})) &= V_{t_i}(x_{t_{i+1}}^0) - V_{t_i}(z^*(t_{i+1})) \\ &\quad + \left(\frac{1}{t_{i+1}} - \frac{1}{t_i}\right)(F(x_{t_{i+1}}^0) - F(z^*(t_{i+1}))) \\ &\leq V_{t_i}(x_{t_i}^{R_i}) - V_{t_i}(z^*(t_i)) \\ &\quad + \left(1 - \frac{t_{i+1}}{t_i}\right)(V_{t_{i+1}}(x_{t_{i+1}}^0) - V_{t_{i+1}}(z^*(t_{i+1}))) \\ &\quad + \left(1 - \frac{t_{i+1}}{t_i}\right)(g(z^*(t_{i+1})) - g(x_{t_{i+1}}^0)), \end{aligned}$$

where the last transition follows from  $V_{t_i}(z^*(t_{i+1})) \geq V_{t_i}(z^*(t_i))$ . Moreover,

$$g(x_{t_{i+1}}^0) - g(z^*(t_{i+1})) \leq g(x_{t_{i+1}}^0) - \text{Opt} \leq \eta_i + \frac{2\nu}{t_i} = \frac{4\nu}{t_i}.$$

Since  $t_{i+1} > t_i$ , the above two inequalities imply

$$\frac{t_{i+1}}{t_i}[V_{t_{i+1}}(x_{t_{i+1}}^0) - V_{t_{i+1}}(z^*(t_{i+1}))] \leq V_{t_i}(x_{t_i}^{R_i}) - V_{t_i}(z^*(t_i)) + \frac{t_{i+1} - t_i}{t_i^2} 4\nu.$$

Whence,

$$t_{i+1}\Delta_{t_{i+1}}(x_{t_{i+1}}^0) \leq t_i\Delta_{t_i}(x_{t_i}^{R_i}) + \frac{t_{i+1} - t_i}{t_i} 4\nu \leq t_i\eta_i + \frac{t_{i+1} - t_i}{t_i} 4\nu = \left(2\frac{t_{i+1}}{t_i} - 1\right) 2\nu. \quad (5.14)$$

We are now in the position to estimate the total iteration complexity  $\text{Comp1}(x^0, \varepsilon, f) := \sum_{i=0}^I R_i \leq \sum_{i=0}^I R(x_{t_i}^0, \eta_i, t_i)$  by using Proposition 3.1, and thereby prove Theorem 3.3. We do so by using the updating regime of the sequences  $\{t_i\}$  and  $\{\eta_i\}$  explained in Section 3. These updating mechanisms imply

$$\begin{aligned} \sum_{i=1}^I R_i &\leq \sum_{i=1}^I 5.3 \left( \nu + 2\nu \left( \frac{2t_i}{t_{i-1}} - 1 \right) + t_i \Omega_g \right) \log \left( 10.6 \left( 2\nu \left( \frac{2t_i}{t_{i-1}} - 1 \right) \right) \right) \\ &\quad + \sum_{i=1}^I \frac{12}{\nu} (\nu + t_i \Omega_g)^2 \\ &\leq \log(21.2(\nu(2/\sigma - 1))) \sum_{i=1}^I 5.3(\nu(4/\sigma - 1) + t_i \Omega_g) + \sum_{i=1}^I \frac{24}{\nu} (\nu^2 + t_i^2 \Omega_g^2) \\ &\leq 24\nu \times I + 21.2\nu/\sigma \log(42.4\nu/\sigma) \times I + 5.3 \log(42.4\nu/\sigma) \Omega_g \sum_{i=1}^I t_i + \frac{24\Omega_g^2}{\nu} \sum_{i=1}^I t_i^2 \\ &\leq \frac{24\nu \log(2\eta_0/\varepsilon)}{\log(1/\sigma)} + \log\left(\frac{42.4\nu}{\sigma}\right) \frac{21.2\nu \log(2\eta_0/\varepsilon)}{\sigma \log(1/\sigma)} \\ &\quad + \log\left(\frac{42.4\nu}{\sigma}\right) \frac{21.2\nu\Omega_g}{\varepsilon(1-\sigma)} + \frac{384\Omega_g^2\nu}{\varepsilon^2(1-\sigma^2)}. \end{aligned}$$

In deriving these bounds, we have used the definition of  $I$  and the following estimates:

$$\sum_{i=1}^I t_i = t_0 \sigma^{-1} \sum_{i=0}^{I-1} (1/\sigma)^i \leq t_0 \frac{\sigma^{-I}}{1-\sigma} \leq \frac{4\nu}{\varepsilon(1-\sigma)},$$

and

$$\sum_{i=1}^I t_i^2 = t_0^2 \sum_{i=1}^I (1/\sigma)^{2i} = \frac{t_0^2}{\sigma^2} \sum_{i=0}^{I-1} (1/\sigma^2)^i \leq \frac{16\nu^2}{\varepsilon^2(1-\sigma^2)}.$$

It remains to bound the complexity at  $i = 0$ . We have

$$\begin{aligned} R_0 &\leq 5.3(\nu + t_0 \Delta_{t_0}(x_{t_0}^0) + t_0 \Omega_g) \log(10.6 t_0 \Delta_{t_0}(x^0)) + \frac{12}{\nu} (\nu + t_0 \Omega_g)^2 \\ &\leq 5.3(\nu + F(x^0) - F(z^*(t_0)) + 2t_0 \Omega_g) \log(10.6(F(x^0) - F(z^*(t_0)) + t_0 \Omega_g)) \\ &\quad + \frac{24}{\nu} (\nu^2 + t_0^2 \Omega_g^2). \end{aligned}$$

Since  $t_0 = \frac{\nu}{\Omega_g}$  and  $\eta_0 = 2\Omega_g$ , we have

$$R_0 \leq 5.3(3\nu + F(x^0) - F(z^*(t_0))) \log(10.6(\nu + F(x^0) - F(z^*(t_0)))) + 48\nu.$$

Adding the two gives the total complexity bound

$$\begin{aligned} \text{Comp}(x^0, \varepsilon, f) &\leq 5.3(3\nu + F(x^0) - F(z^*(t_0))) \log(10.6(\nu + F(x^0) - F(z^*(t_0)))) + 48\nu \\ &\quad + \frac{\nu \log(4\Omega_g/\varepsilon)}{\log(1/\sigma)} \left[ 24 + \log\left(\frac{42.4\nu}{\sigma}\right) \frac{21.2}{\sigma} \right] \\ &\quad + \log\left(\frac{42.4\nu}{\sigma}\right) \frac{21.2\nu\Omega_g}{\varepsilon(1-\sigma)} + \frac{384\Omega_g^2\nu}{\varepsilon^2(1-\sigma^2)}. \\ &= \tilde{O}\left(\frac{\Omega_g^2\nu}{\varepsilon^2(1-\sigma^2)}\right). \end{aligned}$$

## 6 Experimental results

In this section, we give two examples covered by the problem template (P), and report the results of numerical experiments that illustrate the practical performance and scalability of our method. We implement Algorithm 2 using procedure CG and LCG as solvers for the inner loops. We compare the results of our algorithm to two benchmarks: (1) an interior point solution of the problem by SDPT3 [35], and (2) the solution obtained by CGAL [41]. Our performance measure for these experiments is the *relative optimality gap*, which given the value of the objective of the solution computed for each method  $M$  and iteration  $i$ ,  $g_i^M$ , is computed by  $|g_i^M - g^{\text{SDPT3}}|/|g^{\text{SDPT3}}|$ , where  $g^{\text{SDPT3}}$  is the interior point solution. The full description of the setup for these experiments is available in Appendix B. A key takeaway from these numerical experiments is that CG and LCG are not influenced by the problem's scaling and are therefore well-suited to solving ill-posed problems with differently scaled constraints.

## 6.1 Estimating the mixing time of a Markov chain

Consider a continuous-time Markov chain on a weighted graph, with edge weights representing the transition rates of the process. Let  $\mathbf{P}(t) = e^{-Lt}$  be the stochastic semi-group of the process, where  $L$  is the graph Laplacian. From  $L\mathbf{1} = 0$  it follows that  $\frac{1}{n}\mathbf{1}$  is a stationary distribution of the process. From [9] we have the following bound on the total variation distance of the time  $t$  distribution of the Markov process and the stationary distribution  $\sup_{\pi} \|\pi\mathbf{P}(t) - \frac{1}{n}\mathbf{1}\|_{\text{TV}} \leq \frac{1}{2} \sqrt{n} e^{-\lambda t}$ . The quantity  $T_{\text{mix}} = \lambda$  is called the *mixing time*. The constant  $\lambda$  is the second-largest eigenvalue of the graph Laplacian  $L$ . To bound this eigenvalue, we follow the SDP-strategy laid out in [33], and in some detail described in Appendix B.

In the experiments, we generated random connected undirected graphs with 100 – 800 nodes and  $10^3 - 10^4$  edges, and for each edge  $\{i, j\}$  in the graph, we generated a random weight uniformly in  $[0, 1]$ . Figure 1 illustrates the relative optimality gap for the generated results by each method (and the dependence of CG and LCG on the starting accuracy  $\eta_0$ ), CGAL only appears in the right most graphs<sup>2</sup>. We conclude that, despite LCG being generally costly per iteration, it exhibits the best computational performance both in the number of iterations and in time. Moreover, for all of the datasets, the primal-dual method CGAL generated solutions that were far from being feasible, and was not able to reduce the feasibility gap even after 1000 seconds or 10000 iterations, resulting in very poor relative optimality gap. Our conjecture is that the slow convergence rate of CGAL with respect to feasibility is due to the different scaling for the right-hand-side of the constraints, which results in a relative feasibility gap which is very large for constraints with small right-hand-side. To test this conjecture, in the next section we present further experiments testing the performance of the methods as a function of the right-hand-side scaling.<sup>3</sup>

## 6.2 Randomly Scaled SDP

In order to further investigate the robustness of CG, LCG and CGAL to constraint scaling, we’ve created a synthetic data set for a general SDP with inequality constraints. The Synthetic Random Scaling (SRS) problem is formulated as follows:

$$\max\langle \mathbf{C}, \mathbf{X} \rangle \text{ s.t.: } \langle \mathbf{A}_i, \mathbf{X} \rangle \leq b_i, i \in \{1, 2, \dots, m\}, \mathbf{X} \in \mathbb{S}_+^n, \text{tr}(\mathbf{X}) \leq 1, \quad (\text{SRS})$$

where both the objective function coefficient matrix  $\mathbf{C}$  and, the constraint coefficient matrices  $\mathbf{A}_i$ , for  $i = 1, \dots, m$ , are randomly generated PSD matrices with unit Frobenius norm. The coefficients  $b_i$  are defined as  $b_i = \frac{u_i}{i^{p/2}} \langle \mathbf{A}_i, \mathbf{X}_0 \rangle$ , where  $u_i \in [\frac{1}{2}, 1]$  is a uniformly distributed random number,  $p \in \{0, 1, 2\}$ , and  $\mathbf{X}_0$  is a randomly generated PSD matrix with unit trace. Thus, parameter  $p$  controls the scaling of the right-hand-side of the constraints. Specifically, when  $p = 0$  we expect all  $b_i$  to have the same order of magnitude, while for  $p = 2$  constraint  $b_m = O(1/m)b_1$ . As we observed for the Mixing problem in Section B.2, our expectation is for CG and LCG to be impervious to this right-hand-side scaling, and for the performance of CGAL to deteriorate as  $p$  increases. To compare our method with CGAL, the CGAL output was adjusted to obtain a feasible solution. The details of this procedure are provided in Appendix B.3.

For the numerical experiments, we have chosen parameters  $n = 100$  and  $m = 100$ . Figures 2 and 3 show the performance of our methods in terms of the relative optimality gap for problem (SRS), where the “optimal” solution is computed using the SDPT3 solver, as described in Appendix B.3. Since the dataset consists of homogeneous data points, the plots present aggregated results over 30 instances for each value of  $p$ . Figure 2 illustrates the performance of each algorithm in terms

<sup>2</sup>More detailed results are available in Appendix B.

<sup>3</sup>We thank an anonymous referee for suggesting this experiment.

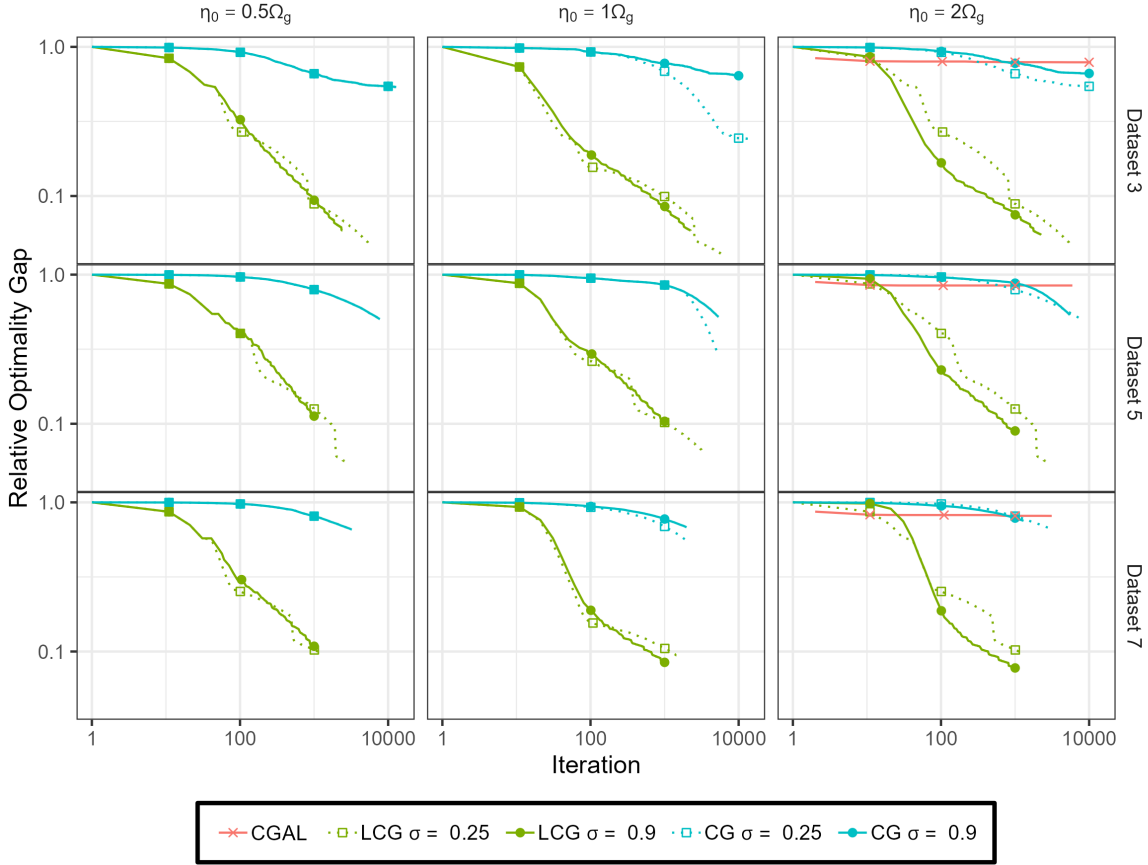


Figure 1: Mixing time problem: relative gap from SDPT3 solution vs. iteration.

of relative optimality gap over iteration count, while Figure 3 presents the performance in terms of runtime, within a time limit of 1000 seconds. The plots indicate that, while in the initial stages of running CG and LCG with a smaller value of  $\sigma$  ( $\sigma = 0.25$ ) are superior, larger values ( $\sigma = 0.9$ ) achieve slightly better overall results. Furthermore, the line search-based method LCG consistently achieves better iteration and time complexity performances than CG.

Importantly, the plots confirm the conjecture that the performance of CGAL deteriorates as  $p$  increases, our methods show consistent performance across different  $p$  values. In fact, CGAL has inferior performance for ill-scaled problems ( $p = 2$ ) compared to CG and LCG, leading to an average optimality gap of up to two orders of magnitude larger. Although Figure 2 shows that CGAL has iteration complexity comparable to or worse than CG and LCG across all values of  $p$ , its low-cost iterations can make it competitive in terms of time complexity, as shown in Figure 3. Specifically, CGAL is able to perform more iterations leading to superior time complexity when  $p = 0$ . However, when  $p = 1$  and especially  $p = 2$ , CGAL's iterations, while still inexpensive, fail to decrease the solution infeasibility, leading to limited improvement. A detailed analysis of the numerical experiments is provided in Appendix B.3.

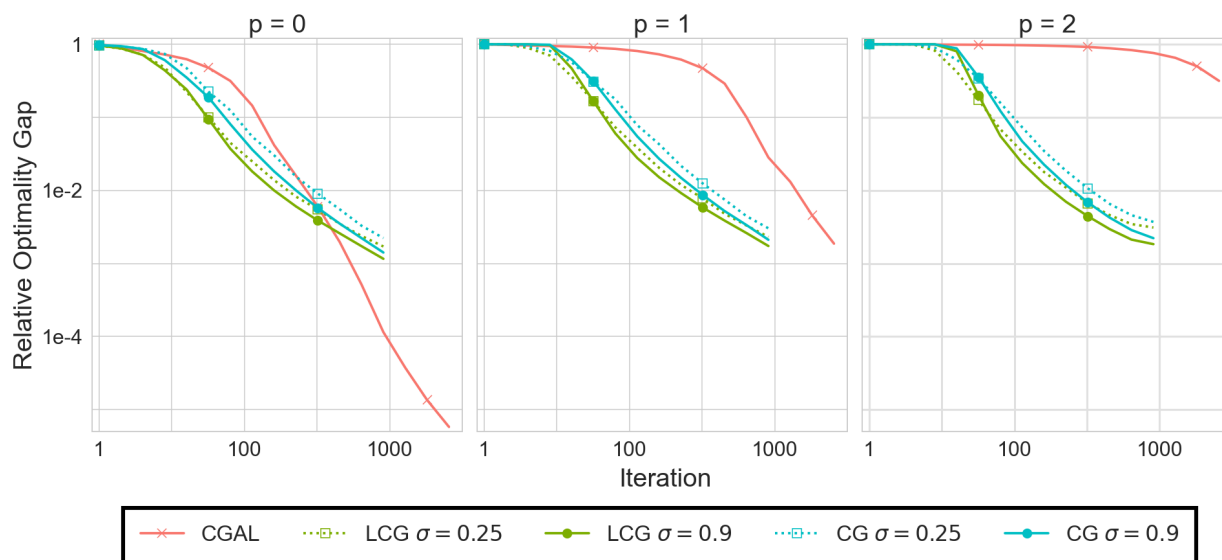


Figure 2: Randomly scaled SDP problem: relative optimality gap vs. iterations for several parameter choices (averaged over 30 instances for each  $p$ )

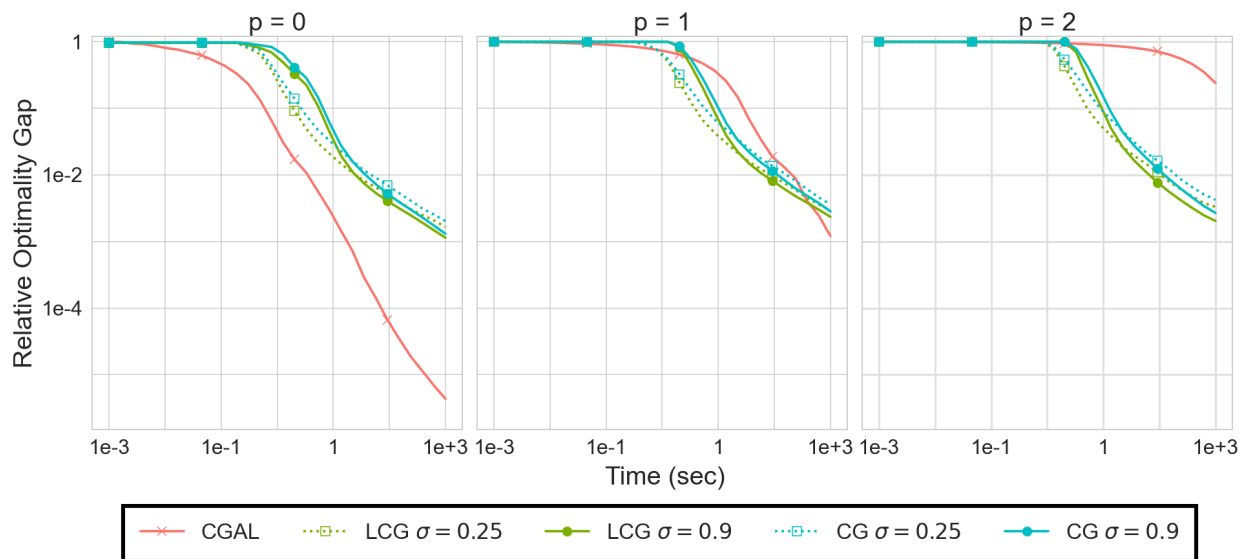


Figure 3: Randomly scaled SDP problem: relative optimality gap vs. time for several parameter choices (averaged over 30 instances for each  $p$ )

## 7 Conclusions

Solving large scale conic-constrained convex programming problems is still a challenge in mathematical optimization and machine learning. In particular, SDPs with a massive amount of linear constraints appear naturally as convex relaxations of combinatorial optimization problems. For such problems, the development of scalable algorithms is a very active field of research [14, 41].

In this paper, we introduce a new path-following/homotopy strategy to solve such massive conic-constrained problems, building on recent advances in projection-free methods for self-concordant minimization [11, 13, 43]. Our theoretical analysis and numerical experiments scheme show that the method is competitive with state-of-the-art solvers in terms of its iteration complexity and gives promising results in practice. Future work will focus on improvements of our deployed CndG solver to accelerate the subroutines.

## References

- [1] Y. Ye, *GSet random graphs*, <https://www.cise.u.edu/research/sparse/matrices/Gset/> (accessed May, 2022).
- [2] S. Arora, E. Hazan, and S. Kale. Fast algorithms for approximate semidefinite programming using the multiplicative weights update method. In *46th Annual IEEE Symposium on Foundations of Computer Science (FOCS'05)*, pages 339–348, 2005. doi: 10.1109/SFCS.2005.35.
- [3] Afonso S. Bandeira, Nicolas Boumal, and Vladislav Voroninski. On the low-rank approach for semidefinite programs arising in synchronization and community detection. In Vitaly Feldman, Alexander Rakhlin, and Ohad Shamir, editors, *29th Annual Conference on Learning Theory*, volume 49 of *Proceedings of Machine Learning Research*, pages 361–382, Columbia University, New York, New York, USA, 23–26 Jun 2016. PMLR. URL <https://proceedings.mlr.press/v49/bandeira16.html>.
- [4] Stephen Boyd and Lieven Vandenberghe. *Convex optimization*. Cambridge university press, 2004. ISBN 1107394007.
- [5] Venkat Chandrasekaran and Parikshit Shah. Relative entropy optimization and its applications. *Mathematical Programming*, 161:1–32, 2017.
- [6] M. Charikar and A. Wirth. Maximizing quadratic programs: extending grothendieck’s inequality. In *45th Annual IEEE Symposium on Foundations of Computer Science*, pages 54–60, 2004. doi: 10.1109/FOCS.2004.39.
- [7] Inc. CVX Research. CVX: Matlab software for disciplined convex programming, version 2.0. <http://cvxr.com/cvx>, August 2012.
- [8] Alexandre d’Aspremont, Francis Bach, and Laurent El Ghaoui. Optimal solutions for sparse principal component analysis. *Journal of Machine Learning Research*, 9(7), 2008.
- [9] Persi Diaconis and Daniel W. Stroock. Geometric bounds for eigenvalues of Markov chains. *Annals of Applied Probability*, 1:36–61, 1991.
- [10] J. C Dunn and S Harshbarger. Conditional gradient algorithms with open loop step size rules. *Journal of Mathematical Analysis and Applications*, 62(2):432–444, 1978. doi: [https://doi.org/10.1016/0022-247X\(78\)90137-3](https://doi.org/10.1016/0022-247X(78)90137-3). URL <https://www.sciencedirect.com/science/article/pii/0022247X78901373>.
- [11] Pavel Dvurechensky, Petr Ostroukhov, Kamil Safin, Shimrit Shtern, and Mathias Staudigl. Self-concordant analysis of Frank-Wolfe algorithms. In Hal Daume III and Aarti Singh, editors, *Proceedings of the 37th International Conference on Machine Learning*, volume 119 of *Proceedings of Machine Learning Research*, pages 2814–2824, Virtual, 13–18 Jul 2020. PMLR. URL <http://proceedings.mlr.press/v119/dvurechensky20a.html>. arXiv:2002.04320.
- [12] Pavel Dvurechensky, Shimrit Shtern, and Mathias Staudigl. First-order methods for convex optimization. *EURO Journal on Computational Optimization*, 9:100015, 2021. ISSN 2192-4406. doi: <https://doi.org/10.1016/j.ejco.2021.100015>. URL <https://www.sciencedirect.com/science/article/pii/S2192440621001428>. arXiv:2101.00935.
- [13] Pavel Dvurechensky, Kamil Safin, Shimrit Shtern, and Mathias Staudigl. Generalized self-concordant analysis of frank-wolfe algorithms. *Mathematical Programming*, 2022. doi: 10.1007/s10107-022-01771-1. URL <https://doi.org/10.1007/s10107-022-01771-1>.
- [14] Khaled Elbassioni, Kazuhisa Makino, and Waleed Najy. Finding sparse solutions for packing and covering semidefinite programs. *SIAM Journal on Optimization*, 32(2):321–353, 2022. doi: 10.1137/20M137570X. URL <https://doi.org/10.1137/20M137570X>.
- [15] Hamza Fawzi, James Saunderson, and Pablo A Parrilo. Semidefinite approximations of the matrix logarithm. *Foundations of Computational Mathematics*, 19:259–296, 2019.
- [16] Leonid Faybusovich and Cunlu Zhou. Self-concordance and matrix monotonicity with applications to quantum entanglement problems. *Applied Mathematics and Computation*, 375:125071, 2020. doi: <https://doi.org/10.1016/j.amc.2020.125071>. URL <https://www.sciencedirect.com/science/article/pii/S0096300320300400>.
- [17] Marguerite Frank and Philip Wolfe. An algorithm for quadratic programming. *Naval Research Logistics Quarterly*, 3(1-2):95–110, 2019/09/05 1956. doi: 10.1002/nav.3800030109. URL <https://doi.org/10.1002/nav.3800030109>.

- [18] Robert M Freund and Paul Grigas. New analysis and results for the frank–wolfe method. *Mathematical Programming*, 155(1-2):199–230, 2016.
- [19] Michel X Goemans and David P Williamson. Improved approximation algorithms for maximum cut and satisfiability problems using semidefinite programming. *Journal of the ACM (JACM)*, 42(6):1115–1145, 1995.
- [20] Frank Göring, Christoph Helmberg, and Markus Wappler. Embedded in the shadow of the separator. *SIAM Journal on Optimization*, 19(1):472–501, 2008. doi: 10.1137/050639430. URL <https://doi.org/10.1137/050639430>.
- [21] Elaine T. Hale, Wotao Yin, and Yin Zhang. Fixed-point continuation for  $\ell_1$ -minimization: Methodology and convergence. *SIAM Journal on Optimization*, 19(3):1107–1130, 2008. doi: 10.1137/070698920. URL <https://doi.org/10.1137/070698920>.
- [22] Michał Horodecki, Paweł Horodecki, and Ryszard Horodecki. Separability of mixed states: necessary and sufficient conditions. *Physics Letters A*, 223(1):1–8, 1996. doi: [https://doi.org/10.1016/S0375-9601\(96\)00706-2](https://doi.org/10.1016/S0375-9601(96)00706-2). URL <https://www.sciencedirect.com/science/article/pii/S0375960196007062>.
- [23] G. Iyengar, D. J. Phillips, and C. Stein. Approximating semidefinite packing programs. *SIAM Journal on Optimization*, 21(1):231–268, 2011. doi: 10.1137/090762671. URL <https://doi.org/10.1137/090762671>.
- [24] Garud Iyengar, David J Phillips, and Cliff Stein. Feasible and accurate algorithms for covering semidefinite programs. *Scandinavian Workshop on Algorithm Theory*, pages 150–162, 2010.
- [25] Martin Jaggi. Revisiting Frank-Wolfe: Projection-free sparse convex optimization. In *International Conference on Machine Learning*, pages 427–435, 2013.
- [26] Simon Lacoste-Julien, Martin Jaggi, Mark Schmidt, and Patrick Pletscher. Block-coordinate Frank-Wolfe optimization for structural SVMs. In Sanjoy Dasgupta and David McAllester, editors, *Proceedings of the 30th International Conference on Machine Learning*, volume 28 of *Proceedings of Machine Learning Research*, pages 53–61, Atlanta, Georgia, USA, 2013. PMLR. URL <https://proceedings.mlr.press/v28/lacoste-julien13.html>.
- [27] Gert RG Lanckriet, Nello Cristianini, Peter Bartlett, Laurent El Ghaoui, and Michael I Jordan. Learning the kernel matrix with semidefinite programming. *Journal of Machine learning research*, 5(Jan):27–72, 2004.
- [28] Monique Laurent and Franz Rendl. Semidefinite programming and integer programming. *Handbooks in Operations Research and Management Science*, 12:393–514, 2005.
- [29] Yurii Nesterov. *Lectures on Convex Optimization*, volume 137 of *Springer Optimization and Its Applications*. Springer International Publishing, 2018.
- [30] Yurii Nesterov and Arkadi Nemirovski. *Interior Point Polynomial methods in Convex programming*. SIAM Publications, 1994.
- [31] M. Nielsen and I Chuang. *Quantum Computation and Quantum Information*. Cambridge: Cambridge University Press., 2010.
- [32] Jiming Peng and Yu Wei. Approximating k-means-type clustering via semidefinite programming. *SIAM Journal on Optimization*, 18(1):186–205, 2007. doi: 10.1137/050641983. URL <https://doi.org/10.1137/050641983>.
- [33] Jun Sun, Stephen Boyd, Lin Xiao, and Persi Diaconis. The fastest mixing markov process on a graph and a connection to a maximum variance unfolding problem. *SIAM Review*, 48(4):681–699, 2022/01/12/ 2006. URL <http://www.jstor.org/stable/20453871>.
- [34] Ryan J. Tibshirani and Jonathan Taylor. The solution path of the generalized lasso. *Ann. Statist.*, 39(3):1335–1371, 2011. doi: 10.1214/11-AOS878. URL <https://projecteuclid.org/443/euclid.aos/1304514656>.
- [35] K. C. Toh, M. J. Todd, and R. H. Tütüncü. Sdpt3 —a matlab software package for semidefinite programming, version 1.3. *Optimization Methods and Software*, 11(1-4):545–581, 01 1999. doi: 10.1080/10556789908805762. URL <https://doi.org/10.1080/10556789908805762>.
- [36] Kilian Q Weinberger and Lawrence K Saul. Distance metric learning for large margin nearest neighbor classification. *Journal of machine learning research*, 10(2), 2009.
- [37] Zaiwen Wen, Wotao Yin, Donald Goldfarb, and Yin Zhang. A fast algorithm for sparse reconstruction based on shrinkage, subspace optimization, and continuation. *SIAM Journal on Scientific Computing*, 32(4):1832–1857, 2010. doi: 10.1137/090747695. URL <https://doi.org/10.1137/090747695>.
- [38] Lin Xiao and Tong Zhang. A proximal-gradient homotopy method for the sparse least-squares problem. *SIAM Journal on Optimization*, 23(2):1062–1091, 2013. doi: 10.1137/120869997. URL <https://doi.org/10.1137/120869997>.
- [39] Alp Yurtsever. SketchyCGAL MATLAB code. URL <https://github.com/alpyurtsever/SketchyCGAL>.
- [40] Alp Yurtsever, Olivier Fercoq, Francesco Locatello, and Volkan Cevher. A conditional gradient framework for composite convex minimization with applications to semidefinite programming. pages 5727–5736. PMLR, 2018. ISBN 2640-3498.

- [41] Alp Yurtsever, Joel A. Tropp, Olivier Fercoq, Madeleine Udell, and Volkan Cevher. Scalable semidefinite programming. *SIAM Journal on Mathematics of Data Science*, 3(1):171–200, 2021. doi: 10.1137/19M1305045. URL <https://doi.org/10.1137/19M1305045>.
- [42] Renbo Zhao. An away-step frank-wolfe method for minimizing logarithmically-homogeneous barriers. *arXiv preprint arXiv:2305.17808*, 2023.
- [43] Renbo Zhao and Robert M. Freund. Analysis of the Frank–Wolfe method for convex composite optimization involving a logarithmically-homogeneous barrier. *Mathematical Programming*, 2022. doi: 10.1007/s10107-022-01820-9. URL <https://doi.org/10.1007/s10107-022-01820-9>.
- [44] Yuriy Zinchenko, Shmuel Friedland, and Gilad Gour. Numerical estimation of the relative entropy of entanglement. *Physical Review A*, 82(5):052336, 2010.

## A Modifications due to inexact oracles

In this appendix we give the missing proofs of the theoretical statements in Sections 4 and 4.2. Consider the function  $\tilde{e}_t(x) := \|\tilde{s}_t(x) - x\|_x$ , where  $\tilde{s}_t(x)$  is any member of the set  $\mathcal{L}_g^{(\delta, \theta)}(\frac{1}{t}\nabla F(x))$  (cf. Definition 4.1). It is easy to see that 5.1 translates to the case with inexact oracle feedback as

$$t^{-1}\tilde{e}_t(x) \leq v/t + \widetilde{\text{Gap}}_t(x) + \Omega_g. \quad (\text{A.1})$$

Moreover, one can show that

$$\tilde{e}_t(x) \geq \frac{t}{\sqrt{v}} \left( \widetilde{\text{Gap}}_t(x) - \Omega_g \right). \quad (\text{A.2})$$

### A.1 Proof of Proposition 4.3

The proof of this proposition mimics the proof of the exact regime (cf. Proposition 3.2), with some important twists. We split the analysis into two phases, bound the maximum number of iterations the algorithms can spend on these phases, and add these numbers up to obtain the worst-case upper bound.

First, for a round  $k$  of  $\text{ICG}(x, t, \eta, \delta, \theta)$ , we use the abbreviations

$$\tilde{s}_t^k = \tilde{s}_t(x_t^k), \quad \tilde{e}_t^k \equiv \|\tilde{s}_t^k - x_t^k\|_{x_t^k}, \quad \tilde{G}_t^k \equiv \widetilde{\text{Gap}}_t(x_t^k), \quad \tilde{a}_t^k \equiv \tilde{a}_t(x_t^k).$$

We further redefine the phases as  $\mathbb{K}_I(t) := \{k \in \mathbb{N} | \widetilde{\text{Gap}}_t(x_t^k) > a_t\}$  (phase I) and  $\mathbb{K}_{II}(t) := \{k \in \mathbb{N} | \widetilde{\text{Gap}}_t(x_t^k) \leq a_t\}$  (phase II), where  $a_t := \frac{v}{t} + \Omega_g$ .

Note that in the analysis we use the inequality  $\Delta_t(x_t^k) > \eta + \theta$  since our goal is to estimate the number of iterations to achieve  $\Delta_t(x_t^k) \leq \eta + \theta$ . Moreover, if the stopping condition  $\widetilde{\text{Gap}}_t(x_t^k) \equiv \tilde{G}_t^k \leq \eta\delta$  holds, we obtain by the definition of the ILMO and inequality (3.5) that

$$\eta\delta \geq \widetilde{\text{Gap}}_t(x_t^k) \geq \delta(\text{Gap}_t(x_t^k) - \theta) \geq \delta(\Delta_t(x_t^k) - \theta), \quad (\text{A.3})$$

which implies that  $\Delta_t(x_t^k) \leq \eta + \theta$ . Thus, in the analysis we also use the inequality  $\tilde{G}_t^k > \eta\delta > 0$ . We start by showing that the sequence  $\{\Delta_t(x_t^k)\}_{k \in \mathbb{N}}$  is monotonically decreasing.

**Monotonicity of  $\Delta_t(x_t^k)$**  Consider  $k \in \mathbb{K}_I(t)$ . Combining the condition  $\tilde{G}_t^k > \frac{\nu}{t} + \Omega_g$  of this phase with (A.2), we deduce that  $\tilde{\mathbf{e}}_t^k \geq \sqrt{\nu} \geq 1$ . This in turn implies  $\frac{t\tilde{G}_t^k}{\tilde{\mathbf{e}}_t^k(\tilde{\mathbf{e}}_t^k + t\tilde{G}_t^k)} < \frac{t\tilde{G}_t^k}{\tilde{\mathbf{e}}_t^k + t\tilde{G}_t^k} < 1$ . Hence, at this iteration algorithm ICG( $x, t, \eta, \delta, \theta$ ) chooses the step size  $\tilde{\alpha}_t^k = \frac{t\tilde{G}_t^k}{\tilde{\mathbf{e}}_t^k(\tilde{\mathbf{e}}_t^k + t\tilde{G}_t^k)}$ . The per-iteration reduction of the potential function can then be estimated just as in the derivation of (5.5):

$$V_t(x_t^{k+1}) \leq V_t(x_t^k) - \frac{1}{t} \omega \left( \frac{t\tilde{G}_t^k}{\tilde{\mathbf{e}}_t^k} \right). \quad (\text{A.4})$$

Note that the r.h.s. is well-defined since  $\tilde{G}_t^k > \eta\delta > 0$  as the stopping condition is not yet achieved. The above inequality, using the definition of the potential function gap as  $\Delta_t(x_t^k) = V_t(x_t^k) - V_t(z^*(t))$ , readily yields

$$\Delta_t(x_t^k) - \Delta_t(x_t^{k+1}) \geq \frac{1}{t} \omega \left( \frac{t\tilde{G}_t^k}{\tilde{\mathbf{e}}_t^k} \right) \geq 0. \quad (\text{A.5})$$

Now, consider  $k \in \mathbb{K}_{II}(t)$ , which means that  $\tilde{G}_t^k \leq \frac{\nu}{t} + \Omega_g$ . There are two cases we need to consider, depending on the step size  $\tilde{\alpha}_t^k$ . We first consider the case where  $\tilde{\alpha}_t^k = 1$ . Then  $t\tilde{G}_t^k \geq \tilde{\mathbf{e}}_t^k(\tilde{\mathbf{e}}_t^k + t\tilde{G}_t^k)$ , which implies  $\tilde{\mathbf{e}}_t^k \in (0, 1)$ . From there we conclude that  $\tilde{G}_t^k \geq \frac{(\tilde{\mathbf{e}}_t^k)^2}{t(1-\tilde{\mathbf{e}}_t^k)}$ , and, by (3.7) and (2.7), that

$$\begin{aligned} V_t(x_t^{k+1}) &\leq V_t(x_t^k) - \tilde{G}_t^k + \frac{1}{t} \omega_*(\tilde{\mathbf{e}}_t^k) \\ &\leq V_t(x_t^k) - \tilde{G}_t^k + \frac{1}{t} \frac{(\tilde{\mathbf{e}}_t^k)^2}{2(1-\tilde{\mathbf{e}}_t^k)} \\ &\leq V_t(x_t^k) - \frac{\tilde{G}_t^k}{2}. \end{aligned}$$

Therefore, using again that  $\tilde{G}_t^k \leq \frac{\nu}{t} + \Omega_g$ , we have

$$\Delta_t(x_t^k) - \Delta_t(x_t^{k+1}) \geq \frac{\tilde{G}_t^k}{2} \geq \frac{(\tilde{G}_t^k)^2}{2(\nu/t + \Omega_g)} \geq \frac{t(\tilde{G}_t^k)^2}{12(\nu + t\Omega_g)^2} \geq 0, \quad (\text{A.6})$$

where the last inequality follows  $\tilde{G}_t^k > \eta\delta > 0$ .

Consider now the case where  $\tilde{\alpha}_t^k < 1$ , i.e.,  $\tilde{\alpha}_t^k = \frac{t\tilde{G}_t^k}{\tilde{\mathbf{e}}_t^k(\tilde{\mathbf{e}}_t^k + t\tilde{G}_t^k)}$ . Then, using this stepsize, just as in the derivation of (5.5) and (A.4), we get

$$V_t(x_t^{k+1}) \leq V_t(x_t^k) - \frac{1}{t} \omega \left( \frac{t\tilde{G}_t^k}{\tilde{\mathbf{e}}_t^k} \right). \quad (\text{A.7})$$

Again, since  $\tilde{G}_t^k \leq \frac{\nu}{t} + \Omega_g$  for  $k \in \mathbb{K}_{II}(t)$ , we have  $\frac{\tilde{G}_t^k}{\tilde{G}_t^k + \nu/t + \Omega_g} \leq \frac{1}{2}$ . Using the monotonicity of  $\omega(\tau)$ , inequality (A.1), and that  $\omega(\tau) \geq \frac{\tau^2}{3}$  for  $\tau \leq 1/2$  [43, Prop. 1], we can develop the bound

$$\frac{1}{t} \omega \left( \frac{t\tilde{G}_t^k}{\tilde{\mathbf{e}}_t^k} \right) = \frac{1}{t} \omega \left( \frac{\tilde{G}_t^k}{\tilde{\mathbf{e}}_t^k/t} \right) \geq \frac{1}{t} \omega \left( \frac{\tilde{G}_t^k}{\tilde{G}_t^k + \nu/t + \Omega_g} \right) \geq \frac{1}{3t} \left( \frac{\tilde{G}_t^k}{\tilde{G}_t^k + \nu/t + \Omega_g} \right)^2.$$

This and (A.7), again by  $\tilde{G}_t^k \leq \frac{\nu}{t} + \Omega_g$ , implies that also in this regime we obtain the estimate

$$\Delta_t(x_t^k) - \Delta_t(x_t^{k+1}) \geq \frac{t(\tilde{G}_t^k)^2}{12(\nu + t\Omega_g)^2}. \quad (\text{A.8})$$

As we see, the above inequality holds on the whole phase II, both when  $\tilde{\alpha}_t^k < 1$  and when  $\tilde{\alpha}_t^k = 1$ . In particular, since  $\tilde{G}_t^k > \eta\delta > 0$ , together with (A.6) imply that  $\{\Delta_t(x_t^k)\}_{k \in \mathbb{N}}$  is monotonically decreasing.

We now move to the analysis of the iteration complexity.

**Analysis for Phase I** Let let  $\{k_i\}_{i \in \mathbb{N}_0}$  denote the increasing set of indices enumerating the elements of the set  $\mathbb{K}_I(t)$ . Since  $k_i \in \mathbb{K}_I(t)$ , it holds that  $\tilde{G}_t^{k_i} > \frac{\nu}{t} + \Omega_g$  and so  $\frac{t\tilde{G}_t^{k_i}}{\nu + t\tilde{G}_t^{k_i} + t\Omega_g} > \frac{1}{2}$ . Together with (A.1), this implies

$$\frac{t\tilde{G}_t^{k_i}}{\tilde{\epsilon}_t^{k_i}} \geq \frac{\tilde{G}_t^{k_i}}{\nu/t + \tilde{G}_t^{k_i} + \Omega_g} = \frac{t\tilde{G}_t^{k_i}}{\nu + t\tilde{G}_t^{k_i} + t\Omega_g} > \frac{1}{2}.$$

Using the monotonicity of  $\omega(\cdot)$  and that  $\omega(\tau) \geq \frac{\tau}{5.3}$  for  $\tau \geq 1/2$  [43, Prop. 1], we further obtain

$$\Delta_t(x_t^{k_i}) - \Delta_t(x_t^{k_{i+1}}) \geq \frac{1}{t} \omega\left(\frac{t\tilde{G}_t^{k_i}}{\tilde{\epsilon}_t^{k_i}}\right) \geq \frac{\tilde{G}_t^{k_i}}{5.3(\nu + t\Omega_g + t\tilde{G}_t^{k_i})}. \quad (\text{A.9})$$

By our definition of the inexact oracle, inequalities (3.5) and  $\Delta_t(x_t^{k_i}) > \eta + \theta$ , we see that

$$\tilde{G}_t^{k_i} \equiv \widetilde{\text{Gap}}_t(x_t^{k_i}) \geq \delta(\text{Gap}_t(x_t^{k_i}) - \theta) \geq \delta(\Delta_t(x_t^{k_i}) - \theta) > \eta > 0.$$

Combining this with (A.9) and the fact that the function  $x \mapsto \frac{x}{a+tx}$  is strictly increasing for  $a, t > 0$  and  $x > 0$ , we obtain

$$\Delta_t(x_t^{k_i}) - \Delta_t(x_t^{k_{i+1}}) \geq \frac{\delta(\Delta_t(x_t^{k_i}) - \theta)}{5.3(t\delta(\Delta_t(x_t^{k_i}) - \theta) + \nu + t\Omega_g)} \geq \frac{\delta(\Delta_t(x_t^{k_i}) - \theta)}{5.3(t\delta(\Delta_t(x_t^0) - \theta) + \nu + t\Omega_g)}, \quad (\text{A.10})$$

where in the first and last inequalities follow from  $\{\Delta_t(x_t^k)\}_{k \in \mathbb{N}_0}$  being monotonically decreasing and  $\Delta_t(x_t^{k_i}) > \eta + \theta \geq \theta$ . Rearranging the terms and defining  $q := \frac{\delta}{5.3(t\delta(\Delta_t(x_t^0) - \theta) + \nu + t\Omega_g)}$ , which we know to be in  $(0, 1)$  since  $\nu \geq 1$  and  $\Delta_t(x_t^0) > \eta + \theta$ , it follows from the previous display that

$$\Delta_t(x_t^{k_{i+1}}) \leq \Delta_t(x_t^{k_i})(1 - q) + q\theta \leq \Delta_t(x_t^0)(1 - q)^i + \theta \leq \exp(-iq)\Delta_t(x_t^0) + \theta. \quad (\text{A.11})$$

On the other hand, we have

$$\Delta_t(x_t^{k_i}) \geq \Delta_t(x_t^{k_i}) - \Delta_t(x_t^{k_{i+1}}) \geq \frac{\tilde{G}_t^{k_i}}{5.3(\nu + t\Omega_g + t\tilde{G}_t^{k_i})} > \frac{1}{10.6t}$$

since  $\frac{t\tilde{G}_t^{k_i}}{\nu + t\tilde{G}_t^{k_i} + t\Omega_g} > \frac{1}{2}$  for  $k_i \in \mathbb{K}_I(t)$ . Moreover, we know that  $\Delta_t(x_t^{k_i}) > \eta + \theta$ , which gives us in combination with (A.11)

$$\max\left\{\frac{1}{10.6t}, \eta + \theta\right\} \leq \Delta_t(x_t^{k_i}) \leq \exp(-iq)\Delta_t(x_t^0) + \theta. \quad (\text{A.12})$$

Solving w.r.t.  $i$ , we see that the number of iterations in  $\mathbb{K}_I(t)$  is bounded as

$$K_t(x_t^0) := \left\lceil \frac{5.3(t\delta(\Delta_t(x_t^0) - \theta) + \nu + t\Omega_g)}{\delta} \log \left( \min \left\{ \frac{10.6t\Delta_t(x_t^0)}{(1 - 10.6t\theta)_+}, \frac{\Delta_t(x_t^0)}{\eta} \right\} \right) \right\rceil. \quad (\text{A.13})$$

**Analysis for Phase II** Let let  $\{\ell_j\}_{j \in \mathbb{N}_0}$  denote the increasing set of indices enumerating the elements of the set  $\mathbb{K}_{II}(t)$ . Let  $N_t(x_t^0)$  be a bound on the number of iterations until  $\Delta_t(x_t^k) \leq \eta + \theta$  belonging to phase II. We will show that setting  $N_t(x_t^0) = \left\lceil \frac{12(\nu + t\Omega_g)^2}{t\delta^2} \left( \frac{1}{\eta} - \frac{1}{\Delta_t(x_t^0) - \theta} \right)_+ \right\rceil$  is such a bound. Indeed, if  $\Delta_t(x_t^{N_t(x_t^0)+1}) \leq \theta$  then the proof is done, otherwise  $\Delta_t(x_t^j) \geq \theta$  for all  $j \leq N_t(x_t^0) + 1$  from monotonicity of the sequence  $\{\Delta_t(x_t^{\ell_j})\}_{\ell_j \in \mathbb{K}_{II}(t)}$ . Calling  $\Delta_t^j \equiv \Delta(x_t^{\ell_j(t)})$  and using the monotonicity of this sequence, we see from (A.8) and (A.3) that, for  $j = 1, \dots, N_t - 1(x_t^0)$ ,

$$\Delta_t^j - \Delta_t^{j+1} \geq \Delta_t^j - \Delta_t(x_t^{\ell_j(t)+1}) \geq \frac{t(\tilde{G}_t^{\ell_j(t)})^2}{12(\nu + t\Omega_g)^2} \geq \frac{t\delta^2(\Delta_t^j - \theta)(\Delta_t^{j+1} - \theta)}{12(\nu + t\Omega_g)^2}.$$

This implies that for  $j = 1, \dots, N_t(x_t^0)$  that

$$\frac{1}{\Delta_t^{j+1} - \theta} - \frac{1}{\Delta_t^j - \theta} \geq \frac{t\delta^2}{12(\nu + t\Omega_g)^2}, \quad j = 1, \dots, N_t(x_t^0).$$

Telescoping this expression together with  $\Delta_t^1 \leq \Delta_t(x_t^0)$ , which stems from the entire sequence  $\{\Delta_t(x_t^k)\}_{k \in \mathbb{N}_0}$  being monotonically decreasing, we see that

$$\frac{1}{\Delta_t^{N_t(x_t^0)+1} - \theta} \geq \frac{(N_t(x_t^0) - 1)t\delta^2}{12(\nu + t\Omega_g)^2} + \frac{1}{\Delta_t^1 - \theta} \geq \frac{(N_t(x_t^0) - 1)t\delta^2}{12(\nu + t\Omega_g)^2} + \frac{1}{\Delta_t(x_t^0) - \theta} \geq \frac{1}{\eta},$$

is satisfied for  $N_t(x_t^0)$ .

We can therefore conclude that the number of iterations required to obtain  $\Delta_t(x_t^k) \leq \eta + \theta$  does not exceed  $N_t(x_t^0) + K_t(x_t^0) + 1$  which is exactly the value of  $\tilde{N}(x^0, \eta, \delta, \theta)$ , thus concluding the proof.

## A.2 Proof of Proposition 4.2

Our analysis concentrates on the behaviour of the algorithm in Phase II since the estimate for number of iterations in Phase I still holds. Here we split the iterates of the set  $\mathbb{K}_{II}(t) = \{k_1(t), \dots, k_p(t)\} \equiv \{k_1, \dots, k_p\}$  into two regimes so that  $\mathbb{K}_{II}(t) = H_t \cup L_t$  with  $L_t := \{k \in \mathbb{K}_{II}(t) | \Delta_t(x_t^k) < \theta\}$  and  $H_t := \{k \in \mathbb{K}_{II}(t) | \Delta_t(x_t^k) \geq \theta\}$ . By monotonicity of the potential function gap, we know that the indices of  $H_t$  ('high states') precede those of  $L_t$  ('low states'). We bound the size of each of these subsets in order to make  $\widetilde{\text{Gap}}_t$  smaller than  $\eta\delta$ . Since the potential function gap is monotonically decreasing, we can organise the iterates on phase II as  $H_t = \{k_1, \dots, k_q\}$  and accordingly,  $L_t = \{k_{q+1}, \dots, k_p\}$  for some  $q \in \{1, \dots, p\}$ .

**Bound on  $H_t$ :** For  $k_j(t) \in H_t$  we know that

$$\Delta_t(x_t^{k_j(t)}) - \Delta_t(x_t^{k_{j+1}(t)}) \geq \Delta_t(x_t^{k_j(t)}) - \Delta_t(x_t^{k_j(t)+1}) \geq \frac{t(\tilde{G}_t^{k_j(t)})^2}{12(\nu + t\Omega_g)^2}. \quad (\text{A.14})$$

Define  $d_j := \delta(\Delta_t(x_t^{k_j(t)}) - \theta)$  for  $j = 1, \dots, q$ , so that  $d_j \geq 0$ . Then, we obtain the recursion

$$d_{j+1} - d_j \leq -\frac{\Gamma_j^2}{M}$$

for  $j \in \{1, \dots, q-1\}$  and  $\Gamma_j \equiv \tilde{G}_t^{k_j(t)} \geq d_j$  and  $\frac{1}{M} \equiv \frac{t\delta}{12(v+t\Omega_g)^2}$ . By [43, Proposition 4], we can conclude that

$$d_q < \frac{M}{q-1} \text{ and } \min\{\Gamma_1, \dots, \Gamma_q\} < \frac{2M}{q-1}.$$

Since we know that  $\min\{\Gamma_1, \dots, \Gamma_q\} \geq \delta\eta$ , we obtain the bound

$$q \leq \frac{2M}{\delta\eta} + 1 = \frac{24(v+t\Omega_g)^2}{t\delta^2\eta} + 1. \quad (\text{A.15})$$

**Bound on  $L_t$ :** On this subset we cannot use the same argument as for the iterates in  $H_t$ , since we cannot guarantee that the sequence  $d_j$  involved in the previous part of the proof is positive. However, we still know that (A.14) applies for the iterates in  $L_t$ . If we telescope this expression over the indices  $q+1, \dots, p$ , and using the fact that  $\Delta_t(x^{k_j(t)}) \in [0, \theta]$ , we see that

$$\begin{aligned} \theta &\geq \Delta_t(x_t^{k_{q+1}(t)}) - \Delta_t(x_t^{k_{p+1}(t)}) \geq \frac{t(p-q)}{12(v+t\Omega_g)^2} \min_{q+1 \leq j \leq p} \left( \tilde{G}_t^{k_j(t)} \right)^2 \\ &\geq \frac{t(p-q)\eta^2\delta^2}{12(v+t\Omega_g)^2} \end{aligned}$$

It follows

$$(p-q) \leq \frac{12\theta(v+t\Omega_g)^2}{t\eta^2\delta^2}. \quad (\text{A.16})$$

**Combining the bounds:** Combining the expressions (A.15) and (A.16) together with the bound (A.13), we see that

$$\begin{aligned} \tilde{R}_t(x_t^0, \eta, \delta, \theta) &= \left\lceil \frac{5.3(t\delta(\Delta_t(x_t^0) - \theta) + v + t\Omega_g)}{\delta} \log \left( \min \left\{ \frac{10.6t\Delta_t(x_t^0)}{(1-10.6t\theta)_+}, \frac{\Delta_t(x_t^0)}{\eta} \right\} \right) \right\rceil \\ &\quad + \left\lceil \frac{12(v+t\Omega_g)^2}{t\delta^2\eta} \left( 2 + \frac{\theta}{\eta} \right) \right\rceil + 1 \end{aligned}$$

defines an upper bound for the length of phase I.

### A.3 Analysis of the outer loop and proof of Theorem 4.4

We set  $\hat{x}_i \equiv x_{t_i}^{\tilde{R}_i}$  the last iterate of procedure ICG( $x_{t_i}^0, t_i, \eta_i, \delta, \theta_i$ ), where  $\tilde{R}_i$  is at most  $R_{\tilde{G}_{t_i}}(x_{t_i}^0, \eta_i, \delta, \theta_i)$  by 4.2. Therefore, we know that  $\widetilde{\text{Gap}}_{t_i}(\hat{x}_i) \leq \eta_i\delta$ , and a-fortiori

$$\Delta_{t_i}(\hat{x}_i) \leq \text{Gap}_{t_i}(\hat{x}_i) \leq \eta_i + \theta_i.$$

By eq. 5.12 and the definition of the  $(\delta, \theta_i)$ -ILMO, we obtain

$$\begin{aligned} g(\hat{x}_i) - g(z^*(t_i)) &\leq \text{Gap}_{t_i}(\hat{x}_i) + \frac{1}{t} F'(\hat{x}_i)[z^*(t_i) - \hat{x}_i] \\ &\leq \frac{\widetilde{\text{Gap}}_{t_i}(\hat{x}_i)}{\delta} + \theta_i + \frac{\nu}{t_i} \\ &\leq \eta_i + \theta_i + \frac{\nu}{t_i}. \end{aligned}$$

Hence, using 2.2, we observe

$$g(\hat{x}_i) - \text{Opt} = g(\hat{x}_i) - g(z^*(t_i)) + g(z^*(t_i)) - \text{Opt} \leq \eta_i + \theta_i + \frac{2\nu}{t_i}.$$

Since  $t_i = \frac{2\nu}{\eta_i}$  and  $\theta_i = \eta_i$ , we obtain  $g(\hat{x}_i) - \text{Opt} \leq 3\eta_i$ . The latter, by the choice of the number of restarts  $I$  implies that

$$g(\hat{z}) - \text{Opt} = g(\hat{x}_I) - \text{Opt} \leq \varepsilon.$$

Our next goal is to estimate the total number of inner iterations based on the estimation for the first epoch  $i = 0$  and summation over epochs  $i = 1, \dots, I$ . For each epoch we use the estimate from 4.2, which we repeat here for convenience

$$\begin{aligned} \tilde{R}_{t_i}(x_{t_i}^0, \eta_i, \delta, \theta_i) &= \left\lceil \frac{5.3(t_i\delta(\Delta_{t_i}(x_{t_i}^0) - \theta_i) + \nu + t_i\Omega_g)}{\delta} \log \left( \min \left\{ \frac{10.6t_i\Delta_{t_i}(x_{t_i}^0)}{(1 - 10.6t_i\theta_i)_+}, \frac{\Delta_{t_i}(x_{t_i}^0)}{\eta_i} \right\} \right) \right\rceil \\ &\quad + \left\lceil \frac{12(\nu + t_i\Omega_g)^2}{t_i\delta^2\eta_i} \left( 2 + \frac{\theta_i}{\eta_i} \right) \right\rceil + 1. \end{aligned} \quad (\text{A.17})$$

We see that we need to estimate the quantities  $t_i(\Delta_{t_i}(x_{t_i}^0) - \theta_i)$  and  $\frac{\Delta_{t_i}(x_{t_i}^0)}{\eta_i}$ , which is our next step. Consider  $i \geq 1$  and observe that

$$\begin{aligned} V_{t_{i+1}}(x_{t_{i+1}}^0) - V_{t_{i+1}}(z^*(t_{i+1})) &= V_{t_i}(x_{t_{i+1}}^0) - V_{t_i}(z^*(t_{i+1})) \\ &\quad + \left( \frac{1}{t_{i+1}} - \frac{1}{t_i} \right) (F(x_{t_{i+1}}^0) - F(z^*(t_{i+1}))) \\ &\leq V_{t_i}(x_{t_i}^{R_i}) - V_{t_i}(z^*(t_i)) \\ &\quad + \left( 1 - \frac{t_{i+1}}{t_i} \right) (V_{t_{i+1}}(x_{t_{i+1}}^0) - V_{t_{i+1}}(z^*(t_{i+1}))) \\ &\quad + \left( 1 - \frac{t_{i+1}}{t_i} \right) (g(z^*(t_{i+1})) - g(x_{t_{i+1}}^0)). \end{aligned}$$

Moreover,

$$g(x_{t_{i+1}}^0) - g(z^*(t_{i+1})) \leq g(x_{t_{i+1}}^0) - \text{Opt} \leq \eta_i + \theta_i + \frac{2\nu}{t_i}.$$

Since  $t_{i+1} > t_i$ , the above two inequalities imply

$$\frac{t_{i+1}}{t_i} [V_{t_{i+1}}(x_{t_{i+1}}^0) - V_{t_{i+1}}(z^*(t_{i+1}))] \leq V_{t_i}(x_{t_i}^{R_i}) - V_{t_i}(z^*(t_i)) + \frac{t_{i+1} - t_i}{t_i} (\eta_i + \theta_i + \frac{2\nu}{t_i}).$$

Whence,

$$\begin{aligned} t_{i+1}(\Delta_{t_{i+1}}(x_{t_{i+1}}^0) - \theta_{i+1}) &\leq t_i\Delta_{t_i}(x_{t_i}^{R_i}) + (t_{i+1} - t_i)(\eta_i + \theta_i + \frac{2\nu}{t_i}) - t_{i+1}\theta_{i+1} \\ &\leq t_i(\eta_i + \theta_i) + (t_{i+1} - t_i)(\eta_i + \theta_i + \frac{2\nu}{t_i}) - t_{i+1}\theta_{i+1} \\ &= 4\nu + (t_{i+1} - t_i) \cdot \frac{6\nu}{t_i} - 2\nu = 2\nu + (1/\sigma - 1)6\nu = 2\nu(3/\sigma - 2), \end{aligned}$$

where we used our assignments  $t_{i+1} = t_i/\sigma$ ,  $\eta_i t_i = \theta_i t_i = 2\nu$ . In the same way, we obtain

$$\begin{aligned} \frac{\Delta_{t_{i+1}}(x_{t_{i+1}}^0)}{\eta_{i+1}} &\leq \frac{t_i}{t_{i+1}\eta_{i+1}}\Delta_{t_i}(x_{t_i}^{R_i}) + \frac{t_{i+1}-t_i}{t_{i+1}\eta_{i+1}}(\eta_i + \theta_i + \frac{2\nu}{t_i}) \\ &\leq \frac{t_i}{t_{i+1}\eta_{i+1}}(\eta_i + \theta_i) + \frac{t_{i+1}-t_i}{t_{i+1}\eta_{i+1}}(\eta_i + \theta_i + \frac{2\nu}{t_i}) \\ &= \frac{4\nu}{t_{i+1}\eta_{i+1}} + \frac{t_{i+1}-t_i}{t_{i+1}\eta_{i+1}}\frac{6\nu}{t_i} = 2 + (1/\sigma - 1)3 = (3/\sigma - 1), \end{aligned}$$

where we again used our assignments  $t_{i+1} = t_i/\sigma$ ,  $\eta_i t_i = \theta_i t_i = 2\nu$ .

Using these bounds, our assignments  $\eta_i = \theta_i = 2\nu/t_i$ , we see that  $1 - 10.6t_i\theta_i < 0$  and the bound (A.17) simplifies to

$$\tilde{R}_i(x_{t_i}^0, \eta_i, \delta, \theta_i) \leq \left\lceil \frac{5.3(2\delta\nu(3/\sigma - 2) + \nu + t_i\Omega_g)}{\delta} \log(3/\sigma - 1) \right\rceil + \left\lceil \frac{18(\nu + t_i\Omega_g)^2}{\nu\delta^2} \right\rceil + 1 \quad (\text{A.18})$$

$$\leq 3 + \frac{5.3(2\delta\nu(3/\sigma - 2) + \nu)}{\delta} \log(3/\sigma - 1) + \frac{18\nu}{\delta^2} \quad (\text{A.19})$$

$$+ t_i \cdot \left( \frac{5.3\Omega_g}{\delta} \log(3/\sigma - 1) + \frac{18\Omega_g}{\delta^2} \right) + t_i^2 \cdot \frac{18\Omega_g^2}{\nu\delta^2}. \quad (\text{A.20})$$

Using the same bounds for  $\sum_i t_i$ ,  $\sum_i t_i^2$  as in the proof of 3.3 (see Section 5.2), we obtain that

$$\begin{aligned} \sum_{i=1}^I \tilde{R}_i &\leq \left( 3 + \frac{5.3(2\delta\nu(3/\sigma - 2) + \nu)}{\delta} \log(3/\sigma - 1) + \frac{18\nu}{\delta^2} \right) \frac{\log(2\eta_0/\varepsilon)}{\log(1/\sigma)} \\ &\quad + \left( \frac{5.3\Omega_g}{\delta} \log(3/\sigma - 1) + \frac{18\Omega_g}{\delta^2} \right) \frac{4\nu}{\varepsilon(1-\sigma)} \\ &\quad + \frac{288\nu\Omega_g^2}{\delta^2\varepsilon^2(1-\sigma^2)}. \end{aligned} \quad (\text{A.21})$$

Finally, we estimate  $\tilde{R}_0$  as follows using (A.17) and that  $t_0\eta_0 = 2\nu$ ,  $t_0 = \nu/\Omega_g$ ,  $\theta_0 = \eta_0$ ,  $\delta < 1$ :

$$\begin{aligned} \tilde{R}_0 &\leq \left\lceil \frac{5.3(t_0\delta\Delta_{t_0}(x^0) + \nu + t_0\Omega_g)}{\delta} \log\left(\frac{\Delta_{t_0}(x^0)}{\eta_0}\right) \right\rceil + \left\lceil \frac{18(\nu + t_0\Omega_g)^2}{\nu\delta^2} \right\rceil + 1 \\ &\leq \frac{5.3(F(x^0) - F(z^*(t_0)) + 3\nu)}{\delta} \log\left(\frac{F(x^0) - F(z^*(t_0)) + \nu}{2\nu}\right) + \frac{72\nu}{\delta^2} + 3. \end{aligned}$$

Combining the latter with (A.21), we obtain that the leading complexity term is  $O\left(\frac{\nu\Omega_g^2}{\delta^2\varepsilon^2(1-\sigma^2)}\right)$ .

We remark that assuming that the oracle accuracies  $\theta_i$  have geometric decay is crucial in order to obtain the same dependence on the accuracy in the complexity as in the exact case. Indeed, if the oracle accuracy is fixed to be  $\theta_i \equiv \theta$ , then the last term in the bound (A.17) contains a term  $\frac{12t_i^2\Omega_g^2\theta}{2\nu\delta^2\eta_i} = \frac{12t_i^3\Omega_g^2\theta}{4\nu^2\delta^2}$ , which after summation will imply that the leading term in the complexity would be  $O(1/\varepsilon^4)$ .

## B Added Details to the Numerical Experiments

In this section we report outcomes obtained by extensive numerical experiments illustrating the practical performance of our method. We implement Algorithm 2 using procedure CG and LCG as solvers for the inner loops. We compare the results of our algorithm to two benchmarks: (1) an interior point solution of the problem, and (2) CGAL, implemented following the suggestions in [41]. In order to enable a fair comparison with CGAL, both CG and LCG also used the LMO implementation of the random Lanczos algorithm provided as part of the CGAL code. The interior point solution was obtained via the Matlab-based modelling interface CVX [7] (version 2.2) with the SDPT3 solver (version 4.0) [35]. The implementation of CGAL was taken from [39]. All experiments have been conducted on an Intel(R) Xeon(R) Gold 6254 CPU @3.10GHz server limited to 4 threads per run and 512G total RAM using Matlab R2019b.

### B.1 MaxCut Problem

The following class of SDPs is studied in [2]. This SDP arises in many algorithms such as approximating MaxCut, approximating the CUTNORM of a matrix, and approximating solutions to the little Grothendieck problem [3, 6]. The optimization problem is defined as

$$\begin{aligned} & \max \quad \langle \mathbf{C}, \mathbf{X} \rangle \\ \text{s.t.} \quad & X_{ii} \leq 1 \quad i = 1, \dots, n \\ & \mathbf{X} \geq 0 \end{aligned} \tag{MAXQP}$$

Let  $\mathbf{Q} := \{y \in \mathbb{R}^n \mid y_i \leq 1, i = 1, \dots, n\}$ , and consider the conic hull of  $\mathbf{Q}$ , defined as  $\mathbf{K} := \{(y, t) \in \mathbb{R}^n \times \mathbb{R} \mid \frac{1}{t}y \in \mathbf{Q}, t > 0\} \subset \mathbb{R}^{n+1}$ . This set admits the  $n$ -logarithmically homogenous barrier

$$f(y, t) = - \sum_{i=1}^n \log(t - y_i) = - \sum_{i=1}^n \log\left(1 - \frac{1}{t}y_i\right) - n \log(t).$$

We can then reformulate (MAXQP) as

$$\begin{aligned} & \min_{\mathbf{X}, t} \quad \{g(\mathbf{X}) := -\langle \mathbf{C}, \mathbf{X} \rangle\} \\ \text{s.t.} \quad & (\mathbf{X}, t) \in \mathbf{X} := \{(\mathbf{X}', t') \in \mathbb{S}^n \times \mathbb{R} \mid \mathbf{X}' \geq 0, \text{tr}(\mathbf{X}') \leq n, t' = 1\}, \\ & \mathcal{P}(\mathbf{X}, t) \in \mathbf{K} \end{aligned} \tag{B.1}$$

where  $\mathcal{P}(\mathbf{X}, t) := [X_{11}; \dots; X_{nn}; t]^\top$  is a linear homogenous mapping from  $\mathbb{S}^n \times \mathbb{R}$  to  $\mathbb{R}^{n+1}$ . Set  $F(\mathbf{X}, t) = f(\mathcal{P}(\mathbf{X}, t))$  for  $(\mathbf{X}, t) \in \mathbb{S}^n \times (0, \infty)$ .

We apply this formulation to the classical MaxCut problem: given an undirected graph  $\mathcal{G} = (\mathcal{V}, \mathcal{E})$  with vertex set  $\mathcal{V} = \{1, \dots, n\}$  and edge set  $\mathcal{E}$ , we seek to find the maximum-weight cut of the graph. The MaxCut problem is formulated as  $\max_{\mathbf{x} \in \{\pm 1\}^n} \mathbf{x}^\top \mathbf{L} \mathbf{x}$ , where  $\mathbf{L}$  is the combinatorial Laplace matrix of graph  $\mathcal{G}$ . A convex relaxation of this NP-hard combinatorial optimization problem can be given by the SDP [19]

$$\max \frac{1}{4} \text{tr}(\mathbf{L}\mathbf{X}) \text{ s.t.: } X_{ii} \leq 1, i \in \{1, 2, \dots, n\}, \mathbf{X} \in \mathbb{S}_+^n,$$

which is the form of (MAXQP) with  $\mathbf{C} = \frac{1}{4}\mathbf{L}$ .

To evaluate the performance of the tested algorithms on this problem, we consider the random graphs G1-G30, published online in [1]. The CG and LCG methods were applied to all datasets with

parameters  $\eta_0 = 2\Omega_g$  and  $\sigma \in \{0.25, 0.5, 0.9\}$ . The solutions were compared to the solution obtained from running CGAL, using the original CGAL code applied to the scaled problem and assuming that all constraint are satisfied with equality. The computations were stopped after either 10,000 seconds of running time. The benchmark solutions for the interior point method for each data set are displayed in Table 1. Table 1 also displays the size of each dataset, the value obtained by solving the MaxCut SDP relaxation using CVX with the SDPT3 solver, and  $\lambda_{\min}(\mathbf{X}^{\text{SDPT3}})$ , that is the minimum eigenvalue of the solution. We observe that for larger graphs the interior-point solver SDPT3 returns infeasible solutions, displaying negative eigenvalues. If this occurs, the value obtained by a corrected solution is used as a reference value instead. This corrected solution  $\tilde{\mathbf{X}}^{\text{SDPT3}}$  is constructed as  $\tilde{\mathbf{X}}^{\text{SDPT3}} = (\mathbf{X}^{\text{SDPT3}} - \lambda_{\min}(\mathbf{X}^{\text{SDPT3}})\mathbf{I})/\alpha$ , where  $\mathbf{I}$  is the identity matrix, and  $\alpha = \max_{i \in \{1, \dots, n\}} \max\{\tilde{X}_{ii}^{\text{SDPT3}}, 1\}$  is the minimal number for which  $\tilde{X}_{ii}^{\text{SDPT3}} \leq 1$  for all  $i = 1, \dots, n$ . The objective value of this corrected solution,  $g(\tilde{\mathbf{X}}^{\text{SDPT3}})$  is also recorded in Table 1 as the feasible value (Feas. value). We therefore label the optimal solution  $g^*$  as the minimum of  $g(\tilde{\mathbf{X}}^{\text{SDPT3}})$  and the minimal value obtained by any of the methods. The performance measure we employ to benchmark our experimental results is the *relative optimality gap*, defined as  $\frac{|g(\mathbf{X}) - g^*|}{|g^*|}$ . Moreover, since CGAL does not necessarily generate feasible solutions, its reported solution  $\mathbf{X}^{\text{CGAL}}$  is corrected to the feasible one  $\tilde{\mathbf{X}}^{\text{CGAL}} = \mathbf{X}^{\text{CGAL}}/(\gamma + 1)$ , where  $\gamma = \max_{i \in \{1, \dots, n\}} \max\{X_{ii}^{\text{CGAL}} - 1, 0\}$  is the *relative feasibility gap* of CGAL. In particular, for every dataset  $D$ , method  $M$ , and parameter choice  $P$ , after each iteration  $i$  we record the objective value  $g_i^{M,P,D}$  of the solution after this iteration (or, in the case of CGAL, the corrected solution), the corresponding relative optimality gap  $r_i^{M,P,D} = |g_i^{M,P,D} - g^*|/|g^*|$ , the time from the start of the run  $t_i^{M,P,D}$  and, in the case of CGAL, the feasibility gap  $\gamma_i^{\text{CGAL},P,D}$  of the current solution.

Figures 4-7 illustrate the performance of our methods for various parameter values and datasets G1-G30 vs. both iteration and time. More specifically, Figures 4 and 6 display, for each iteration  $i$ , the best relative optimality gap  $\min_{j \leq i} \{r_j^{M,P,D}\}$  attained up to that iteration; Figures 5 and 7 display, for each time point  $t$ , the best relative optimality gap  $\min_j \{r_j^{M,P,D} | t_j^{M,P,D} \leq t\}$  obtained up to time  $t$ . Additionally, Tables 2 and 3 report the algorithmic performances of the tested methods for each data base and method, at specific time points  $t \in \{100, 1000, 10000\}$  seconds. Specifically, for each of the time points we compute  $j^* = \operatorname{argmin}_j \{g_j^{M,P,D} | t_j^{M,P,D} \leq t\}$ , and then display the relative optimality gap (Opt. Gap)  $r_{j^*}^{M,P,D}$ , the relative feasibility gap  $\gamma_{j^*}^{\text{CGAL},D}$  for CGAL (Feas. Gap), and the number of iterations  $\max\{j | t_j^{M,P,D} \leq t\}$  performed until that time point (Iter). The smallest relative optimality gap for each data set and time is marked in bold.

Figures 4 and 6, show that the performances of CG and LCG are similar across iterations, with LCG having a slight advantage. Further, the performance of both methods remains nearly unchanged for different values of  $\sigma$ . Note that, for a low number of iterations (smaller than 1000), CG and LCG generally perform better than CGAL. However, beyond that point, CGAL exhibits a sudden improvement in objective value, leading to better performance. When looking at the methods' performances over time in Figures 5 and 7, the initial advantage of CG and LCG seems to disappear, due to the lower per-iteration cost of CGAL. However, a closer look at the results in Tables 2 and 3 reveals that CG achieves the lowest optimality gap in 7 out of 30 datasets after 1000 seconds, and in 13 out of the 30 datasets after 10000 seconds. The former instances can be identified by the fact that CGAL obtains an optimality gap higher than 0.5% after 100 seconds, and has a very slow improvement rate after that point. In contrast, CG obtains a higher optimality gap of approximately 2% at that time but manages to achieve better performance due to its superior optimality gap reduction rate. Additionally, we observe that the costly iterations of LCG result in

Table 1: MaxCut datasets information

Dataset	#Nodes	#Edges	SDPT3			Dataset	#Nodes	#Edges	SDPT3		
			Obj. value	$\lambda_{\min}$	Feas. value				Value	$\lambda_{\min}$	Feas. value
G1	800	19176	12083.2	0	-	G16	800	4672	3175.02	0	-
G2	800	19176	12089.43	0	-	G17	800	4667	3171.25	0	-
G3	800	19176	12084.33	0	-	G18	800	4694	1173.75	0	-
G4	800	19176	12111.5	0	-	G19	800	4661	1091	0	-
G5	800	19176	12100	0	-	G20	800	4672	1119	0	-
G6	800	19176	2667	0	-	G21	800	4667	1112.06	0	-
G7	800	19176	2494.25	0	-	G22	2000	19990	18276.89	-1	14135.95
G8	800	19176	2535.25	0	-	G23	2000	19990	18289.22	-1	14142.11
G9	800	19176	12111.5	0	-	G24	2000	19990	18286.75	-1	9997.75
G10	800	19176	12111.5	0	-	G25	2000	19990	18293.5	-1	9996
G11	800	1600	634.83	0	-	G26	2000	19990	18270.24	-1	14132.87
G12	800	1600	628.41	0	-	G27	2000	19990	8304.5	-1	4141.75
G13	800	1600	651.54	0	-	G28	2000	19990	8253.5	-1	4100.75
G14	800	1600	12111.5	0	-	G29	2000	19990	8377.75	-1	4209
G15	800	4661	3171.56	0	-	G30	2000	19990	8381	-1	4215.5

inferior performance over time compared to CG, as it can only complete a tenth of the iterations within the same time frame. In summary, while CGAL manages to obtain a less than 1% optimality gap quite quickly, in about a third of the instances it gets ‘stuck’ and does not significantly improve the objective function, whereas LCG and CG are more consistent across the instances starting from a higher optimality gap, but making progress in a constant rate throughout their execution, with CG being more efficient in terms of time complexity.

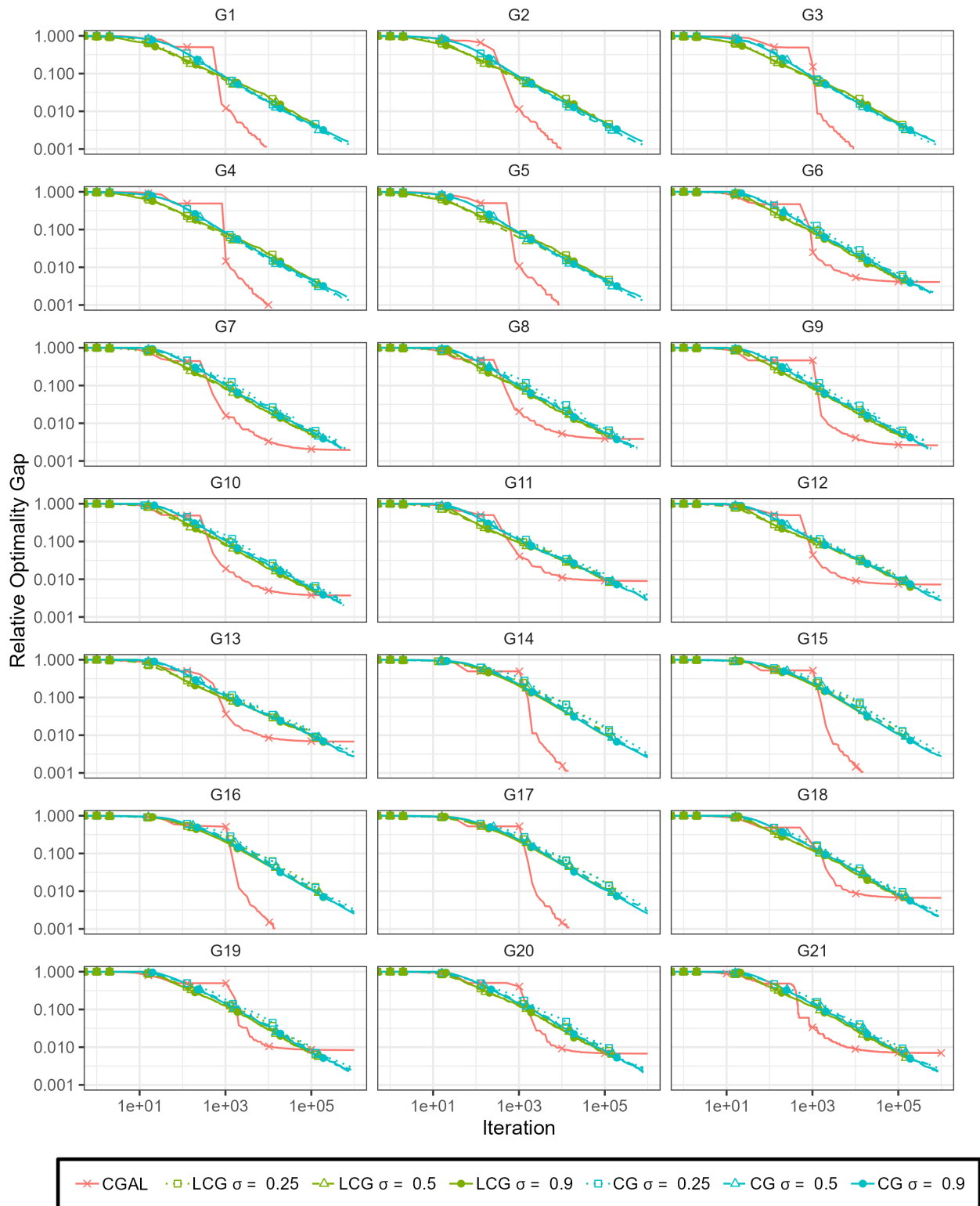


Figure 4: MaxCut datasets G1-G21 relative optimality gap vs. iteration.

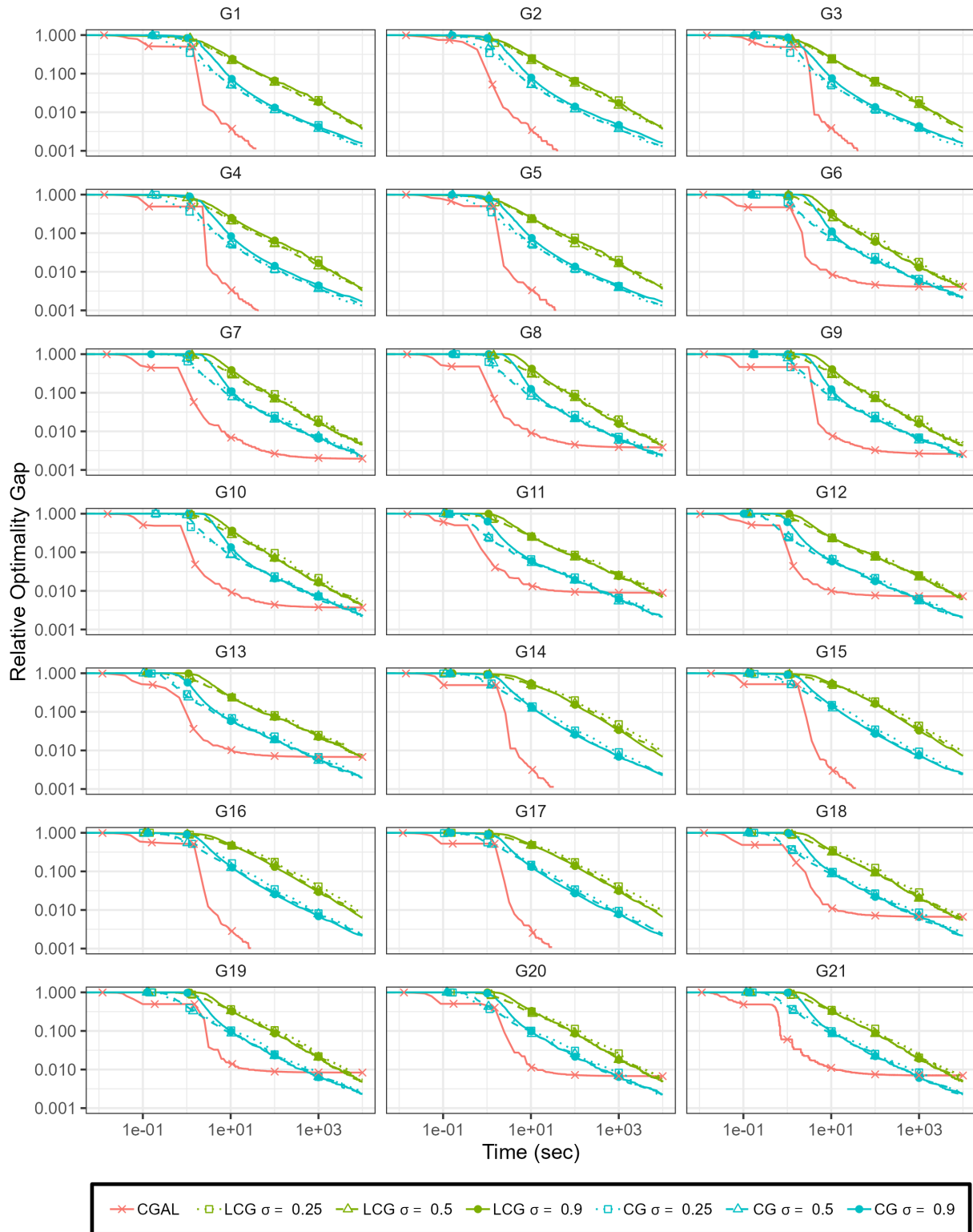


Figure 5: MaxCut datasets G1-G21 relative optimality gap vs. time.

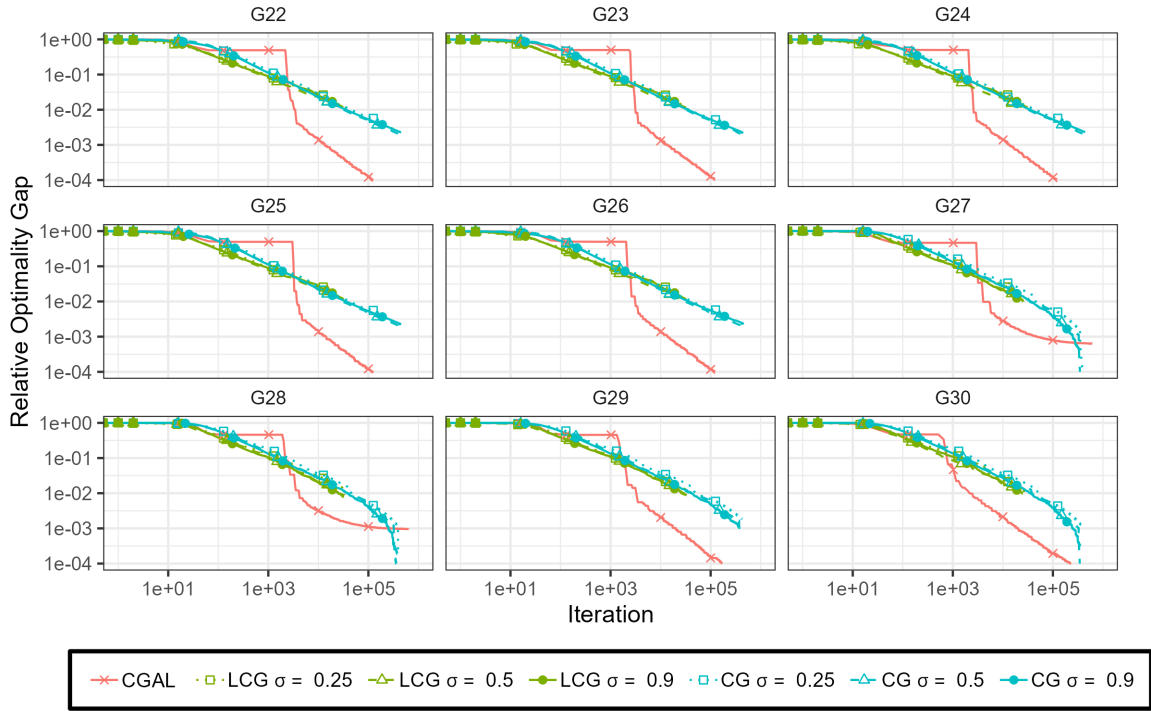


Figure 6: MaxCut datasets G22-G30 relative optimality gap vs. iteration.

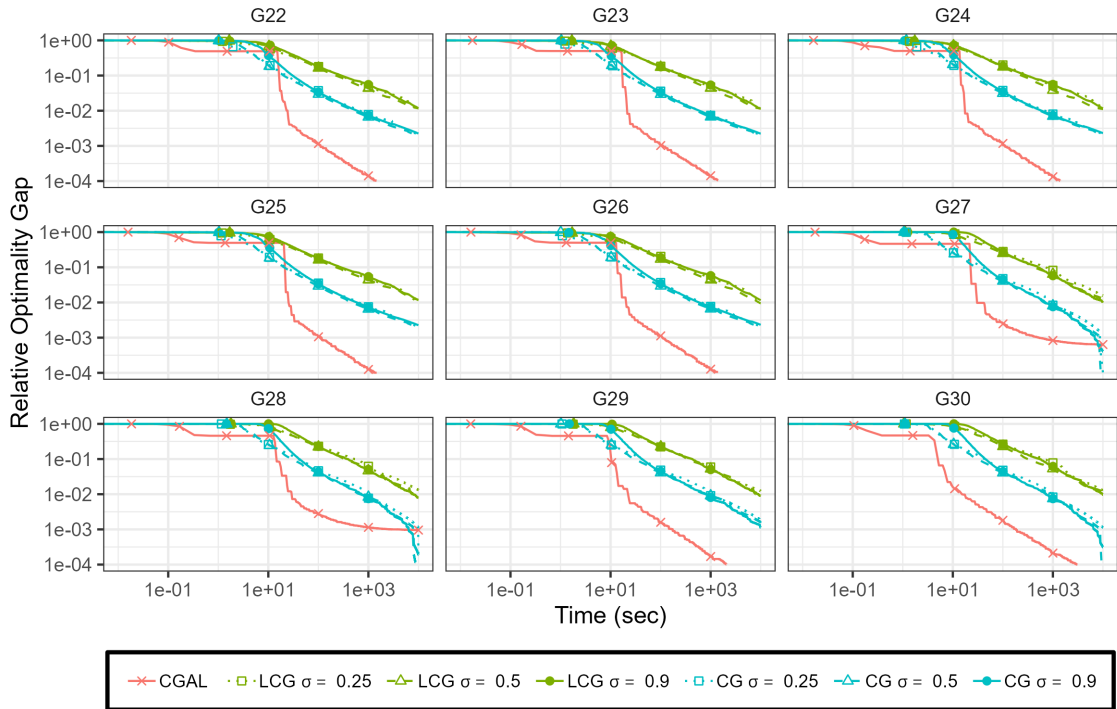


Figure 7: MaxCut datasets G22-G30 relative optimality gap vs. time.

Table 2: Performance for datasets G1-G18 at specific time points. For each data set, each time point, and each method the relative optimality gap (Opt. Gap), the iteration count (Iter) and for CGAL the relative feasibility gap (Feas. Gap) of the solution with the best objective value obtained until that time. The best relative optimality gap for each row is marked in bold.

Data Set	Time (sec)	CGAL			LCG $\sigma=0.25$		LCG $\sigma=0.5$		LCG $\sigma=0.9$		CG $\sigma=0.25$		CG $\sigma=0.5$		CG $\sigma=0.9$	
		Opt. Gap %	Feas. Gap %	Iter	Opt. Gap %	Iter	Opt. Gap %	Iter	Opt. Gap %	Iter	Opt. Gap %	Iter	Opt. Gap %	Iter	Opt. Gap %	Iter
G1	100	<b>0.0452</b>	0.0427	21685	5.3256	1650	5.1013	1592	6.3882	1494	1.1139	19046	1.1743	18468	1.2960	17742
	1000	<b>0.0100</b>	0.0092	144575	1.8670	17024	1.5269	16930	1.7090	16589	0.3782	126215	0.3774	124709	0.4113	127334
	10000	<b>0.0010</b>	0.0010	888035	0.4146	134546	0.3628	141906	0.3890	154157	0.1312	786346	0.1322	728109	0.1565	730861
G2	100	<b>0.0443</b>	0.0416	20514	5.1990	1673	4.9872	1668	6.1180	1614	1.1186	20079	1.1583	17849	1.3328	17078
	1000	<b>0.0076</b>	0.0074	135864	1.8878	17695	1.5429	17554	1.5702	17592	0.3857	136275	0.3675	120983	0.4254	121586
	10000	<b>0.0013</b>	0.0012	816010	0.3419	150126	0.3133	153430	0.4046	148095	0.1317	763621	0.1463	687932	0.1571	715246
G3	100	<b>0.0641</b>	0.0622	21664	5.9692	1416	5.2227	1629	6.1860	1585	1.1050	20425	1.1555	17401	1.3028	17647
	1000	<b>0.0074</b>	0.0071	141485	1.8837	17015	1.3351	17410	1.5635	17266	0.4115	124686	0.3536	120982	0.4347	116904
	10000	<b>0.0008</b>	0.0008	892189	0.3171	151626	0.3283	156878	0.3777	156813	0.1326	763597	0.1405	649211	0.1665	669949
G4	100	<b>0.0686</b>	0.0666	19922	5.6793	1487	5.7132	1355	6.9583	1208	1.0994	19435	1.1341	18535	1.2752	17574
	1000	<b>0.0077</b>	0.0073	133750	2.1315	13938	1.4965	14001	1.7269	14378	0.3918	124072	0.3522	125967	0.4050	123681
	10000	<b>0.0008</b>	0.0008	892189	0.3171	151626	0.3283	156878	0.3777	156813	0.1326	763597	0.1405	649211	0.1665	669949
G5	100	<b>0.0668</b>	0.0644	20334	5.8090	1509	5.7594	1379	6.8983	1338	1.1164	20254	1.1668	16756	1.2883	17533
	1000	<b>0.0125</b>	0.0118	135291	2.0338	14165	1.3668	14650	1.7768	14696	0.4197	124738	0.3487	116404	0.4222	118817
	10000	<b>0.0008</b>	0.0007	888095	0.3882	137871	0.3553	143148	0.3893	146200	0.1322	772666	0.1335	714684	0.1643	694540
G6	100	<b>0.4803</b>	0.0682	19842	8.2189	1541	7.2658	1426	7.0960	1293	2.5433	16239	2.0011	14659	2.1106	12283
	1000	<b>0.4179</b>	0.0100	133015	1.8849	16247	1.7304	14630	1.5365	14492	0.6772	109973	0.5733	94957	0.6847	86027
	10000	0.4078	0.0009	937170	0.4791	172357	0.4163	177925	0.3755	163790	<b>0.2108</b>	720098	0.2232	581993	0.2106	566692
G7	100	<b>0.2743</b>	0.0735	19832	9.9632	1282	7.2801	1206	8.0242	1129	2.2855	16331	1.9467	13740	2.1709	12006
	1000	<b>0.2068</b>	0.0110	133207	2.1909	13391	1.7102	12885	1.7527	12644	0.6705	113963	0.6946	91575	0.6064	89294
	10000	<b>0.1959</b>	0.0009	813946	0.4959	142268	0.4302	129157	0.4549	124502	0.2127	657896	0.2206	525425	0.2223	510794
G8	100	<b>0.4518</b>	0.0627	20101	8.5605	1370	7.5897	1277	7.9211	1179	2.3751	15179	2.1037	13710	2.1617	12686
	1000	<b>0.3945</b>	0.0102	134291	2.0238	13734	1.7576	13463	1.6682	13493	0.7010	104772	0.5873	92671	0.6569	84183
	10000	0.3839	0.0009	820939	0.5342	137709	0.4611	133831	0.4212	129272	<b>0.2134</b>	566425	0.2330	566242	0.2457	480991
G9	100	<b>0.3402</b>	0.0741	20486	8.6602	1454	6.8707	1402	6.7527	1364	2.5177	17074	2.0543	14883	2.1253	12280
	1000	<b>0.2705</b>	0.0105	137199	1.9809	15167	1.7249	14672	1.5419	14895	0.6765	113442	0.5708	101335	0.6687	78602
	10000	0.2603	0.0011	839573	0.5128	148527	0.4597	141307	0.4304	137229	<b>0.2126</b>	578638	0.2375	561210	0.2158	492155
G10	100	<b>0.4693</b>	0.0931	20176	9.1327	1365	7.0820	1293	7.5663	1210	2.3524	16086	2.0193	13699	2.1163	12605
	1000	<b>0.3829</b>	0.0118	134447	2.0525	13854	1.7098	13728	1.5771	13428	0.6489	95647	0.5940	95183	0.5856	89508
	10000	0.3711	0.0008	843504	0.5452	140556	0.4503	139367	0.4136	136075	<b>0.2046</b>	572185	0.2221	525312	0.2224	502739
G11	100	<b>0.9391</b>	0.0293	52396	7.6742	2344	6.8577	2332	7.4084	2073	2.1040	42363	1.8304	36848	1.7089	39655
	1000	0.9021	0.0045	343271	2.3392	25386	1.9903	24475	2.0117	24162	0.6135	361872	0.5343	341395	<b>0.5732</b>	309567
	10000	0.8946	0.0007	1823694	0.7343	196738	0.7811	193144	0.6929	187647	<b>0.2105</b>	2176005	0.2228	1945371	<b>0.2105</b>	1813119
G12	100	<b>0.7673</b>	0.0295	52859	8.1471	2120	7.0435	2302	7.3282	2236	2.1726	38919	1.8728	37346	1.7495	37614
	1000	0.7294	0.0033	342496	2.4091	24045	2.1357	24512	2.3042	23901	0.6337	325029	<b>0.5363</b>	314001	0.5735	276203
	10000	0.7236	0.0007	1901444	0.7065	228102	0.5723	222533	0.6089	205372	<b>0.2002</b>	2311377	0.2094	2029389	0.2037	1692541
G13	100	<b>0.7167</b>	0.0260	50953	7.5696	2414	7.2154	1830	6.6205	2339	2.1816	42733	1.9334	37760	1.8089	36572
	1000	0.6846	0.0050	332950	2.4416	24491	2.1377	23816	1.9294	25070	0.6357	343063	<b>0.5274</b>	312566	0.5570	279764
	10000	0.6775	0.0005	1843586	0.7297	211955	0.7435	204609	0.6543	195695	0.1995	1887493	0.2062	1895654	<b>0.1948</b>	1547687
G14	100	<b>0.0488</b>	0.0401	36050	21.069	1686	16.422	1764	14.932	1636	2.9552	32769	2.6901	30857	2.3423	28826
	1000	<b>0.0062</b>	0.0051	247958	4.4529	18672	3.5753	18026	3.3863	17441	0.8246	243773	0.7049	220892	0.6569	206482
	10000	<b>0.0010</b>	0.0006	1653247	0.9661	175901	0.7821	173581	0.6847	186339	0.2270	1629850	0.2462	1237850	0.2253	1212944
G15	100	<b>0.0495</b>	0.0411	36866	18.219	2085	15.498	2061	14.534	2039	3.2756	35930	2.7522	29819	2.5041	27217
	1000	<b>0.0083</b>	0.0064	251117	4.1913	22101	3.2621	21712	3.0489	20963	0.8459	255448	0.7324	225802	0.6674	204773
	10000	<b>0.0011</b>	0.0007	1579597	0.9704	196785	0.7993	192710	0.7211	183253	0.2433	1550812	0.2374	1314984	0.2514	1151339
G16	100	<b>0.0365</b>	0.0287	41046	16.989	2178	14.670	2150	13.058	2034	2.7754	33679	2.5751	31471	2.3225	30479
	1000	<b>0.0061</b>	0.0049	271597	3.9114	22674	3.1580	22386	2.8169	21605	0.7870	260408	0.7366	228063	0.7303	222851
	10000	<b>0.0010</b>	0.0008	1679075	0.8573	224493	0.6819	227033	0.6209	224707	0.2386	1499401	0.2269	1423609	0.2134	1430100
G17	100	<b>0.0518</b>	0.0434	37335	20.096	1707	17.255	1757	14.974	1703	3.2235	33611	2.7927	29911	2.6083	26684
	1000	<b>0.0090</b>	0.0075	253376	4.5791	18601	3.6161	18267	3.4578	17899	0.8749	243142	0.7551	216924	0.6898	205937
	10000	<b>0.0009</b>	0.0006	1650749	0.9701	232319	0.7884	226754	0.6712	220683	0.2417	1537197	0.2402	1352397	0.2139	1371570
G18	100	<b>0.7302</b>	0.0560	38999	11.727	1795	10.971	1780	9.5330	1586	2.4057	24255	2.0556	22388	2.0462	20555
	1000	0.6753	0.0084	260520	2.7593	18331	2.1365	18265	2.1493	17040	0.7666	185915	0.6925	159283	<b>0.6533</b>	141416
	10000	0.6645	0.0006	1599182	0.6728	182254	0.4799	183154	0.5566	166432	0.2586	1061813	0.2166	962496	<b>0.2154</b>	879504

Table 3: Performance for datasets G19-G30 at specific time points. For each data set, each time point, and each method we record the best relative optimality gap (Opt. Gap), the iteration count (Iter) and for CGAL the relative feasibility gap (Feas. Gap) of the solution with the best objective value obtained until that time. The best relative optimality gap for each row is marked in bold.

Data Set	Time (sec)	CGAL			LCG $\sigma=0.25$		LCG $\sigma=0.5$		LCG $\sigma=0.9$		CG $\sigma=0.25$		CG $\sigma=0.5$		CG $\sigma=0.9$	
		Opt. Gap %	Feas. Gap %	Iter	Opt. Gap %	Iter	Opt. Gap %	Iter	Opt. Gap %	Iter	Opt. Gap %	Iter	Opt. Gap %	Iter	Opt. Gap %	Iter
G19	100	<b>0.8967</b>	0.0492	37083	12.059	1630	10.580	1541	10.506	1527	2.3693	25356	2.2978	22770	2.0119	20054
	1000	0.8444	0.0066	254368	2.6314	16530	2.1796	16473	2.1604	15966	0.6124	162830	0.6152	137255	<b>0.6637</b>	129524
	10000	0.8351	0.0006	1723323	0.5384	205382	0.5075	194687	0.4851	186757	0.2624	1026619	0.2506	842195	<b>0.2320</b>	756654
G20	100	<b>0.7363</b>	0.0538	36281	12.956	1486	10.386	1593	10.453	1462	2.8064	23999	2.4927	21325	2.2067	19130
	1000	0.6819	0.0062	251142	2.9914	15873	2.4176	15989	2.2335	16143	0.7705	162281	0.7034	144692	<b>0.6373</b>	132063
	10000	0.6742	0.0006	1716273	0.6061	208638	0.5587	206001	0.4746	187323	0.2475	1068889	<b>0.2064</b>	924839	0.2231	790836
G21	100	<b>0.7840</b>	0.0726	41830	10.288	1935	7.7700	1998	8.3024	1955	2.4996	24785	2.0761	20738	2.0545	20794
	1000	0.7121	0.0102	275681	2.1759	20341	1.8593	21211	1.8629	20506	0.7668	160845	<b>0.5995</b>	139988	0.6157	136838
	10000	0.7005	0.0008	1610239	0.4848	188165	0.4806	187510	0.4938	178700	0.2522	1016576	<b>0.2235</b>	914508	0.2284	824945
G22	100	<b>0.1174</b>	0.1139	12416	18.1438	300	16.5330	288	18.2411	248	3.7563	7042	2.9849	6751	3.4068	5745
	1000	<b>0.0193</b>	0.0187	90981	4.7658	3319	4.3706	3215	5.5525	2941	0.7828	64426	0.6636	59780	0.7353	58167
	10000	<b>0.0022</b>	0.0021	632496	1.0548	34970	1.1614	31913	1.1801	31293	0.2095	497773	0.1931	447623	0.2247	449915
G23	100	<b>0.1023</b>	0.0980	12410	18.5561	292	17.3589	250	17.8255	256	3.6153	6927	2.9642	6491	3.3613	5583
	1000	<b>0.0149</b>	0.0143	90915	4.7672	3275	4.3952	2940	5.3747	3069	0.7403	60120	0.6684	57688	0.7333	57294
	10000	<b>0.0021</b>	0.0020	631480	1.0797	33094	1.1388	31910	1.1669	32278	0.2062	478154	0.1923	440393	0.2229	449699
G24	100	<b>0.1257</b>	0.1222	12342	20.1997	251	17.6862	259	18.7144	242	3.8042	6856	3.1557	6188	3.4891	5526
	1000	<b>0.0164</b>	0.0157	90383	5.1886	2825	3.8498	2957	5.5847	2858	0.8075	61881	0.6991	55330	0.7356	57577
	10000	<b>0.0020</b>	0.0018	624799	1.2467	30859	1.1084	31608	1.1785	30999	0.2195	475491	0.2035	412481	0.2309	438368
G25	100	<b>0.1057</b>	0.1012	12533	18.5114	300	16.3371	284	17.9667	256	3.5888	6971	2.9573	6687	3.4011	5701
	1000	<b>0.0135</b>	0.0128	91948	4.7165	3368	4.4134	3115	5.4227	3022	0.7561	63518	0.6510	60912	0.7309	58963
	10000	<b>0.0018</b>	0.0017	637281	1.0292	34064	1.1919	32793	1.1593	32361	0.2028	491183	0.1930	448653	0.2257	452544
G26	100	<b>0.1375</b>	0.1337	12736	20.6034	248	17.1955	269	18.7351	245	3.7270	6860	2.9696	6664	3.4397	5703
	1000	<b>0.0151</b>	0.0145	92871	4.9788	3025	4.4023	3025	5.7863	2932	0.7733	62802	0.6581	60555	0.7417	59907
	10000	<b>0.0022</b>	0.0021	635639	1.0644	32298	0.9407	32064	1.1557	32364	0.2074	490930	0.1957	442197	0.2317	461381
G27	100	<b>0.3024</b>	0.2283	11530	28.4263	195	25.0943	214	27.2575	174	4.7957	6361	4.0809	6127	4.4816	4712
	1000	<b>0.0877</b>	0.0246	82946	8.2273	2240	6.4036	2407	5.7783	2351	0.8400	55681	0.8083	52249	0.7602	47704
	10000	0.0646	0.0031	609686	1.5543	25336	0.9938	25525	0.9926	25790	0.0102	390126	<b>0.0000</b>	378324	0.0409	344793
G28	100	<b>0.3037</b>	0.1984	12418	23.2191	281	22.2085	280	23.0712	226	4.6768	6415	4.1060	6054	4.3763	4992
	1000	<b>0.1194</b>	0.0240	91115	6.2536	3044	4.6599	3113	5.0701	3019	0.7727	54325	0.8275	54898	0.7498	50886
	10000	0.0964	0.0026	634335	1.3236	33006	0.8704	33326	0.7890	32323	0.0216	393334	<b>0.0000</b>	397716	0.0190	377339
G29	100	<b>0.1737</b>	0.1651	12428	22.335	291	22.374	276	22.594	244	4.8811	6431	4.1196	6132	4.4864	4976
	1000	<b>0.0238</b>	0.0216	91157	5.9446	3169	5.2525	3145	5.0132	3068	0.9131	57929	0.9055	50524	0.8096	51421
	10000	<b>0.0025</b>	0.0022	637658	1.2430	33012	0.8851	33265	0.9036	32289	0.1865%	421074	0.0965	375627	0.1135	356157
G30	100	<b>0.2294</b>	0.2176	11582	26.6363	217	22.9201	208	26.8685	190	4.8414	6122	4.0918	6027	4.4921	4685
	1000	<b>0.0300</b>	0.0254	86515	7.8141	2482	5.3362	2403	6.1525	2295	0.8334	53756	0.7499	51787	0.7489	47761
	10000	0.0048	0.0017	616813	1.0134	27305	1.1942	24995	0.9684	24960	0.1127	388638	<b>0.0027</b>	364280	0.0314	353046

## B.2 Markov chain mixing rate

We next consider the problem of finding the fastest mixing rate of a Markov chain on a graph [33]. In this problem, a symmetric Markov chain is defined on an undirected graph  $G = (\{1, \dots, n\}, \mathcal{E})$ . Given  $G$  and weights  $d_{ij}$  for  $\{i, j\} \in \mathcal{E}$ , we are tasked with finding the transition rates  $w_{ij} \geq 0$  for each  $\{i, j\} \in \mathcal{E}$  with weighted sum smaller than 1, that result in the fastest mixing rate. We assume that  $\sum_{ij} d_{ij}^2 = n^2$ . The mixing rate is given by the second smallest eigenvalue of the graph's Laplacian matrix, described as

$$L(\mathbf{w})_{ij} = \begin{cases} \sum_{j:\{i,j\} \in \mathcal{E}} w_{ij} & j = i \\ -w_{ij} & \{i, j\} \in \mathcal{E} \\ 0 & \text{otherwise.} \end{cases}$$

From  $L\mathbf{1} = 0$  it follows that  $\frac{1}{n}\mathbf{1}$  is a stationary distribution of the process. From [9], we have the following bound on the total variation distance of the time  $t$  distribution of the Markov process and the stationary distribution  $\sup_{\pi} \|\pi\mathbf{P}(t) - \frac{1}{n}\mathbf{1}\|_{\text{TV}} \leq \frac{1}{2} \sqrt{ne^{-\lambda t}}$ . The quantity  $T_{\text{mix}} = \lambda$  is called the *mixing time*, and  $\lambda \equiv \lambda_2(L(\mathbf{w}))$  is the second-largest eigenvalue of the graph Laplacian  $L(\mathbf{w})$ . To bound this eigenvalue, we follow the strategy laid out in [33]. Thus, the problem can be written as

$$\begin{aligned} \max_{\mathbf{w}} \quad & \lambda_2(L(\mathbf{w})) \\ \text{s.t.} \quad & \sum_{\{i,j\} \in \mathcal{E}} d_{ij}^2 w_{ij} \leq 1 \\ & \mathbf{w} \geq 0. \end{aligned}$$

This problem can also alternatively be formulated as

$$\begin{aligned} \min_{\mathbf{w}} \quad & \sum_{\{i,j\} \in \mathcal{E}} d_{ij}^2 w_{ij} \\ \text{s.t.} \quad & \lambda_2(L(\mathbf{w})) \geq 1 \\ & \mathbf{w} \geq 0. \end{aligned}$$

Due to the properties of the Laplacian, the first constraint can be reformulated as

$$\min_{\mathbf{w}} \quad \sum_{\{i,j\} \in \mathcal{E}} d_{ij}^2 w_{ij} \tag{B.2}$$

$$\text{s.t.} \quad L(\mathbf{w}) \geq \mathbf{I}_{n \times n} - \frac{1}{n} \mathbf{1}\mathbf{1}^\top \tag{B.3}$$

$$\mathbf{w} \geq 0. \tag{B.4}$$

The dual problem is then given by

$$\max_{\mathbf{X} \in \mathcal{S}_+^n} \quad \langle \mathbf{I}_{n \times n} - \frac{1}{n} \mathbf{1}\mathbf{1}^\top, \mathbf{X} \rangle \tag{B.5}$$

$$\text{s.t.} \quad X_{ii} + X_{jj} - 2X_{ij} \leq d_{ij}^2 \quad \{i, j\} \in \mathcal{E}$$

To obtain an SDP within our convex programming model, we combine arguments from [33] and [2]. Let  $\mathbf{X}$  be a feasible point for (B.5). Then, there exists a  $n \times n$  matrix  $\mathbf{V}$  such that  $\mathbf{X} = \mathbf{V}\mathbf{V}^\top$ . It is easy to see that multiplying each row of the matrix  $\mathbf{V}^\top = [\mathbf{v}_1, \dots, \mathbf{v}_n]$  with an orthonormal matrix does not change the feasibility of the candidate solution. Moreover  $X_{ij} = \mathbf{v}_i^\top \mathbf{v}_j$  for all  $1 \leq i, j \leq n$ , so that  $X_{ii} + X_{jj} - 2X_{ij} = \|\mathbf{v}_i - \mathbf{v}_j\|_2^2$ . Since shifting each vector  $\mathbf{v}_i$  by a constant vector  $\mathbf{v}$  would not affect the objective or constraints, we can, without loss of generality, set  $\mathbf{v}_1 = \mathbf{0}$ . This gives the equivalent optimization problem

$$\begin{aligned} \max_{\mathbf{v}_1, \dots, \mathbf{v}_n} \quad & \sum_{i=1}^n \|\mathbf{v}_i\|^2 \\ \text{s.t.} \quad & \|\mathbf{v}_i - \mathbf{v}_j\|^2 \leq d_{ij}^2 \quad \{i, j\} \in \mathcal{E}, \\ & \mathbf{v}_i \in \mathbb{R}^n, \mathbf{v}_1 = \mathbf{0}. \end{aligned} \tag{B.6}$$

This is the geometric dual derived in [33], which is strongly connected to the geometric embedding of a graph in the plane [20]. Thus, setting again  $\mathbf{X} = \mathbf{V}\mathbf{V}^\top$ , we therefore obtain that  $X_{1j} = X_{j1} = 0$

Dataset	# Nodes	# Edges	SDPT3 Value
1	100	1000	15.62
2	100	2000	7.93
3	200	1000	72.32
4	200	4000	17.84
5	400	1000	388.52
6	400	8000	38.37
7	800	4000	333.25
8	800	16000	80.03

Table 4: Mixing datasets characteristics.

for all  $i = 1, \dots, n$  thus reducing the dimension of the problem, and (B.7) can be reformulated as follows:

$$\begin{aligned}
& \max_{\mathbf{X} \in \mathbb{S}_+^{n-1}} \langle \mathbf{I}_{n-1 \times n-1} - \frac{1}{n} \mathbf{1}\mathbf{1}^\top, \mathbf{X} \rangle \\
& \text{s.t.} \quad X_{(i-1)(i-1)} + X_{(j-1)(j-1)} - 2X_{(i-1)(j-1)} \leq d_{ij}^2 \quad \{i, j\} \in \mathcal{E}, i, j > 1 \\
& \quad \quad X_{(j-1)(j-1)} \leq d_{1j}^2 \quad \{1, j\} \in \mathcal{E}
\end{aligned} \tag{B.7}$$

Moreover, since  $\mathbf{X} \in \mathbb{S}_+^{n-1}$ , it follows that  $2|X_{ij}| \geq -\sqrt{X_{ii}X_{jj}}$  and so for any  $\{i, j\} \in \mathcal{E}$  such that  $i, j > 1$ ,  $\sqrt{X_{(j-1)(j-1)}} \leq \sqrt{X_{(i-1)(i-1)}} + \sqrt{d_{ij}}$ . Therefore, since the graph is connected, we can recursively bound each diagonal element of  $\mathbf{X}$  and therefore the trace by a constant  $\alpha$ , and add the trace constraint  $\mathbf{X} = \{\mathbf{X} \in \mathbb{S}^n | \mathbf{X} \geq 0, \text{tr}(\mathbf{X}) \leq \alpha\}$  to the problem formulation without affecting the optimal values. Furthermore, defining  $\mathcal{D} : \mathbb{S}^{n-1} \rightarrow \mathbb{R}^{|\mathcal{E}|}$  by

$$\mathcal{D}(\mathbf{X})_{\{i,j\}} = \begin{cases} X_{(i-1)(i-1)} + X_{(j-1)(j-1)} - 2X_{(i-1)(j-1)}, & i, j > 0, \\ X_{(j-1)(j-1)}, & i = 1. \end{cases}$$

Let  $\mathbf{Q} = \{\mathbf{y} \in \mathbb{R}^{|\mathcal{E}|} | y_{i,j} \leq d_{ij}^2, \{i, j\} \in \mathcal{E}\}$  and  $\mathbf{K} = \{(y, t) \in \mathbb{R}^{|\mathcal{E}|} \times \mathbb{R} | \frac{1}{t} \mathbf{y} \in \mathbf{Q}, t > 0\}$ . This is a closed convex cone with logarithmically homogeneous barrier

$$f(\mathbf{y}, t) = - \sum_{\{i,j\} \in \mathcal{E}} \log(td_{ij}^2 - y_{i,j}) = - \sum_{e \in \mathcal{E}} \log(d_{ij}^2 - \frac{1}{t} y_{i,j}) - |\mathcal{E}| \log(t).$$

This gives a logarithmically homogeneous barrier  $F(\mathbf{X}, t) = f(\mathcal{P}(\mathbf{X}, t))$ , where  $\mathcal{P}(\mathbf{X}, t) = [\mathcal{D}(\mathbf{X}); t] \in \mathbb{R}^{|\mathcal{E}|} \times \mathbb{R}$ . We thus arrive at a formulation of the form of problem (P), which reads explicitly as

$$\begin{aligned}
& \min_{\mathbf{X}, t} \{g(\mathbf{X}) := \langle \mathbf{I}_{n \times n} - \frac{1}{n} \mathbf{1}\mathbf{1}^\top, \mathbf{X} \rangle\} \\
& \text{s.t.} \quad \mathcal{P}(\mathbf{X}, t) \in \mathbf{K} \\
& \quad \quad \mathbf{X} \in \mathbf{X}, t = 1.
\end{aligned} \tag{B.8}$$

We generated random connected undirected graphs of various sizes, and for each edge  $\{i, j\}$  in the graph we generated a random  $d_{ij}^2$  uniformly in  $[0, 1]$ . Table 4 provides the size of each dataset, and the value obtained by solving the Mixing problem SDP using CVX with the SDPT3 solver. In order to compare to the CGAL algorithm, we used the normalisation guidelines specified in [41],

so that the norm of the coefficients vector of each constraint will be equal to each other, and the norm of the constraint matrix and the objective matrix equals 1.

All datasets were run for both CG and LCG options with the following choice of parameters  $\eta_0 \in \{0.5\Omega_g, 1\Omega_g, 2\Omega_g\}$  and  $\sigma \in \{0.9, 0.5, 0.25\}$ . All methods were stopped when either they reached 10000 iterations or 3600 seconds running time, the earlier of the two conditions. Since CGAL does not generate feasible solutions, we computed the deviation from feasibility of its outputted solution  $\mathbf{X}^{\text{CGAL}}$  by

$$\text{Relative Feasibility Gap} = \gamma(\mathbf{X}^{\text{CGAL}}) \equiv \max_{\{i,j\} \in \mathcal{E}} \frac{d_{ij}^2 - \mathcal{D}(\mathbf{X}^{\text{CGAL}})_{ij}}{d_{ij}^2}.$$

We then corrected the solution to a feasible solution  $\tilde{\mathbf{X}}^{\text{CGAL}} = \mathbf{X}^{\text{CGAL}} / (\gamma(\mathbf{X}^{\text{CGAL}}) + 1)$ , however in our numerical experiments it turned out that  $\gamma$  was extremely large, which resulted in  $\tilde{\mathbf{X}}^{\text{CGAL}}$  being very close to the zero matrix with very poor performance. Therefore, we used the following alternative iterative correction method: We set  $\hat{\mathbf{X}}^{\text{CGAL},1} = \mathbf{X}^{\text{CGAL}}$ , and at each iteration  $k$  we identify  $\{i, j\} \in \mathcal{E}$  which leads to the maximum value for  $\gamma(\hat{\mathbf{X}}^{\text{CGAL},k})$  set  $i^* = \operatorname{argmax}_{\{i,j\}} X_{ij}$  and set

$$\hat{\mathbf{X}}_{ij}^{\text{CGAL},k+1} = \begin{cases} \hat{\mathbf{X}}_{ij}^{\text{CGAL},k+1}, & i, j \neq i^*. \\ \hat{\mathbf{X}}_{ij}^{\text{CGAL},k+1} / (\gamma(\hat{\mathbf{X}}^{\text{CGAL},k}) + 1), & i = i^* \text{ or } j = i^*. \end{cases}$$

We terminate the algorithm when  $\gamma(\hat{\mathbf{X}}^{\text{CGAL},k}) = 0$ . The value of the returned  $\hat{\mathbf{X}}^{\text{CGAL}}$  is then computed. As in the previous section, one of our performance measures is the *relative optimality gap*  $\frac{|g(\mathbf{X}) - g(\tilde{\mathbf{X}}^{\text{SDPT3}})|}{|g(\tilde{\mathbf{X}}^{\text{SDPT3}})|}$  between the (corrected) solution of each method and the SDPT3 solution. Specifically, for each dataset  $D$ , method  $M$  and parameter combination  $P$ , we record the objective value  $g_i^{M,P,D}$  (or, for CGAL, the corrected objective value) after iteration  $i$ , the corresponding relative optimality gap  $r_i^{M,P,D} = (g_i^{M,P,D} - g(\tilde{\mathbf{X}}^{\text{SDPT3}})) / g(\tilde{\mathbf{X}}^{\text{SDPT3}})$ , the time  $t_i^{M,P,D}$  elapsed since the start of the run and, only for CGAL, the relative feasibility gap  $\gamma_i^{\text{CGAL},D}$ .

Figures 8-9 illustrate the results for the tested  $\sigma$  and  $\eta_0$  values. Figure 8 displays, for each iteration  $i$ , the best relative optimality gap  $\min_{j \leq i} \{r_j^{M,P,D}\}$  up to that iteration. Figure 9 displays for each time  $t$  the best relative optimality gap  $\min_j \{r_j^{M,P,D} : t_j^{M,P,D} \leq t\}$  obtained up to time  $t$ . Table 5 reports the performances of the tested methods at time points  $t \in \{100, 500, 1000\}$  seconds, in order to examine their algorithmic behavior under different time constraints. Specifically, given a data set  $D$ , a method  $M$ , parameters  $P$  and a time point  $t$ , for CG and LCG we compute  $(j^*, P^*) = \operatorname{argmin}_{j,P} \{r_j^{M,P,D} | t_j^{M,P,D} \leq t\}$ , so the table contains: the parameter values  $P^* = (\eta_0, \sigma)$ , the corresponding objective function value (Obj. Value)  $g_{j^*}^{M,P^*,D}$ , the relative optimality gap (Opt. Gap)  $r_{j^*}^{M,P^*,D}$ , and the number of iterations (Iter) performed until that time, given by  $\max\{j | t_j^{M,P^*,D} \leq t\}$ . For CGAL, since there is no parameter choice, we retrieve  $j^* = \operatorname{argmin}_j \{r_j^{\text{CGAL},D} | t_j^{\text{CGAL},D} \leq t\}$ , and the table records the corresponding objective value (Obj. Value)  $g_{j^*}^{\text{CGAL},D}$ , the relative optimal gap (Opt. Gap)  $r_{j^*}^{\text{CGAL},D}$ , the relative feasibility gap (Feas Gap)  $\gamma_{j^*}^{\text{CGAL},D}$ , as well as the number of iterations (Iter) given by  $\max\{j | t_j^{\text{CGAL},D} \leq t\}$ . The lowest relative optimality gap for each data set and time is marked in bold.

Figures 8 and 9 indicate that the line search version LCG outperforms CG, although in most cases less iterations are performed. One explanation of this phenomenon is that the step size policy employed in CG is based on global optimization ideas which do not take into account the local structure of the problem. LCG instead captures these local features of the problem more accurately, leading to

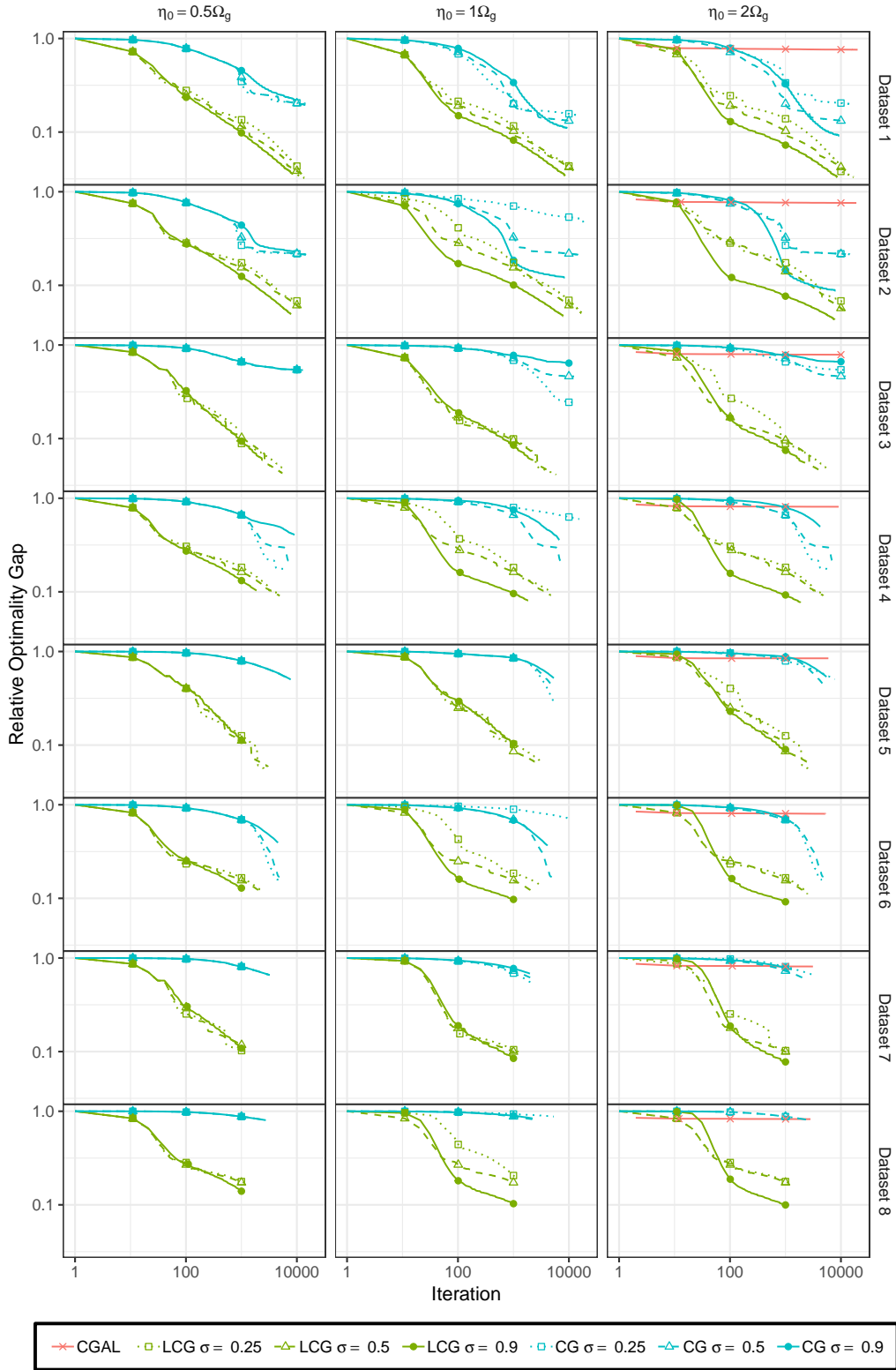


Figure 8: Mixing datasets relative optimality gap vs. iteration for various parameter choices.

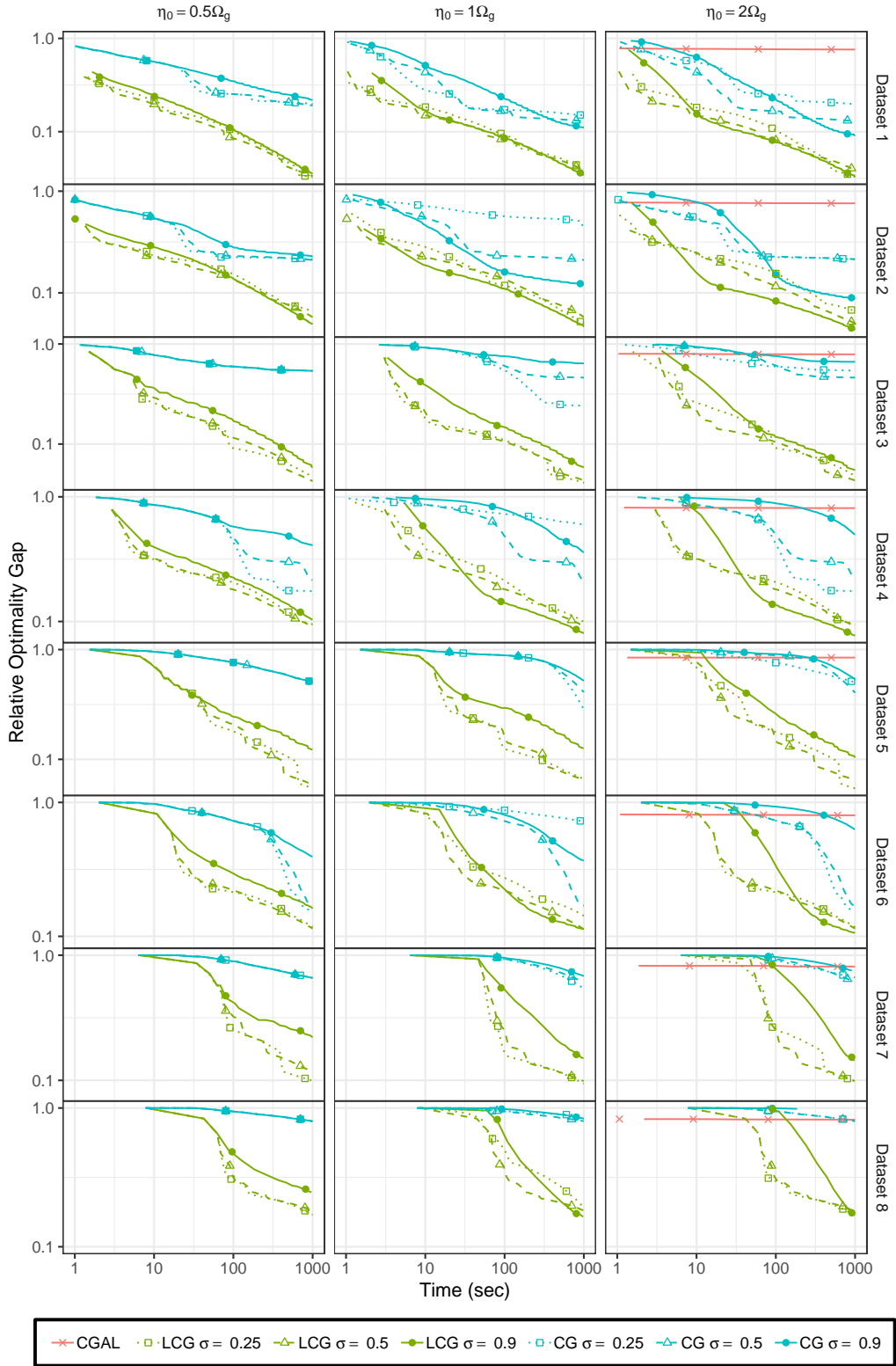


Figure 9: Mixing datasets relative optimality gap vs. time for various parameter choices.

Table 5: Mixing datasets results. For each dataset, time, and algorithm provides the best parameter choice for  $\eta_0$  (in multipliers of  $\Omega_g$ ) and  $\sigma$ , the function value obtained, the relative optimality gap (Opt. Gap), the iteration, and for CGAL the relative feasibility gap (Feas. Gap) of the solution with the best objective value obtained until that time. The best objective value and relative optimality gap for each row are marked in bold.

Data Set	Time (Sec)	CG					LCG					CGAL			
		$\eta_0$ ( $x \cdot \Omega_g$ )	$\sigma$	Obj. Value	Opt. Gap %	Iter	$\eta_0$ ( $x \cdot \Omega_g$ )	$\sigma$	Obj. Value	Opt. Gap %	Iter	Obj. Value	Opt. Gap %	Feas. % Gap %	Iter
MixData1	100	2	0.5	13.03	16.6	2385	2	0.9	<b>14.39</b>	<b>7.9</b>	809	3.68	76.4	21930.2	3090
	500	2	0.9	13.96	10.7	4969	2	0.25	<b>14.97</b>	<b>4.1</b>	9001	3.74	76.1	12304.4	11460
	1000	2	0.9	14.20	9.1	9286	0.5	0.25	<b>15.12</b>	<b>3.2</b>	13598	3.76	75.9	8873.5	19981
MixData2	100	2	0.9	6.71	15.3	957	2	0.9	<b>7.26</b>	<b>8.4</b>	745	1.88	76.2	19184.7	2948
	500	2	0.9	7.17	9.5	4099	2	0.9	<b>7.49</b>	<b>5.5</b>	3873	1.90	76.0	8729.7	10864
	1000	2	0.9	7.23	8.8	8024	2	0.9	<b>7.59</b>	<b>4.3</b>	7758	1.91	76.0	6066.0	18977
MixData3	100	1	0.25	32.86	54.6	1865	0.5	0.25	<b>65.70</b>	<b>9.2</b>	888	15.15	79.1	44622.3	1656
	500	1	0.25	54.34	24.9	8832	1	0.25	<b>68.88</b>	<b>4.8</b>	3289	15.30	78.8	13031.6	6080
	1000	1	0.25	54.87	24.1	14128	1	0.25	<b>69.34</b>	<b>4.1</b>	5851	15.32	78.8	7902.7	10657
MixData4	100	2	0.25	10.28	42.4	1676	2	0.9	<b>15.42</b>	<b>13.6</b>	166	3.33	81.3	116332.0	1440
	500	0.5	0.25	14.69	17.7	4710	2	0.9	<b>16.15</b>	<b>9.5</b>	921	3.36	81.2	57781.9	5203
	1000	0.5	0.25	14.72	17.5	6939	2	0.9	<b>16.47</b>	<b>7.7</b>	1880	3.36	81.2	41696.7	9081
MixData5	100	2	0.25	92.61	76.2	1289	1	0.25	<b>340.02</b>	<b>12.5</b>	415	59.39	84.7	122971.0	946
	500	0.5	0.9	163.46	57.9	4788	0.5	0.5	<b>360.70</b>	<b>7.2</b>	1701	59.31	84.7	126861.0	3397
	1000	1	0.25	277.79	28.5	5359	2	0.25	<b>367.26</b>	<b>5.5</b>	2937	59.90	84.6	64948.0	5939
MixData6	100	1	0.5	10.52	72.6	751	2	0.25	<b>30.11</b>	<b>21.5</b>	256	7.44	80.6	149166.0	811
	500	0.5	0.25	28.98	24.5	2995	2	0.9	<b>33.59</b>	<b>12.5</b>	232	7.60	80.2	103077.0	3004
	1000	0.5	0.25	32.30	15.8	4661	2	0.9	<b>34.24</b>	<b>10.8</b>	482	7.66	80.0	68409.9	5270
MixData7	100	0.5	0.9	35.69	89.3	496	1	0.25	<b>276.90</b>	<b>16.9</b>	82	59.19	82.2	702281.0	478
	500	1	0.25	102.57	69.2	984	0.5	0.25	<b>295.47</b>	<b>11.3</b>	616	62.41	81.3	239810.0	1766
	1000	1	0.25	152.56	54.2	2101	1	0.25	<b>301.48</b>	<b>9.5</b>	1447	62.78	81.2	185699.0	3124
MixData8	100	0.5	0.9	4.49	94.4	306	0.5	0.25	<b>55.80</b>	<b>30.3</b>	66	13.77	82.8	613444.0	431
	500	0.5	0.9	12.03	85.0	1455	2	0.25	<b>63.64</b>	<b>20.5</b>	566	13.99	82.5	282965.0	1593
	1000	0.5	0.9	15.84	80.2	2751	1	0.9	<b>66.98</b>	<b>16.3</b>	133	14.05	82.4	243686.0	2817

better numerical performance. By comparison, CGAL performs quite poorly, with optimality gaps ranging from 70% to 90% roughly; this is closely linked to large relative feasibility gaps, exceeding 10000%. One possible reason for these results is that CGAL's convergence guarantees rely on the magnitude of the dual variables, which in turn depend on the size of the Slater condition gap. Since the right-hand side  $d_{ij}^2$  of the constraints may be very small, this gap will generally be small, causing the norm of the dual variables to become large and slowing convergence. This may also explain the contrast with CGAL's superior performance in the MaxCut example. Additionally, Table 5 does not indicate that there is a preferable choice of parameters for CG and LCG, since the best configuration is different for different data sets and times.

### B.3 Randomly Scaled SDP

Finally, we consider a general SDP problems with inequality constraints, which we use to investigate the sensitivity of the compared methods to problem scaling. The synthetically scaled SDP

(SRS) takes the form

$$\begin{aligned}
& \max \quad \langle \mathbf{C}, \mathbf{X} \rangle \\
& \text{s.t.} \quad \langle \mathbf{A}_i, \mathbf{X} \rangle \leq b_i \quad i = 1, \dots, m \\
& \quad \text{tr}(\mathbf{X}) \leq 1 \\
& \quad \mathbf{X} \geq 0.
\end{aligned} \tag{B.9}$$

Let  $\mathbf{Q} = \{\mathbf{y} \in \mathbb{R}^m \mid y_i \leq b_i, i \in \{1, 2, \dots, m\}\}$  and  $\mathbf{K} = \{(\mathbf{y}, t) \in \mathbb{R}^m \times \mathbb{R} \mid \frac{1}{t}\mathbf{y} \in \mathbf{Q}, t > 0\}$ . This is a closed convex cone with logarithmically homogeneous barrier

$$f(\mathbf{y}, t) = - \sum_{i=1}^m \log(tb_i - y_i) = - \sum_{i=1}^m \log(b_i - \frac{1}{t}y_i) - m \log(t),$$

i.e.,  $F(\mathbf{X}, t) = f(\mathcal{P}(\mathbf{X}, t))$ , where  $\mathcal{P}(\mathbf{X}, t) = [\langle \mathbf{A}_1, \mathbf{X} \rangle; \langle \mathbf{A}_2, \mathbf{X} \rangle; \dots; \langle \mathbf{A}_m, \mathbf{X} \rangle; t] \in \mathbb{R}^m \times \mathbb{R}$ . We thus arrive at a formulation of the form of problem (P), which reads explicitly as

$$\begin{aligned}
& \min_{\mathbf{X}, t} \quad g(\mathbf{X}) := \langle -\mathbf{C}, \mathbf{X} \rangle \\
& \text{s.t.} \quad \mathcal{P}(\mathbf{X}, t) \in \mathbf{K} \\
& \quad (\mathbf{X}, t) \in \mathbf{X} := \{(\mathbf{X}', t') \in \mathcal{S}^n \times \mathbb{R} \mid \mathbf{X}' \geq 0, \text{tr}(\mathbf{X}') \leq 1, t' = 1\}.
\end{aligned} \tag{B.10}$$

We randomly generate the objective function and constraint coefficients to be PSD matrices with unit Frobenius norm where, given a matrix  $M \in \mathbb{R}^{m_1 \times m_2}$ , its Frobenius norm is  $\|M\|_F := \sqrt{\sum_{i=1}^{m_1} \sum_{j=1}^{m_2} M_{ij}^2}$ . Specifically, the constraint matrices for every instance and  $i = 1, \dots, m$  are generated by first sampling  $\mathbf{u}_i \in \mathbb{R}^n$  with components from a standard Gaussian distribution, rounded to the nearest integer, then setting  $\mathbf{A}_i = \mathbf{u}_i \mathbf{u}_i^\top$ , and finally normalizing the matrix to Frobenius norm of 1. Similarly, the objective matrix is generated by sampling  $\mathbf{U}_0 \in \mathbb{R}^{n \times n}$  with components from a standard Gaussian distribution, rounded to the nearest integer, and  $\mathbf{C} = (\mathbf{U}_0 \mathbf{U}_0^\top) / \|(\mathbf{U}_0 \mathbf{U}_0^\top)\|_F$ . Additionally, we generate a PSD reference solution  $\mathbf{X}_0$  by sampling  $\mathbf{V} \in \mathbb{R}^{n \times n}$  with components from a standard Gaussian distribution, then setting  $\mathbf{X}_0 = \mathbf{V} \mathbf{V}^\top$  and, finally, normalizing the result to have a trace equal to 1. The right-hand side constraint coefficients are constructed as  $b_i = \frac{u_i}{p^{1/2}} \langle \mathbf{A}_i, \mathbf{X}_0 \rangle$ , with  $u_i$  is a random variable uniformly distributed over  $[\frac{1}{2}, 1]$ , and  $p \in \{0, 1, 2\}$ , where  $p$  is a parameter that measures the scaling of the constraints. We note that CGAL ran on the normalized problem, using the normalization guidelines specified in [41].

Similarly to the previous examples, the performance metric to benchmark our experimental results is the relative optimality gap, defined  $\frac{|g(\mathbf{X}) - g(\mathbf{X}^{\text{SDPT3}})|}{|g(\mathbf{X}^{\text{SDPT3}})|}$ , where  $\mathbf{X}^{\text{SDPT3}}$  is the optimal solution computed by the interior-point solver SDPT3. We compare our solutions with those generated by CGAL. However, since CGAL does not necessarily produce feasible solutions, its reported solution  $\mathbf{X}^{\text{CGAL}}$  is corrected to ensure feasibility. Specifically, given a relative feasibility gap  $\gamma = \max_{i \in \{1, 2, \dots, m\}} \frac{\max\{\langle \mathbf{A}_i, \mathbf{X} \rangle - b_i, 0\}}{b_i}$ , the corrected solution was given by  $\tilde{\mathbf{X}}^{\text{CGAL}} = \mathbf{X}^{\text{CGAL}} / (1 + \gamma)$ , and the relative optimality gap is obtained by using  $\tilde{\mathbf{X}}^{\text{CGAL}}$ .

For each value of  $p$ , we ran CGAL, LCG and CG on 30 realizations of problems of size  $n = 100$  and  $m = 100$ . All datasets were run for both CG and LCG with parameters  $\eta_0 = 2\Omega_g$  and  $\sigma \in \{0.25, 0.9\}$ . and all methods were stopped when either after 1000 seconds of running time. For every  $p \in \{0, 1, 2\}$ , realization  $R \in \{1, 2, \dots, 30\}$  of the data and algorithm  $M$ , we record the objective value  $g_i^{M,p,R}$  (corrected as explained above for CGAL) obtained after the iteration, the corresponding relative

optimality gap  $r_i^{M,p,R}$ , the time since the start of the run  $t_i^{M,p,R}$  and, for CGAL, the relative feasibility gap  $\gamma_i^{\text{CGAL},p,R}$ .

Table 6: Computational results for randomly scaled SDP datasets. For each time point, value of the parameter  $p$ , and algorithm (CG and LCG with  $\sigma \in \{0.25, 0.9\}$ , and CGAL), the table provides the objective function value (Obj. Value), the relative optimality gap (Opt. Gap), the iteration count and, only for CGAL, the relative feasibility gap (Feas. Gap) of the solution with the best objective value obtained up to that time. For each value of  $p$ , the metrics displayed in the table are aggregated across 30 datasets, and the best relative optimality gap achieved is marked in bold.

Data	Time (sec)	CG $\sigma = 0.25$			CG $\sigma = 0.9$			LCG $\sigma = 0.25$			LCG $\sigma = 0.9$			CGAL			
		Obj. Value	Opt. Gap %	Iter	Obj. Value	Opt. Gap %	Iter	Obj. Value	Opt. Gap %	Iter	Obj. Value	Opt. Gap %	Iter	Obj. Value	Opt. Gap %	Feas. Gap %	Iter
0	100	-186.45	0.671	2067	-186.78	0.4978	1467	-186.79	0.4908	1543	-186.99	0.3875	1305	-187.67	<b>0.0059</b>	0.0183	13349
	500	-187.19	0.2788	6665	-187.34	0.198	6120	-187.28	0.2272	6095	-187.4	0.1666	6201	-187.7	<b>0.0009</b>	0.0049	50070
	1000	-187.33	0.2027	13071	-187.46	0.1308	11662	-187.4	0.1653	11918	-187.5	0.1139	12133	-187.7	<b>0.0004</b>	0.0041	88240
1	100	-143.26	1.3039	1131	-143.56	1.0994	1020	-143.81	0.9277	1099	-144.01	<b>0.786</b>	783	-141.99	1.7272	2.1609	13266
	500	-144.38	0.5311	3976	-144.53	0.423	3841	-144.58	0.3932	3626	-144.66	0.3374	3427	-144.26	<b>0.2718</b>	0.6039	50306
	1000	-144.62	0.3621	7458	-144.73	0.2838	7314	-144.72	0.2955	7014	-144.8	0.235	6790	-144.83	<b>0.1209</b>	0.213	87925
2	100	-107.75	1.5629	767	-108.18	1.1652	686	-108.31	1.0371	612	-108.64	<b>0.7336</b>	569	-32.44	70.2786	265.9191	14138
	500	-108.82	0.5716	2868	-109.02	0.3879	2724	-108.98	0.4199	2727	-109.14	<b>0.276</b>	2603	-65.05	40.3478	74.8299	50504
	1000	-108.98	0.4222	5519	-109.15	0.2695	5283	-108.64	0.3322	5374	-109.22	<b>0.2037</b>	5191	-82.82	24.0898	35.2035	90162

Table 6 displays the performance of CGAL, CG and LCG after time points  $t \in \{100, 500, 1000\}$  seconds for different values of the parameter  $p$ , in order to study algorithmic behaviour under different time constraints. Specifically, for each method  $M$ , parameter value  $p$ , realization  $R$ , and time  $t$ , we compute  $(j^*)^{M,p,R} = \operatorname{argmin}_j \{r_j^{M,p,R} : t_j^{M,p,R} \leq t\}$  and  $k^{M,p,R} = \max\{j : t_j^{M,p,R} \leq t\}$ . The table displays the average objective function value (Obj. Value) given by  $\frac{1}{30} \sum_R \mathcal{G}_{(j^*)^{M,p,R}}^{M,p,R}$ , the average relative optimality gap (Opt. Gap)  $\frac{1}{30} \sum_R r_{(j^*)^{M,p,R}}^{M,p,R}$ , as well as the number of iterations (Iter) until that time given by  $\frac{1}{30} \sum_R k^{M,p,R}$  and, for CGAL, the average feasibility gap (Feas. Gap)  $\frac{1}{30} \sum_R \gamma^{M,p,R}$ . Table 6 shows that CGAL benefits from inexpensive iterations, allowing it to close the optimality gap more quickly than CG and LCG in favorable settings ( $p = 0$ ). However, as  $p$  increases to 2, although CGAL still performs more iterations than our algorithms, it fails to close the infeasibility gap even after 1000 seconds. This leads to a significantly larger optimality gap, as our calculations penalize infeasible solutions. In contrast, CG and LCG demonstrate robust performance, with little variation across different values of  $p$ . In particular LCG reaches an average optimality gap smaller than 1% after 100 seconds for all values of  $p$ , while the average optimality gap of CG increases by a factor of 2-2.5 when moving from  $p = 0$  to  $p = 2$ , but still maintaining less than 1% average optimality gap after 500 seconds for all values of  $p$ .

The performance of the average relative optimality gap with respect to iteration and time for each value of  $p$  is visually depicted in Figures 10 and 11, respectively. In these figures, it can clearly be observed that the performance of CG and LCG is robust to the value of  $p$ , while CGAL's performance deteriorates significantly as  $p$  gets larger. In order to create Figure 10 we first compute, for each iteration  $i$ , algorithm  $M$ , parameter value  $p \in \{0, 1, 2\}$  and realization  $R \in \{1, \dots, 30\}$ , the best relative optimality gap  $\hat{r}_i^{M,p,R} = \min_{j \leq i} \{r_j^{M,p,R}\}$  up to iteration  $i$ . We then plot its average  $\frac{1}{30} \sum_R \hat{r}_i^{M,p,R}$  across all realizations, for each iteration  $i$ . Instead, Figure 11 is obtained by first computing, for each time  $t$ , algorithm  $M$ , parameter value  $p$  and realization  $R$ , the best relative optimality gap  $r_{(j^*)^{M,p,R}}^{M,p,R}$  obtained up to time  $t$  (as defined above), and then by averaging these values across all realizations. These figures elucidate that while CGAL performance deteriorates as  $p$

increases, the performance of CG and LCG is robust to the scaling of the problem, .

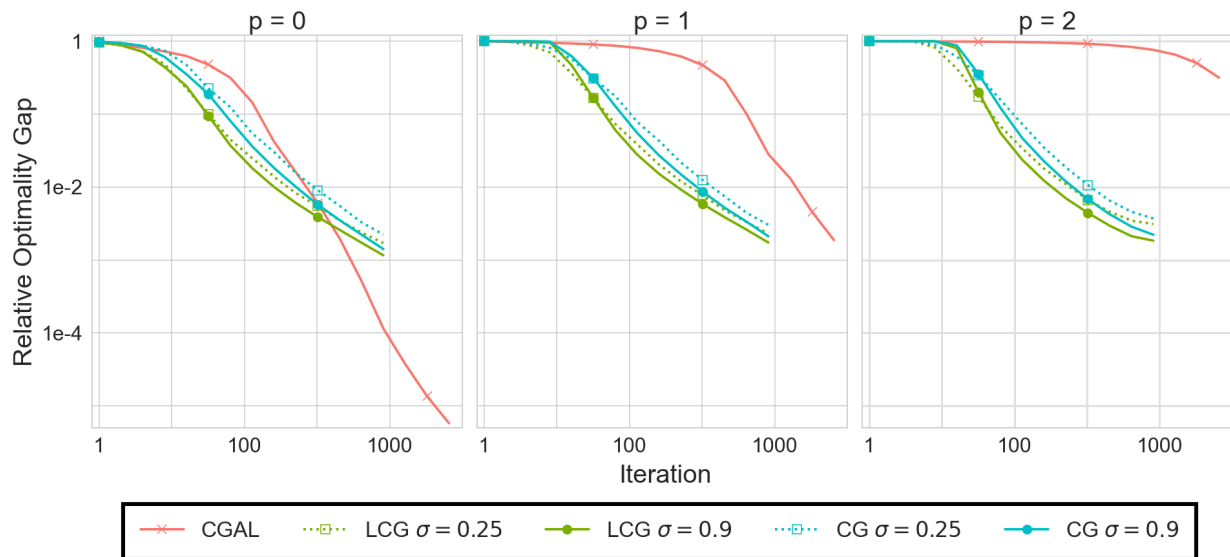


Figure 10: Randomly scaled SDP problem: relative optimality gap vs. iterations for several parameter choices (averaged over 30 instances for each  $p$ )

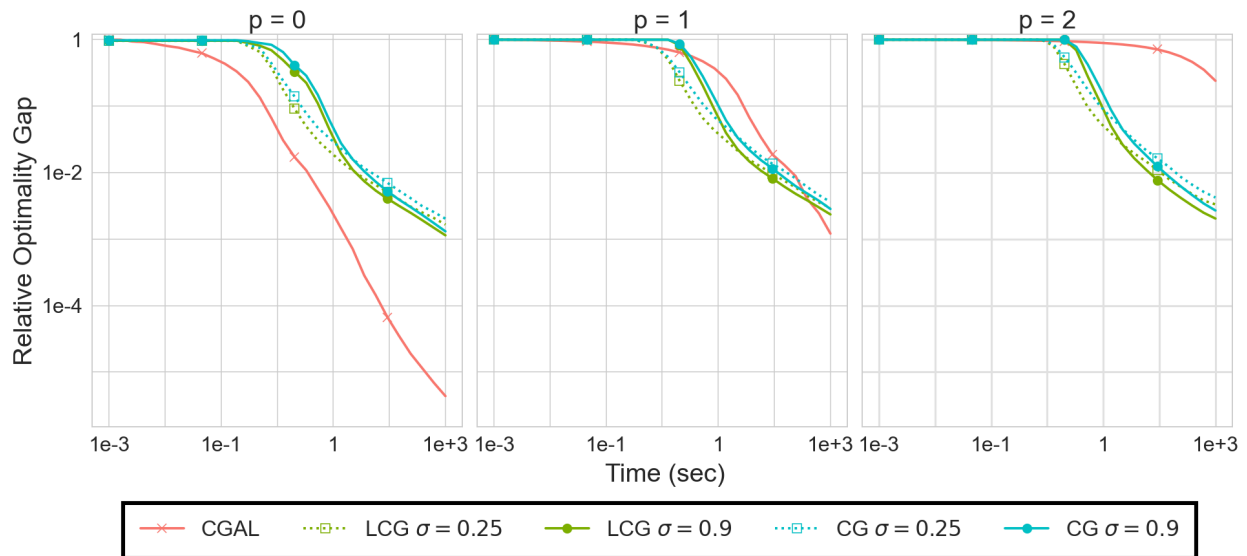


Figure 11: Randomly scaled SDP problem: relative optimality gap vs. time for several parameter choices (averaged over 30 instances for each  $p$ )